TRIBHUVAN UNIVERSITY

INSTITUTE OF ENGINEERING

PULCHOWK CAMPUS

THESIS NO.: M-420-MSREE-2024-2026

Impact assessment of Electric Cooking and Electric Mobility on Grid Demand: A Scenario Based Hourly Load Forecasting Study

by

Prashant Paudyal Sharma

A THESIS

SUBMITTED TO THE DEPARTMENT OF MECHANICAL AND AEROSPACE ENGINEERING IN PARTIAL FULLFILLMENT OF THE REQUIREMENT FOR THE DEGREE OF MASTER OF SCIENCE IN RENEWABLE ENERGY ENGINEERING

DEPARTMENT OF MECHANICAL AND AEROSPACE ENGINEERING

LALITPUR, NEPAL

APRIL 2026

COPYRIGHT

TRIBHUVAN UNIVERSITY

INSTITUTE OF ENGINEERING

PULCHOWK CAMPUS

DEPARTMENT OF MECHANICAL AND AEROSPACE ENGINEERING

The undersigned certify that read, and recommended to the Institute of Engineering for acceptance, a thesis proposal entitled "Impact assessment of Electric Cooking and Electric Mobility on Grid Demand: A Scenario Based Hourly Load Forecasting Study" submitted by Prashant Paudyal Sharma (080MSREE012), in the fulfillment of requirements for the degree of Master of Science in Renewable Energy Engineering.

Asst. Prof. Sanjaya Neupane

Supervisor

Department of Mechanical and Aerospace Engineering

Er. Sumant Sah

Senior Divisional Engineer

Water and Energy Commission Secretariat (WECS)

Tribhuvan University
Institute of Engineering
Department of Mechanical and Aerospace Engineering
Pulchowk Campus

Committee Chairman, Sudip Bhattrai, Ph.D.

Head of Department

Department of Mechanical and Aerospace Engineering

Date: 30 April, 2026

ABSTRACT

Nepal's transition toward electric cooking and electric mobility is expected to substantially increase electricity use, but its impact on hourly grid demand and peak load remains insufficiently understood. Existing planning approaches largely focus on annual energy requirements, whereas system reliability and infrastructure adequacy depend more directly on the timing and concentration of demand. This study develops a scenario-based hourly load forecasting framework to assess the impact of electric cooking and electric mobility on future grid demand. Annual baseline electricity demand was projected using macroeconomic and electricity-sector indicators through an LSTM-based forecasting approach, while additional demand from electric vehicles and electric cooking was incorporated using projected adoption pathways. The combined scenario projects total electricity demand to reach 28.74 TWh by 2030. To represent operational demand behavior, a physics-informed LSTM was used to forecast high-resolution baseline load profiles under annual energy consistency constraints. Electric cooking demand was modeled separately through a disaggregation framework that integrates appliance stock growth, usage intensity, and a learned time-of-day cooking profile. The final hourly demand profile was obtained by combining baseline, EV, and cooking-related loads and was used to evaluate peak-demand impacts. Results indicate that electric cooking strongly intensifies evening demand and sharpens system peaks when combined with rising baseline and EV loads. The integrated forecast identifies a maximum peak demand of approximately 2748.61 MW at 19:00 under the analyzed scenario. The study shows that future grid planning in Nepal should move beyond annual energy targets and explicitly account for peak-demand stress arising from end-use electrification.

Keywords: Electricity Demand Forecasting; Electric Cooking; Electric Mobility; Hourly Load Forecasting; Peak Demand; Physics Informed Neural Network (PINN)

ACKNOWLEDGEMENT

I would like to express my sincere gratitude to the Pulchowk Campus, Department of Mechanical and Aerospace Engineering, for providing me with the academic environment and resources necessary to complete this research.

I am especially thankful to my supervisor, Asst. Prof. Sanjaya Neupane, for his continuous guidance, valuable insights, and constructive feedback throughout this study. His support played a crucial role in shaping the direction and quality of this work.

I would also like to acknowledge the Load Dispatch Center (LDC), Syuchatar, for providing the hourly electricity demand data, which formed the backbone of this research.

My sincere thanks go to the external examiner, Er. Sumant Shah from the Water and Energy Commission Secretariat (WECS), for his valuable evaluation and suggestions.

I would also like to thank my classmates of the MSREE 2080 batch and MSc. Hostel mates in creating an insightful environment throughout the Masters study. With your presence, this study trip has been made interesting and informative. Finally, I want to express my utmost gratitude to my family as it has been able to support me through thick and thin. My academic life has been based on their understanding and sacrifices.

Finally, I would like to thank everyone who directly or indirectly contributed to the successful completion of this thesis.

TABLE OF CONTENTS

LIST OF TABLES

LIST OF FIGURES

LIST OF ABBREVIATIONS

Abbreviation	Full Form
ARIMA	Auto-Regressive Integrated Moving Average
BAU	Business-As-Usual
EV	Electric Vehicle
GWh	Gigawatt-hour
GDP	Gross Domestic Product
INPS	Integrated Nepal Power System
kWh	kilowatt hour
LSTM	Long Short-Term Memory
MAE	Mean Absolute Error
MAPE	Mean Absolute Percentage Error
ML	Machine Learning
MW	megawatt
NDC	Nationally Determined Contribution
NEA	Nepal Electricity Authority
PINN	Physics-Informed Neural Network
RMSE	Root Mean Square Error
TWh	terawatt hour
$\mathbf{x}_d \in \mathbb{R}^{36}$	$\mathbf{x}_d$ is the vector of 36 features

CHAPTER ONE: INTRODUCTION

1.1 Background

The 21st century is characterized by a fundamental paradigm shift in the global energy landscape, driven by the escalating threats of global warming, localized air pollution, and the rapid depletion of conventional fossil fuel reserves (Sinha et al., 2023). This transition necessitates a departure from carbon-intensive energy systems toward a framework anchored in renewable energy sources (RES) such as solar, wind, and hydropower (Deb et al., 2017). Central to this transformation is the concept of deep electrification, which involves substituting fossil fuels with electricity in end-use sectors that have traditionally been difficult to decarbonize [Steinberg et al., 2017]. Among these, the transportation and residential cooking sectors represent the most critical frontiers, forming what is increasingly recognized as the "dual electrification challenge" (Kafle, 2025b).

The international community, through the United Nations' Sustainable Development Goal 7 (SDG 7), has prioritized universal access to affordable, reliable, sustainable, and modern energy by 2030 (Odoi-Yorke, 2024). Access to energy is often described as the "golden thread" that weaves together economic growth, human development, and environmental sustainability (Lombardi et al., 2019). However, a significant "access-use paradox" persists; while global electrification rates have improved with nearly 1.2 billion people gaining access between 2000 and 2012 approximately 733 million people still lack basic electricity, and nearly 2.4 billion rely on inefficient, polluting fuels for their daily cooking needs (Lombardi et al., 2019; *Search | World Bank Data360*, n.d.).

The transportation sector is a primary driver of this energy transition, as it currently accounts for approximately 62.3% of global liquid fuel consumption and 22% of global CO2 emissions (Adhikari et al., 2020). The shift toward electric vehicles (EVs) is essential for achieving net-zero targets, with the global EV fleet projected to grow from 10 million units in 2021 to over 300 million by 2035 (Li & Jenn, 2024). This massive influx of mobile loads presents a unique challenge for power system operators, as uncontrolled charging can lead to severe grid congestion, transformer overloading, and degraded power quality (Birk Jones et al., 2022). Simultaneously, the electrification of the residential sector through electric cooking (e-cooking) is emerging as a vital

strategy for improving public health and energy equity (Gould et al., 2023).

Traditional cooking practices relying on solid biomass (wood, charcoal, and dung) are responsible for approximately 3.2 to 4 million premature deaths annually due to household air pollution (HAP), disproportionately affecting women and children (Scott et al., 2024). Furthermore, the unsustainable collection of fuelwood contributes to 2% of global greenhouse gas emissions and accelerates deforestation (Scott et al., 2024). While many developing nations initially promoted Liquefied Petroleum Gas (LPG) as a "bridge fuel," it remains a non-renewable fossil fuel often subject to volatile international prices and supply chain vulnerabilities (Gould et al., 2023). Consequently, high-efficiency e-cooking technologies, such as induction hobs and Electric Pressure Cookers (EPCs), are now viewed as the most sustainable long-term solution for clean cooking (Leach et al., n.d.; Scott et al., 2024).

The dual integration of EVs and e-cooking onto existing distribution networks creates a complex load synchronization problem (Birk Jones et al., 2022). Because both charging and cooking activities often coincide with existing system peak hours typically the early morning and evening, they pose a cumulative threat to the stability and reliability of the power distribution system (PDS) (Clements et al., 2020a; Kafle et al., 2026; Scott et al., 2024). In many developing regions, such as Nepal, the distribution infrastructure was originally designed for minimal lighting-led loads, meaning that the introduction of high-power appliances like 2 kW induction stoves or Level 2 EV chargers can exceed local transformer capacities even at low penetration levels (Clements et al., 2020a; Kafle et al., 2026).

In the specific context of Nepal, the energy transition is intertwined with the pursuit of energy sovereignty (Giri et al., 2026). The country is endowed with vast hydropower potential, estimated at 83,000 MW, yet it remains heavily dependent on imported petroleum products, which accounted for 17% of total merchandise imports in 2024 (Jha et al., 2025; Kafle, 2025b). While the government has set ambitious targets such as achieving 28,000 MW of generation by 2035 and ensuring that 90% of all vehicle sales are electric by 2030 the "readiness" of the distribution grid remains a critical bottleneck (Jha et al., 2025; Kafle et al., 2026). Understanding the synergistic impact of these two burgeoning sectors on hourly load profiles is therefore paramount for formulating evidence-based infrastructure planning and demand side management

(DSM) strategies that can sustain a resilient, low-carbon future (Kafle, 2025b).

1.2 Statement of Problem

Nepal has set ambitious electricity sector targets, including expanding renewable generation capacity to 28,500 MW by 2035. However, this target represents a broader national generation goal that includes export-oriented development and does not directly reflect domestic electricity demand requirements. As a result, energy planning discussions often emphasize installed capacity and annual energy balance (GWh), while giving limited attention to peak demand (MW) and temporal load dynamics.

At the same time, rapid electrification trends particularly electric cooking and electric mobility are expected to significantly increase domestic electricity consumption. While these transitions contribute to higher annual energy demand, their more critical impact lies in the concentration of demand during specific hours of the day. Electric cooking loads are typically aligned with residential peak periods, and electric vehicle charging behavior often coincides with evening household routines. This temporal overlap creates a compounding peak effect, increasing peak demand and placing additional stress on the power system.

Despite these challenges, conventional forecasting approaches primarily focus on aggregate demand and fail to capture high-resolution temporal variations and technology-driven demand interactions. Consequently, there remains a critical gap in understanding how electrification will influence hourly load behavior and peak demand in Nepal.

Therefore, there is a need for an integrated, scenario-based forecasting framework that combines macro-level demand drivers with high-resolution load modeling to accurately assess future electricity demand patterns and peak load impacts under electrification scenarios.

1.3 Objectives

1.3.1 Main objective

To assess the impact of electric cooking and electric mobility on future grid demand in Nepal through a scenario-based hourly load forecasting framework.

1.3.2 Specific objectives

The specific objectives of this research are:

- To calculate and forecast baseline electricity demand using macroeconomic and demographic indicators.
- To model and integrate future electricity demand from electric cooking and usage of electric vehicles based on adoption trends and policy targets.
- To generate hourly electricity demand profiles using a physics-informed neural network while ensuring consistency with annual energy projections.
- To estimate the hourly contribution of electric cooking demand using a data-driven disaggregation model based on appliance stock, usage behavior, and temporal distribution patterns.
- To analyze the impact of electrification on peak demand magnitude, timing, and frequency for national grid planning purposes.

1.4 Limitations

The following limitations should be considered when interpreting the results;

- Macro Forecasting: Fossil fuel transition dynamics are not explicitly modeled.
- Cooking Model: Cooking demand is DL-based without primary data validation.
- Scenario Integration: Assumes stable policy and economic conditions.
- External Uncertainty: Climate, extreme events, and economic shocks are not considered.

CHAPTER TWO: LITERATURE REVIEW

2.1 Electric Mobility (EVs) and Grid Integration

2.1.1 Global Adoption Trends & Barriers: Developed vs. Developing Contexts

The global transition toward electric mobility is progressing at a significant, albeit geographically uneven, pace. Analysts project that the number of light-duty electric vehicles (EVs) and their associated charging plugs will multiply to over 300 million and 175 million, respectively, by 2035 an order of magnitude increase from 2021 levels (Li & Jenn, 2024; Powell et al., 2022). In developed markets, adoption has been driven by aggressive climate policies and substantial infrastructure investment. For instance, California has enacted ambitious goals that position it as a global leader, yet studies indicate that meeting 2030 targets will require infrastructure upgrades for nearly 20% of existing distribution feeders (Jenn & Highleyman, 2022). Similarly, Norway reported that half of all vehicles sold in 2018 were EVs, supported by extensive fiscal incentives and a robust public charging network (Mali et al., 2022).

In contrast, developing nations like Nepal face a unique trajectory defined by historical early adoption and modern structural bottlenecks. Nepal's engagement with electric mobility began as early as 1975 with the introduction of Chinese-aided electric trolley buses, followed by the successful rollout of the Safa Tempo (battery-operated three-wheelers) in the early 1990s to mitigate Kathmandu's deteriorating air quality (Baral et al., 2000; Mali et al., 2022). However, the modern transition is hindered by inconsistent fiscal policies; for example, Nepal's customs and excise duties on private EVs have fluctuated between 10% and 60% in recent budget cycles, significantly impacting market stability (Jha et al., 2025; Mali et al., 2022). While total vehicle registration in Nepal reached over 5.5 million by 2024, motorcycles continue to dominate with an 81% share, and the uptake of four-wheeler EVs remains limited by high purchase prices and a shortage of charging infrastructure along major highways (Jha et al., 2025; Neupane et al., 2024). Technical barriers, such as a shortage of skilled technicians and concerns regarding battery life in local conditions, further compound these adoption hurdles (Adhikari et al., 2020; Calise et al., 2023).

2.1.2 Technical Grid Impacts: Stability, Waveform Distortions, and Power Losses

The integration of intensive EV charging loads onto the Power Distribution System

(PDS) introduces a range of technical challenges that can compromise grid reliability. A primary concern is power system stability, particularly when uncontrolled charging coincides with existing system peaks (Kene & Olwal, 2023; Roy et al., 2023). Research indicates that even a modest 10% increase in EV charging penetration can result in an 18% increase in total PDS demand, potentially leading to total blackouts if not managed through coordinated schemes (Roy et al., 2023). Furthermore, the non-linear characteristics of power electronic converters used in EV chargers are major sources of waveform distortions (Deb et al., 2017; Kadurek et al., 2009; Li & Jenn, 2024; Veldman & Verzijlbergh, 2015).

These distortions are generally categorized into several types:

- **Current Harmonics:** Generated by EVSE (Electric Vehicle Supply Equipment) transducers, these can lead to component overheating and reduced system efficiency (Deb et al., 2017).
- **Supraharmonics:** Distortions in the 2 kHz to 150 kHz range, induced by high-frequency switching in modern chargers, affect sensitive electronic devices and exacerbate thermal stress.
- **Voltage Sags and Swells:** The rapid start-up of EV loads can cause voltage sags (0.1–0.9 pu), risking data loss and equipment damage, while sudden disconnections can trigger voltage swells (1.1–1.4 pu) that may lead to hardware failure (Saha et al., 2021).
- **Power Losses:** The increase in the RMS value of grid line current due to EV charging has been shown to elevate grid losses by approximately 40% during off-peak hours and up to 62% during peak charging periods (Roy et al., 2023).

2.1.3 Transformer and Infrastructure Degradation

One of the most critical long-term impacts of EV integration is the accelerated aging of distribution assets, specifically power transformers. The high active power demand from Level 2 chargers significantly increases the transformer's hot-spot temperature (HST), which is the primary driver of winding insulation degradation (Roy et al., 2023). Probabilistic assessments using tools like "HotSpotter" demonstrate that unmanaged charging, particularly on smaller 10–25 kVA transformers common in residential areas, can lead to frequent overloading (Roy et al., 2023).

The relationship between transformer loading and life-cycle reduction is exponential; for example, a persistent 150% load can result in an aging acceleration factor (FAA) of 18.65, meaning the asset ages 18 times faster than under nominal conditions (Roy et al., 2023). In rural or poorly planned urban grids, where transformers were originally sized for minimal lighting loads, the addition of a single EV can exceed nameplate capacities, forcing early replacement of expensive equipment (Roy et al., 2023). Mitigation strategies, such as Time-of-Use (TOU) rates, have proven effective at reducing HST by shifting loads to night hours, though uncoordinated "timer-peaks" immediately following the start of off-peak periods can create secondary stress events (Birk Jones et al., 2022; Roy et al., 2023)

2.1.4 Modeling Methodologies: Empirical Data vs. Bottom-Up Simulations

Assessing the impact of EVs requires robust modeling frameworks, which have evolved from simplistic assumptions to complex, data-driven simulations. Most existing literature relies on bottom-up simulation modeling, which utilizes stochastic processes or trip-chain analysis to chain independent origin-destination trips together (Birk Jones et al., 2022). Tools like "EVI-Pro" and "Caldera" employ agent-based approaches to represent each EV as an individual load, allowing researchers to quantify impacts on line loading and voltage violations across diverse feeder compositions (residential, commercial, and industrial) (Birk Jones et al., 2022).

However, a critical gap exists between simulated predictions and actual consumer behavior. Empirical studies leveraging high-frequency smart meter data have revealed that simulations often over-estimate both the environmental benefits and system costs of in-home charging (Qiu et al., 2022). For instance, a study of 1,600 EV homes in Arizona utilized a difference-in-differences (DID) approach and found that actual load changes were smaller than predicted due to "rebound effects" in driving where consumers drive more after adopting an EV, resulting in less home electricity use during specific hours (Qiu et al., 2022). Furthermore, methodological refinements suggest that EV charging assessments require high-resolution data; using time steps of 10 minutes or lower, determined via Bootstrap distribution analysis, is essential for achieving a confidence interval of 95% or higher in grid impact results (Demirci et al., 2023; Jenn & Highleyman, 2022). Combining travel demand models with empirical charging records remains the gold standard for projecting future grid requirements at

high granularity (Li & Jenn, 2024).

2.2 Electric Cooking (e-Cooking): Technologies, Habits, and Demand

2.2.1 Transition from Traditional Fuels: Economics and Environmental Benefits

The transition from traditional biomass and fossil fuels to electric cooking (e-cooking) is increasingly recognized as a cornerstone of sustainable development and energy sovereignty in the Global South (Malla et al., 2025; Odoi-Yorke, 2024). Globally, nearly 2.4 billion people continue to rely on inefficient and polluting fuels for their daily cooking needs, resulting in approximately 4 million premature deaths annually due to household air pollution (HAP) (Scott et al., 2024). In Nepal, unprocessed solid biomass fuels remain the primary energy source for approximately 60% of households, while urban centers have seen a rapid uptake of imported Liquefied Petroleum Gas (LPG) (Bhandari & Pandit, 2018; Malla et al., 2025). This reliance on biomass not only contributes to deforestation and forest degradation but also releases significant amounts of black carbon and CO2, which are critical drivers of climate change (Clements et al., 2020a; Odoi-Yorke, 2024).

From a macroeconomic perspective, substituting imported LPG with domestically produced hydropower offers a pathway to reducing trade deficits and enhancing energy security (Bhandari & Pandit, 2018; Jha et al., 2025). For instance, in the fiscal year 2023/24, Nepal imported LPG worth NRs 55.6 billion, accounting for 3.5% of the country's total import bill (Malla et al., 2025). Shifting toward e-cooking could save between $21.8 million and $70.8 million annually, providing essential capital for future large-scale renewable energy projects (Bhandari & Pandit, 2018). At the household level, while electricity is often perceived as more expensive, empirical studies demonstrate that it is frequently cheaper than fossil fuels and comparable to charcoal when labor costs for fuel collection are included (Clements et al., 2020a; Scott et al., 2024). Furthermore, when external social costs particularly the health impacts of PM2.5 are factored in, electricity emerges as the most cost-effective cooking option for society (Malla et al., 2025).

2.2.2 Appliance Efficiency: Comparative Analysis of e-Cooking Technologies

The technical feasibility and economic viability of e-cooking are heavily dependent on the thermal efficiency of the appliances utilized. Modern electric cooking devices can be classified into three distinct categories based on their heat transfer mechanisms:

- **Pressurized Cooking (Electric Pressure Cookers - EPCs):** EPCs are identified as the most efficient electric cooking technology, combining insulation, automated temperature control, and high-pressure operation (Scott et al., 2024). By reaching boiling points above 112 °C, EPCs deliver a different "cooking service" that significantly reduces cooking time and energy consumption (Scott et al., 2024). Studies indicate that charcoal stoves use 15 times more energy than an EPC to cook the same meal, and EPCs can save over 40% of energy compared to standard resistive hotplates (Saha et al., 2021; Scott et al., 2024).
- **Direct Heating (Induction Hobs and Rice Cookers):** Induction hobs use high-frequency magnetic fields to directly heat ferromagnetic cookware, achieving efficiencies of approximately 84% to 90% (Guayanlema et al., 2024; Lombardi et al., 2019). This direct energy coupling eliminates thermal losses from hot surfaces not in contact with the pot (Scott et al., 2024). Similarly, rice cookers utilize direct heating and insulation, typically saving about 20% of energy compared to hotplates (Scott et al., 2024).
- **Hot Surface Hobs (Resistive Hotplates and Infrared Stoves):** These appliances use electrical resistance to heat a surface onto which a pot is placed. Conventional resistive coil hotplates are the least efficient, with measured efficiencies ranging from 50% to 72% depending on pot-to-surface contact (Scott et al., 2024). Infrared hobs offer only marginal improvements over hotplates and are generally classified alongside other inefficient thermal surface devices(Scott et al., 2024).

2.2.3 Load Profile Characteristics and the "Peak Coincidence" Problem

The integration of e-cooking onto distribution grids introduces a complex load synchronization challenge known as the "peak coincidence" problem (Clements et al., 2020a). Household cooking activities in regions like Nepal and Tanzania typically exhibit two distinct peaks: a morning peak between 5:00 AM and 9:00 AM and an evening peak between 5:00 PM and 9:00 PM (Clements et al., 2020a). These cooking windows almost perfectly align with existing residential peak demand for lighting and entertainment, compounding the stress on distribution assets (Clements et al., 2020a; Kafle, 2025b)

Empirical data from rural Nepali mini-grids show that even a small number of induction cookers can push a system to its full capacity, causing frequent brownouts where voltages drop below 150 V, making cooking virtually impossible [Clements et al., 2020; Silwal et al., 2020]. High-resolution stochastic modeling reveals that induction stoves can triple the peak power requirement of a residential feeder, passing from 6 kW to over 30 kW in community-scale simulations [Lombardi et al., 2019; Sacchi, 2018]. This phenomenon establishes a "peak-feasibility constraint," where low average energy consumption (kWh) coexists with high peak demand (kVA) that exceeds local transformer ratings (Kafle et al., 2026).

Furthermore, traditional cooking habits often involve "fuel stacking," where households use electricity for quick tasks like boiling water but revert to biomass for energy-intensive dishes like beans or flatbreads (chapati) (Clements et al., 2020a). While stacking reduces the total energy demand on the grid, it does not necessarily mitigate the instantaneous peak demand if cooking tasks still coincide with the evening peak (Kafle et al., 2026; Lombardi et al., 2019). Behavioral change strategies, such as shifting meal preparation windows to midday when solar generation is abundant, offer potential for peak shaving, though their success relies heavily on consumer education and the use of efficient, insulated appliances like EPCs (Malla et al., 2025; Shrestha et al., 2024).

2.3 Demand Side Management (DSM) and Mitigation Strategies

The integration of high-power electrified loads, such as electric vehicle (EV) charging stations and induction cooktops, necessitates a transition from passive grid management to active Demand Side Management (DSM) strategies (Kene & Olwal, 2023; Odoi-Yorke, 2024). DSM encompasses a range of technologies and policies designed to influence the timing and magnitude of consumer electricity use, ensuring that new demand does not compromise grid stability or require prohibitively expensive infrastructure upgrades (Amir et al., 2024; Birk Jones et al., 2022; Lombardi et al., 2019). These strategies are particularly vital for mitigating the "peak coincidence" problem, where the simultaneous operation of EVs and e-cooking appliances threatens to exceed the thermal and voltage limits of existing distribution transformers (Birk Jones et al., 2022; Malla et al., 2025).

2.3.1 Time-of-Use (TOU) Pricing: Effectiveness and Behavioral Response

Time-of-Use (TOU) pricing is an established mechanism for load shifting, utilizing variable cost structures to incentivize customers to move high-energy activities to off-peak periods (Birk Jones et al., 2022). In the context of electric mobility, empirical evidence from a large-scale study of 1,600 EV households in Arizona demonstrated that consumers are highly responsive to price signals (Qiu et al., 2022). These households significantly increased their charging duration during "super off-peak" hours (typically 11:00 PM to 5:00 AM) when rates were lowest, effectively flattening the residential load profile (Qiu et al., 2022). Similarly, TOU rates have been shown to reduce peak load demand on distribution feeders by approximately 5%, provided that charging start times are not perfectly synchronized (Birk Jones et al., 2022).

However, the implementation of TOU pricing introduces a critical technical risk known as the "timer-peak" or "TOU Immediate" problem (Birk Jones et al., 2022). If a large number of EVs are programmed to begin charging exactly when an off-peak rate commences (e.g., at midnight), the resulting surge in demand can create a secondary peak that is more intense than the original evening peak (Birk Jones et al., 2022; Jenn & Highleyman, 2022). Simulation studies indicate that such uncoordinated "immediate" charging can increase peak demand on residential feeders by as much as 20%, potentially causing transformer overloading and voltage violations (Birk Jones et al., 2022). For e-cooking, the effectiveness of TOU pricing is often more constrained by social factors; while households may shift laundry or EV charging to night hours, the temporal flexibility of meal preparation is limited by cultural habits and hunger, requiring more sophisticated interventions beyond simple pricing signals (Lombardi et al., 2019; Odoi-Yorke, 2024).

2.3.2 Managed Charging and Smart Cooking: Randomized Start Times and "GridShare" Technologies

To address the limitations of static TOU pricing, managed charging and "smart" cooking technologies employ active control to distribute load more evenly. One highly effective strategy is the randomization of charging start times (Birk Jones et al., 2022). By using on-vehicle or charger-based software to randomly assign start times within an off-peak window, utilities can prevent the "immediate" demand spike, ensuring that EV loads are spread out over several hours (Birk Jones et al., 2022). This approach has been

found to match the line-loading performance of a grid with no EVs at all, making it the most robust method for minimizing infrastructure strain (Birk Jones et al., 2022).

In the residential cooking sector, the "GridShare" technology provides a compelling example of smart DSM for weak grids (Clements et al., 2020a). Tested in a micro-hydropower mini-grid in Bhutan, the GridShare device communicates the real-time state of the grid to households through a simple LED interface (Yangka & Diesendorf, 2016). If the grid is near capacity, the device alerts users, and in some configurations, it can temporarily curtail power to high-load appliances like rice cookers (Clements et al., 2020a; Yangka & Diesendorf, 2016). The results were transformative, reducing the number and duration of severe brownouts by over 92% and encouraging 42% of respondents to intentionally shift their cooking times (Yangka & Diesendorf, 2016). Such community-based agreements and "staggered" appliance rollout strategies are essential for allowing low-amperage distribution networks to support the high-power requirements of induction stoves (Leary et al., 2022; Malla et al., 2025).

2.3.3 Vehicle-to-Grid (V2G) and Energy Storage: EVs as Flexible Grid Resources

The most advanced DSM strategy involves transforming EVs from passive loads into active grid resources through **Vehicle-to-Grid (V2G)** technology (Demirci et al., 2023; Morais et al., 2014). Because EVs remain parked for approximately 90% to 95% of the day, their onboard battery banks represent a massive, underutilized source of decentralized energy storage (Demirci et al., 2023; Jenn & Highleyman, 2022). V2G allows for bidirectional power flow, enabling EVs to discharge energy back into the grid during peak demand periods or to stabilize frequency and voltage (Deb et al., 2017; Demirci et al., 2023)]. This flexibility can substantially reduce the need for centralized spinning reserves and peaker power plants, which often remain idle for 90% of the year (Jenn & Highleyman, 2022).

From a technical perspective, V2G can provide critical ancillary services, including:

- **Peak Load Shaving:** Discharging batteries during evening peaks to reduce the burden on distribution transformers (Deb et al., 2017; Morais et al., 2014).
- **Voltage Regulation and Reactive Power Compensation:** Shunt-connected EVs can inject reactive power to improve voltage profiles and reduce line losses (Demirci et al., 2023).

- **Renewable Energy Integration:** Storing excess solar or wind energy produced during the day (valley filling) and releasing it when generation drops, thereby mitigating the intermittency of renewable sources (Jenn & Highleyman, 2022).

Despite this potential, widespread V2G adoption faces significant hurdles. Chief among these is **battery degradation**, as the additional charge-discharge cycles required for grid support can shorten the operational life of the vehicle's battery (Kene & Olwal, 2023). Furthermore, only about 40% of the EV fleet may be plugged in simultaneously at any given time, limiting the total capacity available for large-scale grid events (Jenn & Highleyman, 2022). For V2G to become commercially viable, utilities must develop business models that provide sufficient revenue for EV owners to offset degradation costs while addressing consumer concerns regarding "range anxiety" and privacy (Jenn & Highleyman, 2022; Kene & Olwal, 2023). Combined with local energy storage systems (BESS), V2G represents a cornerstone of the future "smart grid" that can sustain both clean cooking and clean mobility without catastrophic grid failure (Odoi-Yorke, 2024).

2.4 Integrated Load Forecasting and Scenario Analysis

2.4.1 Advanced Forecasting Methodologies: Stochastic and Neural Network Approaches

The inherent variability of electrified loads driven by human behavior, weather, and socio-economic factors necessitates the shift from deterministic models to probabilistic and machine learning-based forecasting (Jenn & Highleyman, 2022; Sinha et al., 2023). Modern load forecasting is generally categorized into bottom-up simulation and empirical data-driven modeling (Li & Jenn, 2024). Central to bottom-up simulations is the Monte Carlo (MC) method, which allows researchers to account for the stochastic nature of vehicle arrival times, initial state of charge (SoC), and the duration of cooking tasks (Roy et al., 2023). By iteratively sampling from probability distribution functions, MC simulations can generate high-resolution synthetic datasets of thousands of electric vehicles (EVs) and households, providing a robust statistical foundation for impact assessments at the transformer level (Yangka & Diesendorf, 2016).

Recent advancements in Artificial Neural Networks (ANN) have significantly improved the accuracy of short-term load forecasting (STLF) by capturing non-linear relationships that traditional regression models often overlook (Kene & Olwal, 2023;

Miri et al., 2021). In particular, Recurrent Neural Networks (RNNs), specifically Long Short-Term Memory (LSTM) and Gated Recurrent Unit (GRU) architectures, have proven highly effective in predicting EV charging load variations and residential demand profiles (Alizadegan et al., 2025; Ghanbari & Borna, 2021; Waqas & Humphries, 2024). These models utilize historical datasets, including weather variables and consumption patterns, to minimize Root Mean Square Error (RMSE) in load predictions. Furthermore, hybrid optimization strategies, such as combining GRU-NN with Genetic Algorithms (GA) or Particle Swarm Optimization (PSO), allow for the simultaneous optimization of network stability and energy cost minimization (Zheng et al., 2017).

2.4.2 Scenario-Based Modelling: BAU, Sustainable Development, and Net-Zero Pathways

To evaluate long-term energy transitions, researchers employ multi-scenario frameworks, typically modeled using platforms like LEAP (Long-range Energy Alternative Planning), OSeMOSYS, and MARKAL (Bhandari & Pandit, 2018; Kafle, 2025a; Yangka & Diesendorf, 2016)]. These scenarios serve as "pathways" to explore how different policy interventions impact the grid:

- **Business-as-Usual (BAU):** This scenario represents the continuation of current trends without major policy shifts. In the context of Nepal, BAU trajectories suggest a persistent 50% reliance on biomass and a tripling of imported fossil fuels by 2035, leaving the nation vulnerable to international energy price shocks (Bhandari & Pandit, 2018; Kafle et al., 2026).
- **Sustainable Development (SD/NDC):** Aligned with Nationally Determined Contributions (NDCs), this pathway accelerates the adoption of clean cooking and electric mobility. Forecasts for Nepal suggest that an NDC-aligned push could reduce fossil fuel imports by 80% by 2035, shifting a third of the total energy demand to the national grid (Kafle et al., 2026; *Nationally Determined Contribution (NDC) 3.0 Government of Nepal Kathmandu*, 2025).
- **Net-Zero Emissions (NZE/LTS):** The most ambitious pathway, consistent with a 2045–2050 target, envisions near-total electrification of the transport and residential sectors (Jha et al., 2025; Kafle, 2025b). This scenario requires a massive build-out of renewable capacity estimated at 28-30 GW for Nepal to

sustain a per-capita electricity consumption increase of five times current levels.

2.4.3 Synergistic Impacts: Combined Load Patterns on Distribution Feeders

The most critical challenge in modern power system planning is the synchronization of new high-power loads (Birk Jones et al., 2022; Jenn & Highleyman, 2022)]. When analyzing the synergistic impacts of EVs and e-cooking, researchers have identified a "compounding effect" on residential feeders (Clements et al., 2020b; Li & Jenn, 2024). Load synchronization occurs because both charging and cooking behaviors are influenced by standard work-life cycles; for instance, the return from work often triggers both the connection of an EV to a home charger and the commencement of evening meal preparation (Li & Jenn, 2024).

Empirical evaluation of over 5,000 feeders reveals that the timing of peak demand is a product of local land-use and building types (Li & Jenn, 2024). Feeders in residential areas experience a dramatic "night peak" due to the synergy between baseload lighting and home-dominant EV charging, while commercial feeders may peak in the afternoon due to workplace charging (Li & Jenn, 2024). For weak grids in the Global South, this synchronization can be catastrophic; stress tests indicate that even at 25% coincidence, the combined load of induction stoves and basic household needs can exceed the rated capacity of local 50 kVA transformers (Clements et al., 2020a; Malla et al., 2025)

This creates a distribution-planning failure where system operators may perceive "spare capacity" based on low average monthly energy (kWh) consumption, while failing to account for the peak apparent power (kVA) requirements of coincident high-load appliances (Malla et al., 2025). Consequently, the integration of these dual sectors must be managed as a distribution-readiness problem rather than just a generation issue, requiring coordinated infrastructure reinforcement, time-series hosting capacity (TSHC) analysis, and staggered load control to ensure the grid does not become a bottleneck for the energy transition (Malla et al., 2025; Roy et al., 2023).

2.5 The Context of Nepal: Opportunities and Structural Constraints

2.5.1 Hydropower Potential vs. Distribution Weakness: The Paradox of Grid Readiness

Nepal occupies a unique position in the global energy transition, possessing an immense theoretical hydropower potential of approximately 83,000 MW, of which 42,000 MW

is considered commercially exploitable (Adhikari et al., 2020; Jha et al., 2025; Malla et al., 2025)]. As of the 2024/25 fiscal year, the country's total installed capacity has reached 3,591 MW, representing a fourfold increase since 2011, yet this still utilizes less than 10% of the nation's technically feasible resources [Kafle, 2025]. In pursuit of energy sovereignty and decarbonization, the Government of Nepal has articulated an ambitious "Energy Development Roadmap," setting targets to achieve 14,000 MW of generation by 2030 and 28,500 MW by 2035 (*Nationally Determined Contribution (NDC) 3.0 Government of Nepal Kathmandu*, 2025). However, the successful leveraging of this "white gold" is fundamentally constrained by a fragile and under-capacitated distribution network, creating a stark "access-use paradox" (Kafle et al., 2026).

While Nepal has achieved nearly universal electricity access, with 98% of the population connected to either the national grid or isolated off-grid systems, this access is often defined by minimal service capability (*NEPAL ELECTRICITY AUTHORITY*, n.d.). Approximately 90% to 95% of residential connections in Nepal are restricted to a 5-ampere (A) single-phase service, which provides a sanctioned capacity of only about 1.1 kVA (Shrestha et al., 2024). This capacity is sufficient for basic lighting and low-power communication devices but is structurally inadequate for the thermal loads required by modern induction stoves (typically 2 kW) or Level 2 electric vehicle (EV) chargers (Scott et al., 2024). To support stable electric cooking, planners suggest that household connections must be upgraded to a minimum of 15A, yet current infrastructure investments remain focused on generation and high-voltage transmission rather than last-mile distribution readiness (Shrestha et al., 2024).

The technical implications of this distribution weakness are most evident at the transformer level. Stress-testing simulations in rural settlements demonstrate that even a 25% coincidence rate for induction cooking among 82 households can push a 50 kVA transformer to its maximum rated capacity (Kafle et al., 2026). At higher adoption levels, the coincident demand for cooking and EV charging creates step changes in apparent power (kVA) that lead to severe voltage instability and frequent brownouts, where voltages drop below 150 V, rendering induction appliances non-functional (Clements et al., 2020b; Kafle et al., 2026). Consequently, without a coordinated "readiness screen" that evaluates transformer headroom and connection amperage, the promotion of high-load appliances risks regressive impacts, including asset degradation

and bill shocks for low-income households (Malla et al., 2025).

2.5.2 Policy Landscape: Analysis of E-Mobility and Clean Cooking Targets

Nepal's policy framework for energy transition is characterized by high-level ambition tempered by inconsistent implementation and fiscal volatility. The foundational document for the transportation sector, the National Action Plan for Electric Mobility (2018), aims to halve fossil fuel consumption by 2050 and proposes the establishment of dedicated institutions for financing e-mobility (Jha et al., 2025; *Nationally Determined Contribution (NDC) 3.0 Government of Nepal Kathmandu*, 2025). This is complemented by the Second Nationally Determined Contribution (NDC), which sets specific milestones for 2025 and 2030, including ensuring that 25% of all private vehicle sales and 20% of public transport sales are electric by 2025, rising to 90% and 60% respectively by 2030 (Mali et al., 2022). Despite these targets, the market remains volatile due to fluctuating fiscal policies; for instance, customs and excise duties on private EVs have seen drastic year-on-year changes, such as a 5% increase in excise duty for vehicles up to 50 kW in 2024, which undermines consumer confidence (Jha et al., 2025).

In the residential sector, clean cooking targets are equally robust but face similar implementation hurdles. The government's Long-Term Strategy (LTS) for Net-Zero Emissions envisions carbon neutrality by 2045, supported by a target to ensure that 25% of households use electric stoves as their primary cooking method by 2030 (Shrestha et al., 2024). Specific initiatives, such as the "Women's First Program" and the "Quit LPG Connect Electricity" campaign, aim to distribute 1 million electric stoves by 2029 (Malla et al., 2025). However, the actual use of electricity for cooking remains critically low at less than 1% of total households, far behind the target of 7% set for 2021 (Malla et al., 2025).

Policy analysis reveals significant "implementation gaps" where high-level goals are not backed by detailed technical roadmaps for grid reinforcement or standardized charging infrastructure. Furthermore, financial barriers persist; while the Nepal Rastra Bank (NRB) initially allowed for 80% financing of personal EVs, this limit was recently reduced to 60%, even as financing for conventional internal combustion engine (ICE) vehicles was increased to 60%, effectively equalizing the lending terms and removing a key incentive for EV adoption (Jha et al., 2025). To bridge these gaps,

researchers emphasize the need for a "one-window policy" that integrates tax incentives, tariff adjustments (such as time-of-use pricing), and mandatory standard-setting for appliances and charging stations to ensure that Nepal's policy ambitions translate into a resilient, low-carbon (Jha et al., 2025; Mali et al., 2022).

2.6 Research Gaps and Synthesis

2.6.1 The Decoupling of Electrification Sectors in Existing Literature

A fundamental gap identified in current energy transition scholarship is the thematic and methodological decoupling of electric mobility and clean cooking sectors [Kafle et al., 2025]. While both domains are recognized as vital pillars for achieving Sustainable Development Goal 7 (SDG 7), they are predominantly treated as separate policy and technical siloes (*Sustainable Development Goals | United Nations Development Programme*, n.d.). Existing Energy System Optimization Models (ESOMs) for Low- and Middle-Income Countries (LMICs) typically focus on cost and emission outcomes at a national or wholesale level, often leaving the granular, simultaneous impact of these two burgeoning loads on local distribution assets unexplored (Li & Jenn, 2024). This research fragmentation is particularly problematic given the shared objective of these sectors to substitute fossil fuels with renewable electricity, which creates a competitive and synergistic demand for limited grid capacity (Odoi-Yorke, 2024).

2.6.2 Scarcity of Combined Impact Studies on Distribution Assets

The most critical research gap lies in the lack of combined studies assessing both EV and e-cooking on the same distribution assets in the Global South (Lombardi et al., 2019). Most grid integration literature focuses either on the technical challenges of EV charging (Roy et al., 2023) or the feasibility of e-cooking (Lombardi et al., 2019; Scott et al., 2024). However, because both charging behaviors and cooking cycles are governed by standard residential work-life patterns, they are likely to exhibit high temporal synchronization (Clements et al., 2020b; Li & Jenn, 2024).

In the unique context of Nepal, where residential infrastructure is often limited to 5-ampere (A) connections, the introduction of just one of these loads such as a 2 kW induction stove can already exceed sanctioned household capacity (Clements et al., 2020a). There is a complete dearth of research that quantifies the compounded hourly load profiles when an EV and multiple induction stoves are integrated onto a single 50 kVA or 100 kVA distribution transformer in a developing nation (Roy et al., 2023).

Without this integrated analysis, system operators may miscalculate "distribution-grid readiness," risking localized blackouts and accelerated asset degradation (Kafle et al., 2026).

2.6.3 Methodological Gap: From Monthly Energy to Hourly Coincident Peak

Literature analysis reveals a persistent "distribution-planning failure" where assessments rely on monthly energy consumption (kWh) rather than hourly peak apparent power (kVA). In suppressed-demand systems like rural Nepal, households may have low average energy use, suggesting spare capacity to planners, yet the step changes in demand caused by coincident cooking and charging tasks can exceed the peak feasibility of the network (Kafle et al., 2026).

Furthermore, while bottom-up simulations are common, there is a lack of empirical validation for these models in the Global South (Jenn & Highleyman, 2022). As demonstrated by empirical studies in more developed markets, actual consumer behaviors—such as the "rebound effect" in driving or irregular plug-in frequencies often deviate significantly from theoretical predictions (Qiu et al., 2022). There is an urgent need for high-resolution studies that utilize 10-minute interval data to capture the stochastic nature of these dual loads in LMIC settings where the margin for error in grid stability is significantly lower (Jenn & Highleyman, 2022).

2.6.4 The "Access-Use Paradox" and Distribution Bottlenecks

Recent synthesis of the Nepali energy sector highlights the "access-use paradox," where near-universal grid connection (98%) coexists with a persistent reliance on biomass and LPG (99%) for cooking. This gap exists because electrification has been delivered as a "coverage-driven" intervention rather than a "service-ready" one. While Nepal's generation goals are ambitious targeting 28,500 MW by 2035 the distribution network remains a primary bottleneck.

The literature lacks a unified framework that evaluates "grid readiness" as a multi-criteria problem involving:

- **Connection Amperage:** Upgrading 5A to 15A or 30A service (Shrestha et al., 2024).
- **Transformer Headroom:** Analyzing load coincidence factor (CF) at the neighborhood level (Kafle et al., 2026).

- **Tariff Design:** Mitigating "bill shocks" for low-income households transitioning to high-load appliances(Malla et al., 2025).
- **Asset Degradation:** Quantifying the thermal aging of transformers under combined EV-cooking stress (Roy et al., 2023).

2.6.5 Synthesis: The Need for an Integrated Scenario-Based Study

To address these multifaceted gaps, this study proposes a scenario-based hourly load forecasting approach that explicitly bridges the transport and residential cooking sectors. By modeling the combined impact on specific distribution feeders, the study moves beyond the "appliance-only" diffusion focus and treats clean cooking and mobility as a distribution-planning and affordability problem. This synthesis is vital for moving from a "coverage-led" to a "service-ready" electrification paradigm, ensuring that Nepal’s vast hydropower potential can be leveraged without compromising grid reliability or social equity.

CHAPTER THREE: RESEARCH METHODOLOGY

3.1 Research Design and Computational Framework

This research develops a multi-stage forecasting and load disaggregation framework to assess the impact of electric cooking and electric mobility on future grid demand. The methodology is intentionally hierarchical. First, annual electricity demand drivers are forecasted at the macro level. Second, annual energy demand is decomposed into baseline demand, electric cooking demand, and electric vehicle demand. Third, annual targets are translated into daily and hourly load patterns using a physics-informed recurrent forecasting framework. Finally, an appliance-level disaggregation model is employed to estimate the temporal contribution of electric cooking within the aggregate load profile.

The complete methodology is not a single model, but an integrated pipeline composed of four main computational blocks:

1. Annual macro-driver and baseline demand forecasting using baseline_disaggregation_forecast.py.
2. Hourly load model training with energy consistency constraints using pinn_train.py.
3. Recursive generation of future daily and hourly profiles using pinn_forecast.py.
4. Electric cooking load disaggregation and cooking-share estimation using model_v2.py.

This chapter documents each block in formal detail so that the full computational workflow can be reproduced from the dissertation alone.

The methodology offers several strong features. First, it separates structural baseline demand from electrification-driven demand, which improves interpretability. Second, it combines annual-scale scenario planning with daily-scale and hourly-scale temporal modeling. Third, the PINN design embeds an energy-balance principle into the recurrent forecasting model. Fourth, the cooking disaggregation model does not rely on black-box decomposition alone; instead, it incorporates stove stock growth, bounded usage intensity, and a normalized temporal allocation mechanism.

The methodology is therefore not a single predictive algorithm but a layered

computational architecture that moves from annual energy planning to intra-day demand behavior. This structure makes it suitable for assessing not only future electricity consumption but also the timing, shape, and peak-demand implications of electrification.

3.2 Overall Methodological Structure

The methodological structure adopted in this dissertation is shown in Figure 1.

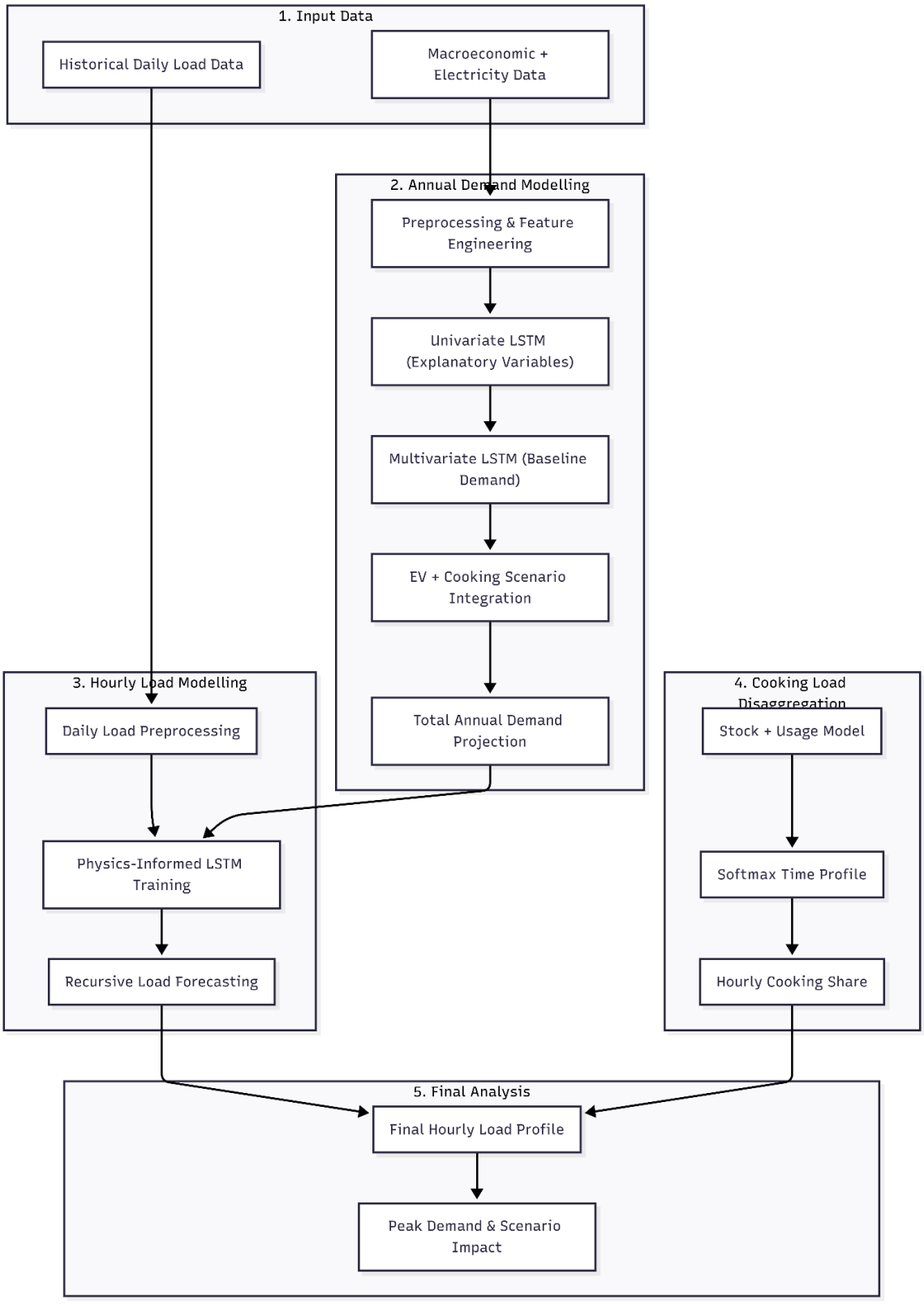

Figure 1: Overall dissertation workflow

The research workflow is therefore both top-down and bottom-up. It is top-down because annual energy expectations constrain the forecasting pipeline. It is bottom-up

because end-use behavior, particularly cooking usage patterns, is modeled at sub-daily resolution and then mapped back to total load and peak demand.

3.3 Data Inputs and Variable Definition

3.3.1 Annual-scale explanatory variables

The annual forecasting stage uses historical socioeconomic and electricity indicators stored in the annual dataset. The primary explanatory variables included in the implemented code are:

- Gross Domestic Product (GDP)
- Total population
- Urban population by percentage
- Electricity consumption per capita
- Electricity access
- Induction cooker energy
- Electric vehicle energy demand

The target variable for the annual forecasting stage is the historical total electricity demand. However, the implemented methodology first constructs a baseline demand component by removing the historical electric cooking and EV components from total demand.

The implemented decomposition is:

$$E_{\text{base},t} = E_{\text{total},t} - E_{\text{cook},t} - E_{\text{EV},t} \tag{3.1}$$

where:

- $E_{\text{base},t}$ is the baseline annual electricity demand in year t,
- $E_{\text{total},t}$ is the observed total annual electricity demand,
- $E_{\text{cook},t}$ is annual electric cooking energy demand,
- $E_{\text{EV},t}$ is annual electric vehicle electricity demand.
- All units are in TWh

This formulation isolates the underlying non-electrification-related demand trend so

that the baseline forecasting model is not forced to learn policy-driven electrification demand as part of ordinary structural growth.

3.3.2 Daily and hourly load data

The sub-annual stage uses the file 3yrdata_smoothed_11500gwh.csv, which stores daily demand observations across 31 time intervals per day. In the implemented code, the first column is a day index and the remaining 31 columns correspond to intra-day demand values. These intervals are not assumed to be uniformly spaced; instead, interval durations are explicitly computed from the time labels and used in energy integration steps. This design is important because it allows the annual energy constraint to operate on physically meaningful integrated load rather than merely on pointwise averages.

3.3.3 Daily cooking-demand data representation

The electric cooking disaggregation model uses the same 31-point intra-day representation and combines it with:

- Synthetic or reconstructed daily stove sales
- Cumulative active stove stock
- Calendar features
- Daily load profile observations

The cooking model therefore operates as an end-use reconstruction framework embedded within the daily load structure.

3.4 Data Preprocessing and Feature Engineering

3.4.1 Chronological ordering and deterministic reproducibility

Before model development, all annual records are sorted chronologically by year. Random seeds are fixed for NumPy and PyTorch to reduce variability in optimization and improve experiment reproducibility. The code explicitly sets deterministic seeds where required for repeatable training.

3.4.2 Scaling and normalization

Separate MinMax scaling is applied in different parts of the pipeline. At the annual forecasting level, individual explanatory variables are scaled independently before

training the corresponding univariate LSTM models. The multivariate baseline model also operates on scaled feature vectors. For the hourly PINN stage, the entire daily demand matrix is scaled before sequence construction, and the fitted scaler is stored using joblib for later inverse transformation during forecasting.

MinMax normalization is expressed as:

$$x_i^* = \frac{x_i - x_{min}}{x_{max} - x_{min}} \tag{3.2}$$

where:

- $x_i^*$is the normalized value
- $x_i$is the original observation

For some annual demand calculations, the target series is transformed using the natural logarithm before scaling in order to stabilize growth behavior and reduce the dominance of large absolute values. This is implemented in the baseline annual demand model as:

$$z_t = log\left(E_{base,t}\right) \tag{3.3}$$

and the LSTM is trained to predict the scaled version of (z_t).

3.4.3 Temporal encoding

The hourly forecasting model incorporates cyclical time features. In the code, the day index is transformed into day-of-week and month-like cyclical signals using sine and cosine functions. These are intended to preserve periodic continuity across temporal boundaries.

For a generic cycle length T, the cyclical transformation is:

$$x_{sin} = sin\left(\frac{2\pi t}{T}\right), x_{cos} = cos\left(\frac{2\pi t}{T}\right) \tag{3.4}$$

where; t is the particular day and T is cycle length

In the implemented models, these are used for:

- Day-of-week seasonality
- Month-level seasonality

- Day-of-year seasonality in the cooking disaggregation model

3.4.4 Derived features for annual demand forecasting

The annual baseline forecasting code introduces several methodological treatments to improve realism:

1. **Electricity access saturation**: future electricity access is hard-coded to 99%, reflecting near-saturation assumptions.
2. **Urban population monotonicity**: urban population percentage is modeled on the basis of first differences and constrained to maintain positive increments, ensuring a strictly increasing future path until saturation.
3. **Cooking energy scenario input**: future induction cooking energy is calculated from predefined cumulative stove sales values using a per-stove daily consumption assumption.
4. **EV energy scenario input**: future EV electricity demand is injected as scenario-driven annual values rather than being endogenously learned.

These treatments are not incidental coding shortcuts; they are explicit methodological assumptions used to embed policy and diffusion constraints into the forecasting process.

3.5 Stage I: Annual Macro-Driver and Baseline Demand Forecasting

This stage is implemented in baseline_disaggregation_forecast.py. The objective is to forecast annual electricity demand by first forecasting key explanatory variables and then using them to predict baseline demand.

3.5.1 Script-level flowchart for baseline_disaggregation_forecast.py

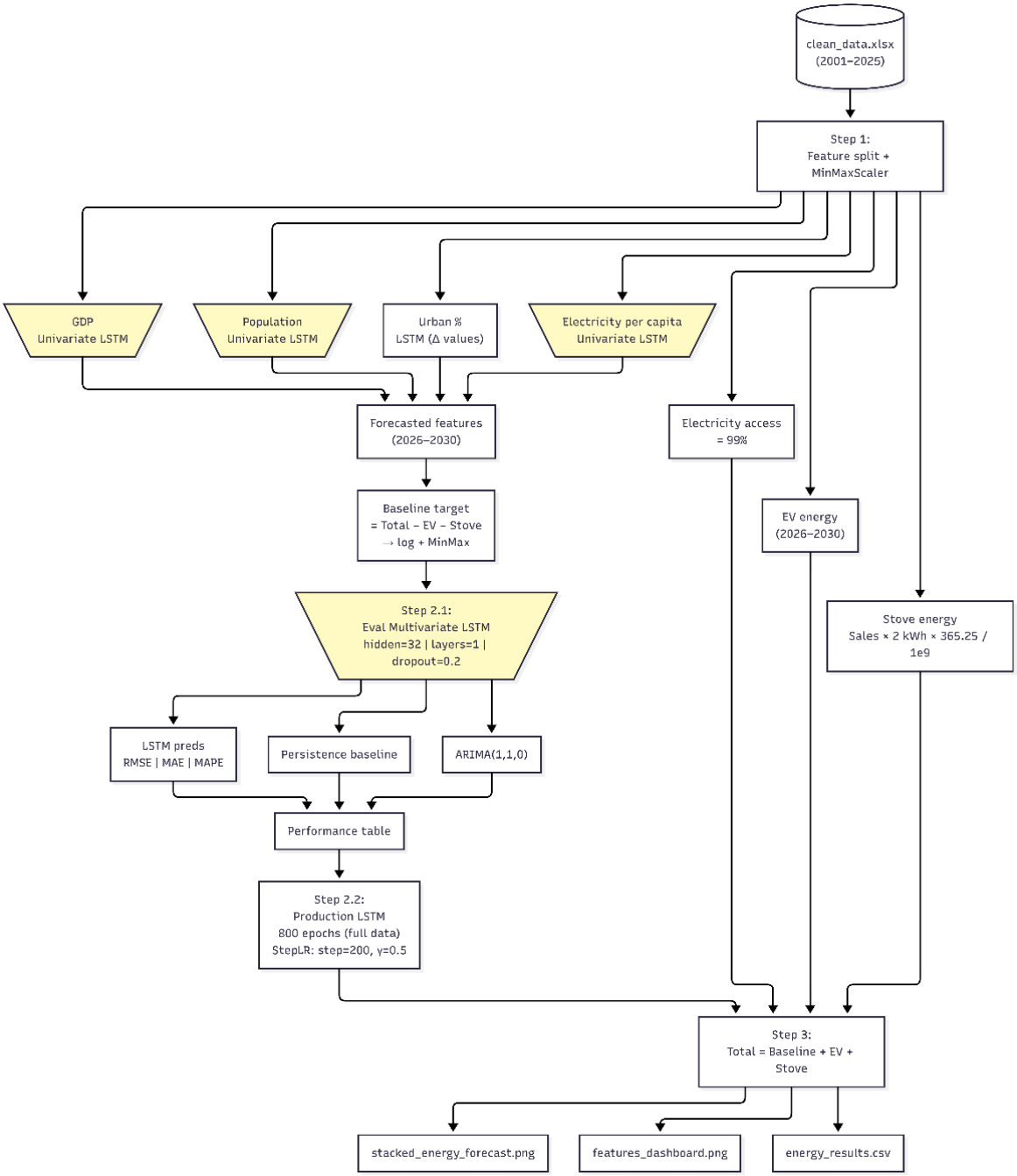

Figure 2: Annual Macro-Driver and Baseline Demand Forecasting model

3.5.2 Univariate forecasting of annual explanatory variables

The annual forecasting block trains a separate univariate LSTM for each feature that is not manually constrained. The implemented sequence generator uses a lookback window of 2 years. Thus, for a generic feature x_t, the training input-output mapping is:

$$[x_{t-2}, x_{t-1}] \rightarrow x_t \tag{3.5}$$

This is recursively extended for future forecasting. After each prediction, the newly predicted value is appended to the input window to forecast the next period.

The code uses a simple LSTM architecture for univariate forecasting:

- Input dimension = 1,
- Hidden units = 32,
- A fully connected hidden layer with 16 units,
- Relu activation,
- Final linear output layer.

The recurrent structure of the LSTM can be expressed through the standard equations:

$$\begin{aligned} f_t &= \sigma\left(W_f x_t + U_f h_{t-1} + b_f\right) \\ i_t &= \sigma(W_i x_t + U_i h_{t-1} + b_i) \\ \tilde{c}_t &= \tanh(W_c x_t + U_c h_{t-1} + b_c) \\ c_t &= f_t \odot c_{t-1} + i_t \odot \tilde{c}_t \\ o_t &= \sigma(W_o x_t + U_o h_{t-1} + b_o) \\ h_t &= o_t \odot \tanh(c_t) \end{aligned} \tag{3.6}$$

where f_t, i_t, and $o_t$are the forget, input, and output gates, respectively.

3.5.3 Scenario-based electric cooking energy construction

In this study, cumulative induction stove adoption is projected using a linear regression model fitted to historical adoption data. The resulting relationship is given by:

$$N_y = 196664x - 4 \times 10^8 \tag{3.7}$$

where:

- x = calendar year,
- N_y = cumulative number of electric cooking stoves in year y.

The projected adoption trajectory is calibrated to align with Government of Nepal targets, which envision approximately 2.1 million households adopting electric cooking by 2030.

The daily electricity consumption of each induction stove is estimated using LPG-to-electric energy equivalence. Based on literature values:

- One 14.2 kg LPG cylinder is consumed in 41.9 days,

- LPG cooking efficiency = 48.27%,
- Induction cooking efficiency = 88.62%.

After accounting for the difference in thermal efficiencies, the equivalent electricity requirement is estimated as:

- $e_{\text{unit}} = 2.36\text{kWh}$ per stove per day.

The annual electricity demand associated with electric cooking is then computed as:

$$E_{\text{cook},y} = \frac{N_y \times 2.36 \times 365.25}{10^9} \tag{3.8}$$

where:

- $E_{\text{cook},y}$= annual cooking electricity demand (TWh/year),
- N_y= cumulative stove stock.

This formulation converts projected appliance adoption directly into annual electricity demand while preserving a clear engineering basis.

3.5.4 Scenario-based EV energy construction

Electric vehicle electricity demand is estimated using a polynomial regression model fitted to historical and projected EV adoption data. The fitted equation is:

$$E_{\text{EV},y} = 0.003x^3 - 18.255x^2 + 36858x - 2 \times 10^7 \tag{3.9}$$

where:

- x= calendar year,
- $E_{\text{EV},y}$= annual electricity demand from EV charging (TWh/year).

The historical and projected EV adoption data used to derive this relationship are provided in the appendices.

This polynomial formulation captures the nonlinear acceleration of electric vehicle deployment and the corresponding increase in charging demand. The resulting annual EV electricity demand is subsequently added to the baseline demand forecast and disaggregated into hourly charging profiles for scenario-based load analysis.

3.5.5 Multivariate LSTM for baseline annual demand

Once the future macroeconomic features are generated, a multivariate Long Short-Term

Memory (LSTM) network is trained to forecast the annual baseline electricity demand, defined as the total electricity demand after excluding the contributions of electric cooking and electric mobility. In baseline_disaggregation_forecast.py, the baseline target is explicitly constructed as:

$$E_{\text{base},t} = E_{\text{total},t} - E_{\text{cook},t} - E_{\text{EV},t} \tag{3.10}$$

The input feature vector for each year consists of five macro-level explanatory variables:

1. Gross Domestic Product (GDP)
2. Total Population
3. Urban Population Percentage
4. Electricity Consumption per Capita
5. Electricity Access Rate

Let $X_t \in \mathbb{R}^5$ denote the macroeconomic feature vector at year t. A two-year lookback window is used, so the model learns the mapping:

$$[X_{t-2}, X_{t-1}] \rightarrow z_t \tag{3.11}$$

where:

$$z_t = \log(E_{base,t}) \tag{3.12}$$

The logarithmic transformation stabilizes the growth trend and improves learning performance. After prediction, the model output is inverse-transformed and exponentiated to recover the annual baseline demand in physical units (TWh/year).

The implemented architecture contains:

- One LSTM layer with input size equal to the number of macro features (m=5)
- Hidden state dimension h = 32 in the actual instantiated models used for evaluation and production
- Dropout layer with dropout rate of 0.2
- Fully connected layer with 16 neurons

- ReLU activation
- Final linear layer producing a single scalar output

The computational flow can be summarized as:

$$\hat{z}_t = W_2\,\mathrm{ReLU}(W_1\,\mathrm{Dropout}(h_t) + b_1) + b_2$$

where $h_t$is the final hidden state of the LSTM.

3.5.6 Validation against benchmark models

Before final production forecasting, the annual code evaluates the multivariate LSTM using a held-out test period consisting of the last five historical years. The code then compares LSTM predictions with two benchmark approaches:

1. **Persistence model**: assumes the next-year demand equals the previous observed value.
2. **ARIMA (1,1,0)**: used as a conventional statistical benchmark.

Prediction errors are evaluated using:

$$RMSE = \sqrt{\frac{1}{n}\sum_{i=1}^{n}(y_i - \hat{y}_i)^2} \tag{3.13}$$

$$MAE = \frac{1}{n}\sum_{i=1}^{n} |\, y_i - \hat{y}_i \,| \tag{3.14}$$

$$MAPE = \frac{100}{n}\sum_{i=1}^{n} \left| \frac{y_i - \hat{y}_i}{y_i + \epsilon} \right| \tag{3.15}$$

where ϵ is a small positive constant preventing division by zero.

This benchmarking is methodologically important because it demonstrates whether the deep learning model adds value beyond simple trend persistence and classical time-series modeling.

3.5.7 Final annual total demand reconstruction

After retraining the multivariate LSTM on the full historical set, future baseline demand is forecasted and then recombined with EV and cooking demand:

$$E_{\text{total},y} = E_{\text{base},y} + E_{\text{EV},y} + E_{\text{cook},y} \tag{3.16}$$

where; energy is in TWh

The code exports the combined annual dataset and creates stacked plots of baseline demand, EV demand, and cooking demand.

3.6 Stage II: Physics-Informed Training of the Hourly Load Model

This stage is implemented in pinn_train.py. The objective is not merely to predict the next daily load curve from previous curves, but to do so while respecting annual energy consistency.

3.6.1 Script-level flowchart for pinn_train.py

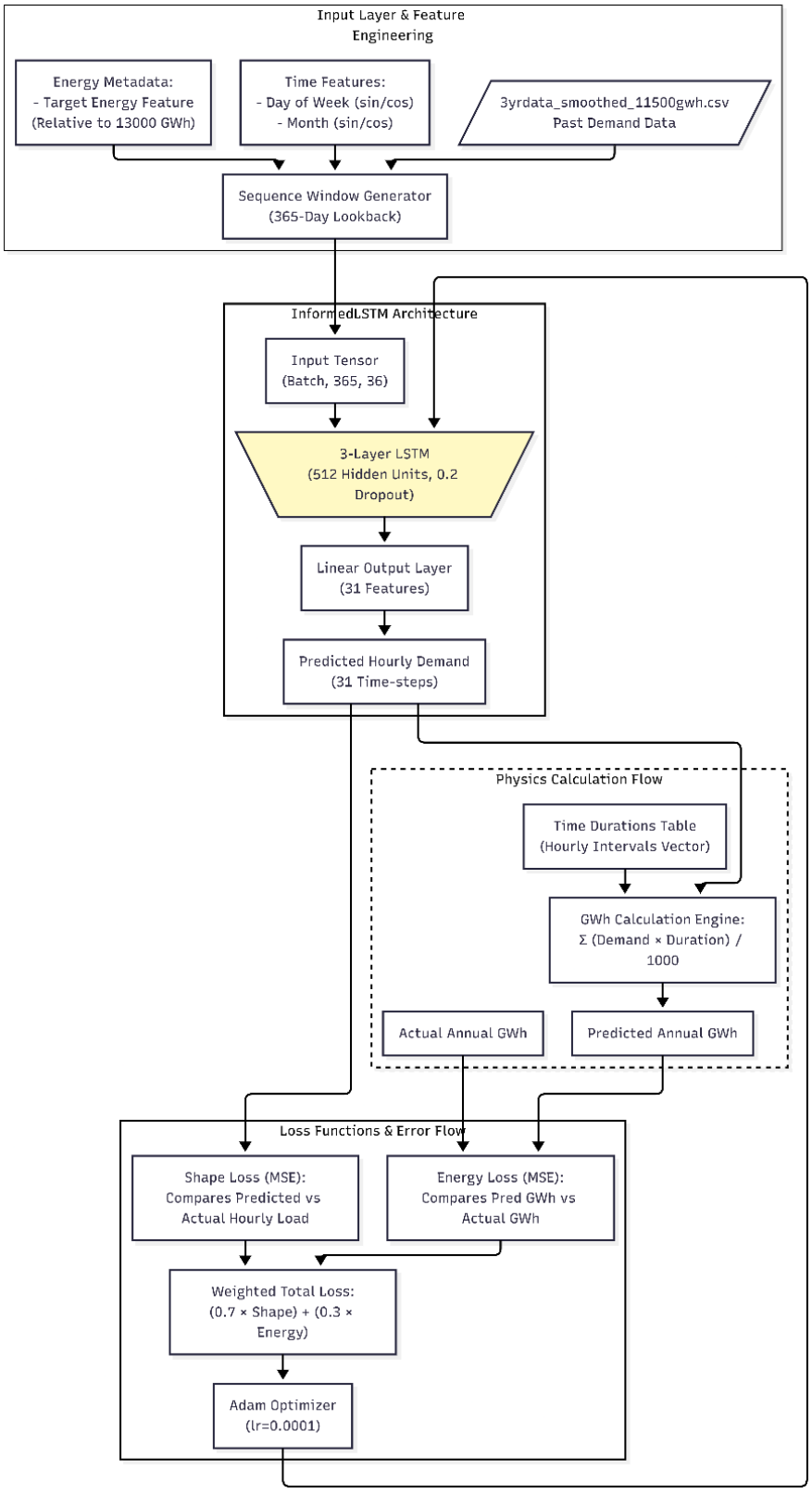

Figure 3: Algorithm for Prediction of future demand profile

3.6.2 Construction of the informed input sequence

The PINN training code begins by loading daily load profiles and constructing additional features. Each training sample is formed from:

- The scaled 31-point daily demand profile
- One scalar feature representing the annual target level associated with the day
- Four temporal features: day-of-week sine, day-of-week cosine, month sine, month cosine

Hence, the effective input size is:

[31 + 1 + 4 = 36]

For each daily observation indexed by day (d), the code determines the corresponding year and inserts a normalized energy feature derived from the annual target dictionary. This is a key methodological element because it injects annual energy context directly into the sequence model.

3.6.3 Sequence length and target design

The training code uses a sequence length of 365 days. Therefore, each training sample is formed as:

$$[\mathbf{x}_{d-364}, \mathbf{x}_{d-363}, \ldots, \mathbf{x}_d] \rightarrow \mathbf{y}_{d+1} \tag{3.17}$$

Where;

- $\mathbf{x}_d \in \mathbb{R}^{36}$ is input of 36 features
- $\mathbf{y}_{d+1} \in \mathbb{R}^{31}$is the next-day load profile

This design allows the model to learn seasonal recurrence over roughly one annual cycle.

3.6.4 Model architecture

The PINN training code defines an InformedLSTM with:

- Input size = 36,
- Hidden layer size = 512,
- Number of lstm layers = 3,

- Dropout = 0.2,
- Output size = 31.

Thus, the model receives a sequence of 365 daily feature vectors and returns a 31-point predicted daily load curve.

In **compact form**, the model can be expressed as:

$$\hat{\mathbf{y}}_{d+1} = F_\theta(\mathbf{X}_{d-364:d}) \tag{3.18}$$

where F_θ denotes the recurrent neural network parameterized by θ.

3.6.5 Physics-informed loss design

The most significant methodological feature of the Physics-Informed Neural Network (PINN) stage is its two-phase loss formulation, which combines conventional profile matching with an annual energy conservation constraint. Rather than relying solely on pointwise prediction accuracy, the model is trained to reproduce both the short-term shape of daily load curves and the long-term annual electricity totals specified by scenario targets. In pinn_train.py, the loss weights are explicitly set to $\lambda_{\text{shape}} = 0.7$and $\lambda_{\text{energy}} = 0.3$.

Shape Loss

The first component of the objective function is the shape loss, which measures the mean squared error between the predicted and observed 31-point daily demand profiles:

$$L_{\text{shape}} = \frac{1}{31B} \sum_{b=1}^{B} \sum_{j=1}^{31} \left(\hat{y}_{b,j} - y_{b,j}\right)^2 \tag{3.19}$$

where:

- B= batch size,
- j= time interval index,
- $\hat{y}_{b,j}$= predicted normalized demand,
- $y_{b,j}$= observed normalized demand.

This term ensures that the network learns realistic intraday load shapes and temporal dynamics.

Daily Energy Calculation

To evaluate compliance with annual energy targets, each predicted daily load curve is converted into daily energy by integrating power over the durations of the 31 time intervals:

$$E_{\text{day}} = \sum_{j=1}^{31} \hat{P}_j \ \Delta t_j \tag{3.20}$$

where:

- $\hat{P}_j$= predicted power at interval j(MW),
- Δt_j= duration of interval j(hours),
- E_{day}= daily energy (MWh).

The interval durations are computed directly from the timestamps in the dataset and are stored in the training code.

Annual Energy Loss

The predicted daily energies are summed over all days belonging to a modeled year to obtain the annual integrated energy. The annual energy penalty is then defined as:

$$L_{\text{energy}} = \left(E_{\text{pred,year}} - E_{\text{actual,year}}\right)^2 \tag{3.21}$$

where:

- $E_{\text{pred,year}}$= predicted annual energy (GWh),
- $E_{\text{actual,year}}$= target annual energy specified by the scenario.

This term acts as a physics-based constraint that enforces consistency between the hourly forecasts and externally defined annual energy targets.

Total Annual-Level Loss

The two loss components are combined as:

$$L_{\text{total}} = \lambda_{\text{shape}} L_{\text{shape,annual}} + \lambda_{\text{energy}} L_{\text{energy}} \tag{3.22}$$

with the implemented weights:

$$\lambda_{\text{shape}} = 0.7, \lambda_{\text{energy}} = 0.3$$

These values indicate that 70% of the optimization emphasis is placed on reproducing realistic daily load shapes, while 30% is devoted to satisfying annual energy constraints.

Significance

This two-phase loss formulation is the core innovation of the PINN framework. The shape loss preserves short-term temporal realism, while the energy loss guarantees that aggregated forecasts exactly follow policy-driven annual demand trajectories. Consequently, the model produces hourly load forecasts that are simultaneously data-driven, physically consistent, and scenario-compliant.

3.6.6 Two-phase optimization strategy

The code does not combine the two losses in a single mini-batch loss at every step. Instead, it uses a two-phase optimization process inside each epoch and for each yearly segment:

- **Phase 1**: mini-batch optimization using shape loss.
- **Phase 2**: annual block optimization using annual profile loss plus energy loss.

This is a practical and conceptually elegant approximation to physics-informed training. Phase 1 teaches the model to reproduce realistic daily shapes. Phase 2 penalizes cumulative deviation from integrated annual energy. The dissertation should explicitly emphasize this staged optimization because it is one of the most novel aspects of the implemented methodology.

3.6.7 Learning-rate scheduling and model persistence

The training code uses the Adam optimizer with learning rate (10^{-4}) and a ReduceLROnPlateau scheduler with factor 0.5 and patience 50 epochs. Training runs for 1100 epochs. The scaler is saved as scaler_pinn.pkl and the trained model is saved as informed_lstm_v4.pth.

3.7 Stage III: Recursive Forecasting of Future Hourly Profiles

The trained Physics-Informed Neural Network (PINN) is used to recursively generate future daily load profiles. After training is completed, the model and the associated scaler are reloaded, and the historical dataset is transformed into informed feature vectors containing normalized demand, annual energy context, and cyclical calendar features.

3.7.1 Recursive forecasting logic

The forecasting procedure follows an autoregressive recursive strategy. Let F_θ denote

the trained PINN model and let L be the sequence length used for forecasting. The model predicts the next daily load profile based on the most recent Ldays:

$$\hat{y}_{d+1} = F_\theta(X_{d-L+1:d}) \tag{3.23}$$

where:

- $\hat{y}_{d+1}$ = predicted 31-point daily demand profile for day $d + 1$,
- $X_{d-L+1:d}$ = feature sequences from the previous 21 days,
- F_θ= trained PINN model.

In the implementation, the model predicts a normalized daily profile, which is then inverse-transformed to MW values using the stored scaler. The predicted scaled profile itself is appended to the input sequence and becomes part of the next forecasting step, enabling fully recursive multi-day prediction.

3.7.2 Annual target injection during forecasting

For every new forecast day, the script determines the corresponding forecast year and inserts an energy feature derived from the annual target dictionary. Hence, the recursive forecasting process remains conditioned on annual energy context even after the historical series ends.

This step is essential because otherwise the recursive process would only propagate shape information and would lose the macro-scale demand growth signal.

3.7.3 Forecast horizon and outputs

The forecast horizon is constructed by combining the remaining days of the partially observed year plus the full subsequent year. The script then produces:

- Daily peak-demand plot,
- Individual plots for each intra-day time slot,
- Combined historic-plus-forecast csv export,
- Forecast-only excel file,
- Annual energy for the forecasted year

The annual electricity demand of the forecast year is obtained by integrating all predicted daily load curves over their corresponding interval durations:

$$E_{\text{forecast year}} = \frac{1}{1000} \sum_{d \in \text{year}} \sum_{j=1}^{31} \hat{P}_{d,j}\, \Delta t_j \tag{3.24}$$

where:

- $\hat{P}_{d,j}$= forecasted power at interval $j$on day d(MW),
- Δt_j= duration of interval j(hours),
- division by 1000 converts MWh to GWh.

This calculation provides a final consistency check to confirm that the recursively forecasted hourly profiles collectively satisfy the prescribed annual energy target.

3.8 Stage IV: Electric Cooking Load Disaggregation and Cooking-Share Estimation

This stage is implemented in model_v2.py. It is the most behaviorally detailed component of the pipeline. The objective is to estimate the portion of the daily load profile attributable to electric cooking by combining stock growth, usage intensity, temporal cooking distribution, and non-cooking base load.

3.8.1 3.8.1 Script-level flowchart for model_v2.py

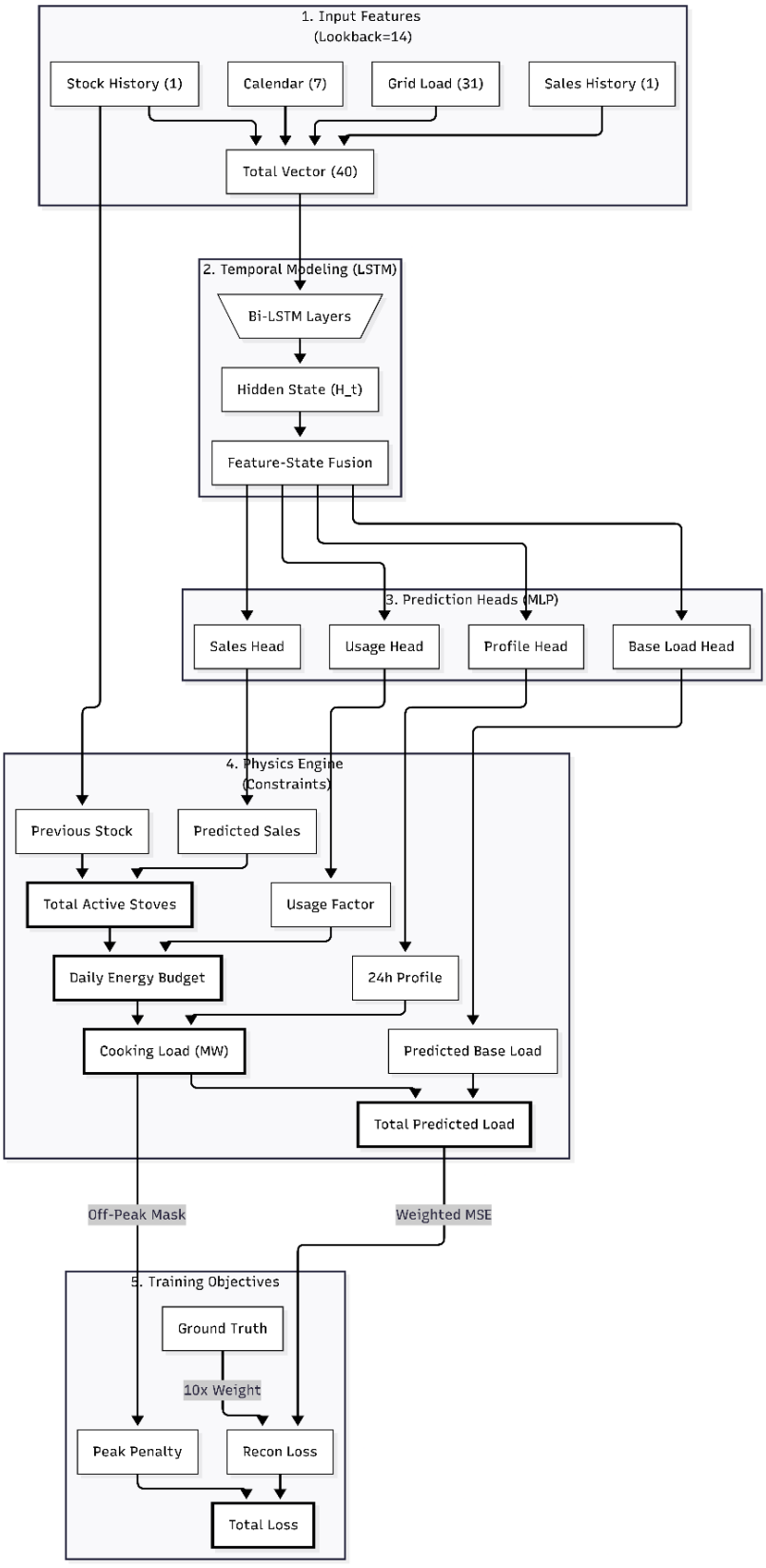

Figure 4: Cooking Profile Harvesting Model

3.8.2 Conceptual basis of the cooking disaggregation model

The cooking disaggregation model is based on the idea that electric cooking demand is not directly observed as a separate time series in the total load profile. It must therefore be inferred indirectly using a structured model. The implemented structure decomposes daily demand into two latent components:

$$L_{\text{total},d} = L_{\text{base},d} + L_{\text{cook},d} \tag{3.25}$$

where:

- $\mathbf{L}_{\text{total},d} \in \mathbb{R}^{31}$ is the observed daily load curve
- $\mathbf{L}_{\text{base},d} \in \mathbb{R}^{31}$ is the non-cooking base-load curve
- $\mathbf{L}_{\text{cook},d} \in \mathbb{R}^{31}$ is the cooking-induced load curve
- All units are in MW

The cooking component is constrained by stock, usage factor, and temporal distribution.

3.8.3 Synthetic stock and sales reconstruction

The code does not use directly observed daily stove sales. Instead, it constructs a synthetic daily sales sequence from annual sales totals and then computes cumulative active stock:

$$N_d = N_0 + \sum_{r=1}^{d} S_r \tag{3.26}$$

where**:**

- N_0 is the initial active stove stock
- S_r is daily stove sales
- N_d is active stock on day d

The resulting stock trajectory becomes a model input. This means the disaggregation model is partly informed by appliance diffusion dynamics rather than only by load shape patterns.

3.8.4 Input construction and lookback design

The model uses a 14-day lookback window. For each training example, the input tensor contains:

- Normalized 31-slot load profile
- 1 Normalized sales
- 1 Normalized active stock
- 7 calendar features

Hence the feature dimension per day is:

$$31 + 1 + 1 + 7 = 40$$

The input sequence is therefore:

$$\mathbf{X}_d \in \mathbb{R}^{40} \tag{3.27}$$

The target includes the next-day normalized load profile, current calendar features, current active stock, next active stock, and the day index.

3.8.5 Calendar features used in the cooking model

The cooking model uses a richer calendar representation than the PINN forecasting model. It includes cyclical features for:

- Day of week
- Month
- Day of year
- Normalized year position

These features are expected to capture weekly cooking rhythm, seasonal behavior, and long-term drift in adoption and use patterns.

3.8.6 Multi-head network architecture

The cooking disaggregation model consists of a shared LSTM backbone and four task-specific heads. After the LSTM encodes the 14-day input sequence, the final hidden state is concatenated with the current calendar feature vector, producing a fused latent representation. This fused representation is then passed to four output branches:

1. **Sales head**: predicts next-day stove sales.

2. **Usage head**: predicts a bounded usage factor.
3. **Profile head**: predicts a 31-slot softmax probability distribution over the day.
4. **Base-load head**: predicts the base-load profile directly.

This can be represented as:

$$\mathbf{h}_d = \text{LSTM}(\mathbf{X}_d) \tag{3.28}$$

$$\mathbf{u}_d = [\mathbf{h}_d;\ \mathbf{c}_d] \tag{3.29}$$

where $\mathbf{c}_d$ denotes the current calendar feature vector. The model heads then produce:

$$\begin{aligned} \hat{S}_{d+1} &= f_{\text{sales}}(\mathbf{u}_d) \\ \hat{\alpha}_d &= f_{\text{usage}}(\mathbf{u}_d) \\ \hat{\mathbf{p}}_d &= f_{\text{profile}}(\mathbf{u}_d) \\ \hat{\mathbf{L}}_{\text{base},d} &= f_{\text{base}}(\mathbf{u}_d) \end{aligned} \tag{3.30}$$

3.8.7 Bounded usage factor and softmax daily profile

The usage branch output is passed through a sigmoid-based affine transformation so that the daily usage multiplier remains bounded between 0.65 and 1.55:

$$\hat{\alpha}_d = 0.65 + 0.90 \cdot \sigma(z_d) \tag{3.31}$$

where; $\hat{\alpha}_d$ is daily usage multiplier

This ensures that the estimated cooking energy remains within a physically interpretable range.

The profile branch uses a softmax layer to allocate cooking energy across the 31 daily time slots:

$$\hat{p}_{d,j} = \frac{\exp\,(z_{d,j})}{\sum_{k=1}^{31} \exp\,(z_{d,k})} \tag{3.32}$$

with:

$$\sum_{j=1}^{31} \hat{p}_{d,j} = 1 \tag{3.33}$$

This guarantees that the daily cooking energy budget is fully distributed across the day.

3.8.8 Mapping stock and usage into daily cooking energy

The model first converts the predicted next-day stove sales and the current number of active induction stoves from normalized values back to their physical units. It then estimates the total daily cooking energy according to:

$$E_{\text{cook},d} = \frac{(N_d + \hat{S}_{d+1}) e_{\text{unit}} \hat{\alpha}_d}{1000} \tag{3.34}$$

where:

- $E_{\text{cook},d}$= total cooking energy on day d(MWh/day)
- N_d= number of active induction stoves on day d
- $\hat{S}_{d+1}$= predicted stove sales for the next day
- $e_{\text{unit}} = 2.36$kWh per stove per day
- $\hat{\alpha}_d$= predicted daily usage factor

The usage factor $\hat{\alpha}_d$is constrained between 0.65 and 1.55 through the usage head of the neural network, allowing the model to capture day-to-day variations in cooking intensity. In the implementation, this factor is computed as $u_t = 0.65 + 0.90 \times \sigma(\cdot)$, where $\sigma(\cdot)$is the sigmoid activation.

The calculated daily cooking energy is then distributed across the 31 time intervals using the learned softmax probability profile and a trainable grid-scaling parameter g:

$$\hat{L}_{\text{cook},d,j} = \frac{E_{\text{cook},d}\, g\, \hat{p}_{d,j}}{\sigma_L} \tag{3.35}$$

where:

- $\hat{L}_{\text{cook},d,j}$= normalized cooking demand at time interval j
- $\hat{p}_{d,j}$= learned probability of cooking at interval j, with $\sum_j \hat{p}_{d,j} = 1$
- g= trainable grid-scaling coefficient
- σ_L= standard deviation of the historical load used for normalization

The softmax profile ensures that the entire daily cooking energy budget is allocated across the 24-hour period while preserving the relative likelihood of cooking activity at each time interval. The grid-scaling factor is implemented as $g = \exp(\theta_g)$,

guaranteeing a strictly positive value during training.

Finally, the predicted cooking load is superimposed onto the estimated baseline load to reconstruct the total household electricity demand:

$$\hat{L}_{\text{total},d,j} = \hat{L}_{\text{base},d,j} + \hat{L}_{\text{cook},d,j} \tag{3.36}$$

where:

- $\hat{L}_{\text{base},d,j}$= predicted baseline demand excluding cooking
- $\hat{L}_{\text{total},d,j}$= final reconstructed total demand

This formulation enables the model to maintain physical consistency by explicitly linking appliance stock, per-unit energy consumption, usage behavior, and temporal cooking patterns. As shown in model_v2.py, the cooking component is calculated from active stove stock and predicted sales, normalized using the load standard deviation, and added directly to the baseline output generated by a separate network branch.

3.8.9 Peak-focused reconstruction loss

The cooking disaggregation model is trained using a specialized loss function rather than a conventional uniform mean squared error (MSE). The objective function incorporates prior knowledge of household cooking behavior by assigning greater importance to predefined cooking peak periods and penalizing any cooking demand predicted outside these expected time windows. This approach allows the model to be guided not only by statistical fit but also by behavioral realism.

Let Ω_{peak}denote the set of time indices corresponding to typical cooking periods (morning, midday, and evening), and let $w_j$represent the reconstruction weight assigned to time interval j, with larger values for $j \in \Omega_{\text{peak}}$. The weighted reconstruction loss is defined as:

$$L_{\text{recon}} = \frac{1}{31B} \sum_{b=1}^{B} \sum_{j=1}^{31} w_j \left(\hat{L}_{b,j} - L_{b,j}\right)^2 \tag{3.37}$$

where:

- $B$is the batch size,
- $\hat{L}_{b,j}$is the predicted total load,

- $L_{b,j}$is the observed load, and
- $w_j = 10$ for peak cooking intervals and $w_j = 1$otherwise.

In model_v2.py, peak-hour weights are explicitly set to 10.0 to emphasize accuracy during cooking-intensive periods.

To ensure that cooking demand is concentrated only during realistic time windows, an off-peak regularization term is introduced. Let $\hat{L}_{\text{cook},b,j}$denote the predicted cooking load, and let γbe a penalty coefficient. The off-peak penalty is given by:

$$L_{\text{offpeak}} = \gamma \frac{1}{31B} \sum_{b=1}^{B} \sum_{j \notin \Omega_{\text{peak}}} \hat{L}^2_{\text{cook},b,j} \tag{3.38}$$

where:

- $\gamma = 50$ in the implemented model,
- the summation is performed only over intervals outside the designated cooking periods.

This penalty strongly discourages the allocation of cooking energy to non-cooking hours and forces the base-load branch to explain demand variations during those periods.

The total objective function used to train the cooking model is therefore:

$$L_{\text{cook model}} = L_{\text{recon}} + L_{\text{offpeak}} \tag{3.39}$$

By combining weighted reconstruction with behavioral regularization, the model simultaneously achieves accurate statistical fitting and realistic temporal disaggregation. This loss formulation is central to the model's ability to identify induction cooking demand patterns that are both data-consistent and physically plausible.

3.8.10 Evaluation outputs of the cooking model

After training, the cooking disaggregation script exports:

- Daily predicted total load
- Base-load and cooking-load decomposition

- Average cooking load percentage over 24 hours
- Latest-day cooking share percentage
- Latest 365 days of estimated cooking profiles
- Visualization of decomposition, learned profile, cooking share, sales trend, and stock trend

The average cooking share at time slot $j$is computed as:

$$CS_j = 100 \times \frac{\bar{L}_{\text{cook},j}}{\bar{L}_{\text{total},j}} \tag{3.40}$$

where the overbar denotes averaging over the evaluation set.

3.9 Final Data Processing and Load Reconstruction

After generating baseline, EV, and cooking demand components, a final data processing stage is implemented to ensure consistency between annual energy targets and hourly demand profiles.

The process consists of three steps:

1. **Scaling factor extraction (scale.py):**
   Initial normalization factors are derived from model outputs.
2. **Calibration step:**
   These factors are manually adjusted to ensure that the aggregated hourly demand matches the projected annual energy targets.
3. **Upscaling and combination (upscale.py and combine_final.py):**
   The adjusted scaling factors are applied to each demand component (baseline, EV, cooking), and the final hourly demand is obtained by:

$$L_{total,t} = L_{base,t} + L_{EV,t} + L_{cook,t} \tag{3.41}$$

3.10 Interconnection of the Four Scripts in the Dissertation Workflow

Although each script can be described independently, the dissertation should emphasize that they form one integrated workflow.

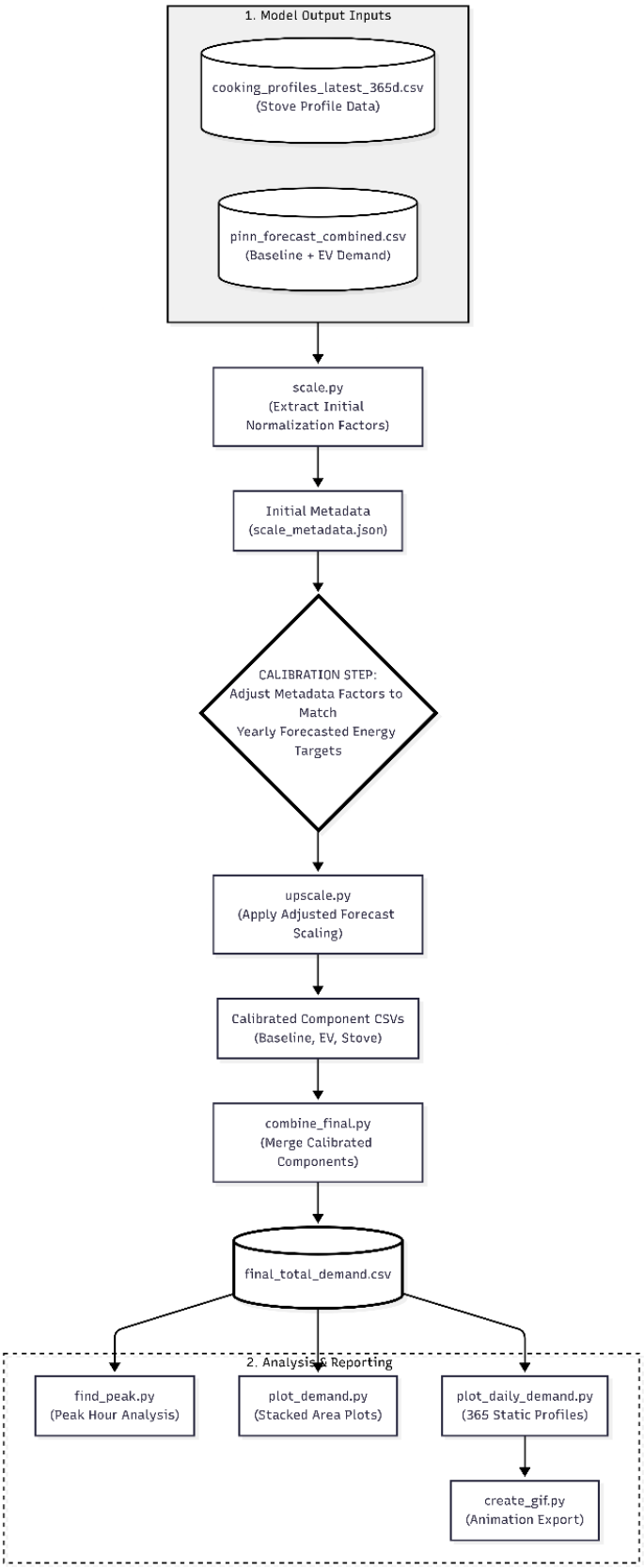

Figure 5: Final Data Processing of the pipeline

The annual module establishes the future energy-demand envelope. The PINN module learns daily load shapes under annual energy constraints. The forecasting script extends these shapes into the future. The cooking model finally interprets part of the aggregate profile as electric cooking demand using behavioral and stock-driven structure.

3.11 Hyperparameters and Training Configuration

For dissertation completeness, the major implemented hyperparameters are summarized below.

3.11.1 Annual baseline forecasting block

- Univariate lookback window: 2 years
- Future forecast horizon: 5 years
- Univariate LSTM hidden units: 32
- Univariate epochs: 250
- Multivariate LSTM hidden units: instantiated with 32 during evaluation and final forecasting
- Multivariate dropout: 0.2
- Multivariate training epochs: 250
- Initial learning rate: 0.005 for univariate block and 0.002 for main multivariate baseline model
- Test period: last 5 years

3.11.2 PINN hourly training block

- Input dimension: 36
- Output dimension: 31
- Hidden layer size: 512
- Number of LSTM layers: 3
- Dropout: 0.2
- Sequence length during training: 365 days

- Batch size: 16
- Epochs: 1100
- Optimizer: Adam
- Learning rate: 0.0001
- Scheduler: ReduceLROnPlateau, factor 0.5, patience 50
- Shape-loss weight: 0.7
- Energy-loss weight: 0.3

3.11.3 PINN forecasting block

- Recursive sequence length during forecasting: 21 days
- Forecast outputs: daily peak, 9:00 AM trend, all time-slot trajectories, forecast CSV, forecast Excel

3.11.4 Cooking disaggregation block

- Number of daily time steps: 31
- Lookback window: 14 days
- Hidden size: 128
- Dense size: 64
- Number of LSTM layers: 2
- Dropout: 0.2
- Batch size: 32
- Epochs: 800
- Learning rate: 0.001
- Usage factor range: 0.65 to 1.55
- Base active stoves: 528,080
- Daily energy per stove: 2.36 kWh/day

These details should appear in the dissertation because they determine model capacity, convergence behavior, and reproducibility.

3.12 Evaluation Strategy

The dissertation should distinguish clearly between evaluation at the annual scale and evaluation at the sub-daily scale.

3.12.1 Annual-scale evaluation

The annual baseline-demand model is explicitly benchmarked against persistence and ARIMA and evaluated on a held-out test period using RMSE, MAE, and MAPE.

3.12.2 Hourly-scale evaluation

The PINN model is evaluated more implicitly through:

- Visual comparison of historical and forecast daily peaks,
- Integrated annual energy consistency,
- Profile continuity across recursive forecasts,
- Time-slot-specific forecast plots.

3.12.3 Disaggregation evaluation

The cooking model is evaluated through:

- Reconstruction accuracy of the total load profile,
- Plausibility of cooking concentration in peak cooking hours,
- Stability of predicted active stock growth,
- Interpretable cooking-share percentages.

CHAPTER FOUR: RESULTS AND DISCUSSION

This chapter presents the results obtained from the proposed multi-stage electricity demand forecasting framework and provides a detailed discussion of their implications for future grid planning. The framework integrates annual energy forecasting, scenario-based demand disaggregation, hourly load prediction, and final calibration to produce a consistent and realistic representation of future electricity demand.

Unlike conventional approaches that rely solely on annual or hourly forecasting, this study combines both temporal scales to capture not only the magnitude of future electricity demand but also its temporal distribution. In particular, the effects of electric mobility and electric cooking are explicitly incorporated into the forecasting process, enabling a comprehensive assessment of their impact on grid demand.

The results are structured in a sequential manner. First, the performance of the annual forecasting model is evaluated to establish its reliability. This is followed by the presentation of macro-level drivers and baseline demand projections. Subsequently, the contributions of electric vehicles (EVs) and electric cooking to total energy demand are analyzed. The chapter then proceeds to discuss hourly load forecasting, demand disaggregation, and final calibration processes, culminating in an integrated assessment of peak demand and grid-level impacts.

The discussion throughout this chapter emphasizes not only the numerical results but also their physical interpretation and relevance to power system planning, particularly in the context of a hydropower-dominated electricity system.

4.1 Performance of the Annual Forecasting Model

4.1.1 Evaluation Framework

To ensure the reliability of the annual electricity demand forecasts, a chronological validation strategy was adopted. The dataset spanning from 2001 to 2025 was divided into a training set (2001–2020) and a test set (2021–2025). This approach ensures that the model is evaluated on unseen future data, thereby reflecting realistic forecasting conditions.

The proposed Long Short-Term Memory (LSTM) model was benchmarked against two commonly used baseline approaches:

- A **Persistence model**, which assumes that future demand remains equal to the most recent observed value.
- An **ARIMA (1,1,0)** model, representing a classical statistical time-series forecasting technique.

The evaluation was carried out using three standard performance metrics: Root Mean Square Error (RMSE), Mean Absolute Error (MAE), and Mean Absolute Percentage Error (MAPE). These metrics provide complementary insights into absolute error magnitude, average deviation, and relative error, respectively.

4.1.2 Model Performance Results

The comparison of model performance on the test period (2021–2025) is summarized in Table 1.

Table 1: Model Performance Comparison (2021–2025)

Metric	LSTM Model	Persistence	ARIMA (1,1,0)
RMSE	0.4858	1.2482	3.9267
MAE	0.4222	1.1903	3.4724
MAPE (%)	4.38	12.46	33.18

The LSTM model achieves a Mean Absolute Percentage Error (MAPE) of approximately **4.38%**, significantly outperforming both the Persistence model and the ARIMA model. The Persistence model, while simple, fails to capture the underlying growth trend, resulting in more than double the error. The ARIMA model performs considerably worse, with a MAPE exceeding 30%, indicating its inability to adequately model the nonlinear and non-stationary characteristics of the dataset.

4.1.3 Discussion of Model Behavior

The superior performance of the LSTM model can be attributed to its ability to capture temporal dependencies and nonlinear relationships among the input variables. Electricity demand in developing energy systems is influenced by multiple interacting factors, including economic growth, demographic changes, and technological adoption. These relationships are inherently nonlinear and evolve over time, making them difficult to model using traditional statistical techniques.

The LSTM architecture is particularly well-suited for this task due to its memory

mechanism, which allows it to retain information from previous time steps and learn long-term dependencies. This enables the model to recognize gradual trends, such as increasing electricity consumption per capita, as well as structural changes, such as rapid urbanization.

In contrast, the ARIMA model relies on linear assumptions and differencing operations to achieve stationarity. While effective for short-term forecasting in stable systems, it struggles to generalize in contexts where demand growth is driven by evolving socio-economic conditions. The Persistence model, being purely naïve, does not incorporate any trend or structural information, leading to poor predictive performance.

4.1.4 Reliability and Suitability for Scenario Forecasting

The low error metrics achieved by the LSTM model indicate a high level of predictive accuracy and robustness. A MAPE of approximately 5% is generally considered acceptable for long-term energy forecasting, particularly in systems characterized by rapid growth and structural transitions.

More importantly, the model demonstrates strong generalization capability, as evidenced by its performance on unseen test data. This is critical for scenario-based forecasting, where the model must extrapolate beyond historical patterns to predict future demand under changing conditions.

The validated performance of the LSTM model provides a reliable foundation for subsequent stages of the analysis, including the incorporation of electric mobility and electric cooking scenarios. By ensuring that the baseline demand forecast is accurate, the study can confidently assess the incremental impact of electrification on total grid demand.

4.1.5 Implications for the Overall Study

The results of the model evaluation establish that the chosen forecasting approach is both accurate and appropriate for the study objectives. This has two important implications:

First, the projected baseline demand can be considered a realistic representation of future electricity needs in the absence of additional electrification scenarios. Second, the subsequent addition of EV and cooking demand can be interpreted as incremental effects, rather than artifacts of model error.

Therefore, the reliability of the annual forecasting model underpins the entire analytical framework of this study and ensures that the final integrated demand projections are grounded in a robust predictive foundation.

4.2 Forecasted Macro Drivers and Baseline Demand

4.2.1 Overview of Macro Level Drivers

The future trajectory of electricity demand is fundamentally influenced by macroeconomic and demographic variables. In this study, key drivers including Gross Domestic Product (GDP), total population, urban population share, electricity access, and electricity consumption per capita were forecasted using optimized univariate Long Short-Term Memory (LSTM) models. These variables were subsequently used as inputs to the multivariate LSTM model for baseline electricity demand prediction.

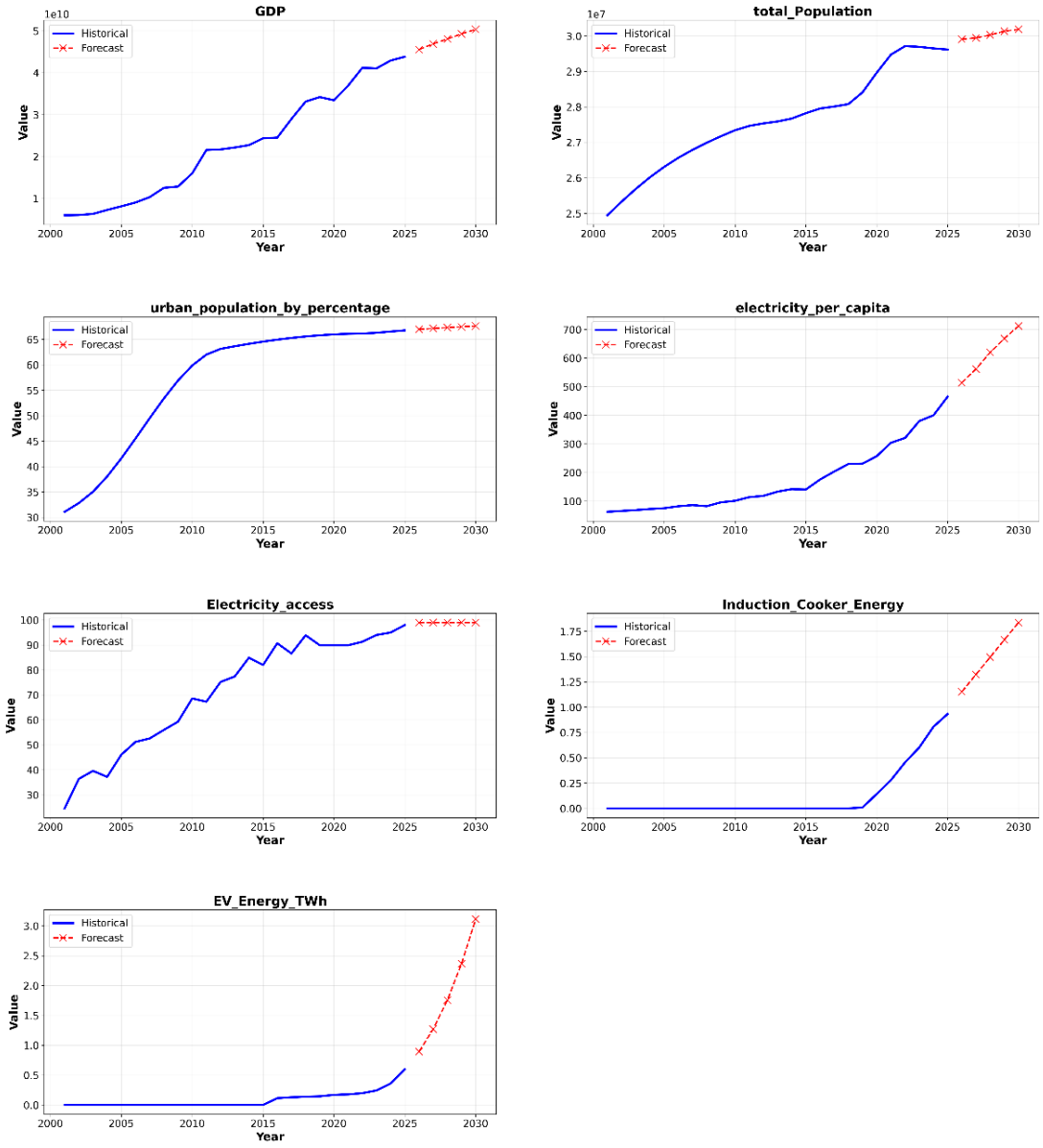

Figure 6: Historical and Forecasted Macro-Level Drivers

The projected trends of these drivers provide critical insight into the structural evolution of electricity demand, independent of electrification scenarios such as electric mobility and electric cooking. Therefore, this subsection establishes the baseline conditions upon which scenario-based demand increments are later superimposed.

A comprehensive visualization of both historical and forecasted macro-level drivers is presented in the feature dashboard (Figure 1), which illustrates the temporal evolution of each variable from 2001 to 2030.

4.2.2 Gross Domestic Product (GDP) Growth

The forecast results indicate a steady and sustained increase in GDP over the forecast horizon (2026–2030). This trend reflects continued economic development and expansion of industrial and service sectors.

From an energy perspective, GDP growth is one of the strongest determinants of electricity demand, as it correlates with increased industrial activity, commercial energy use, and household consumption. The rising GDP trajectory therefore contributes directly to the upward trend in baseline electricity demand.

The smooth and consistent nature of the GDP forecast suggests that the model successfully captures long-term economic growth patterns without introducing unrealistic volatility.

4.2.3 Population Growth

The total population is projected to increase gradually over the forecast period, reaching approximately 29.9 million by 2030. Although the growth rate is relatively moderate, the cumulative effect of population increase contributes significantly to total electricity demand.

Population growth influences electricity demand through increased residential consumption, expansion of infrastructure, and greater demand for public services. Even in the absence of electrification scenarios, a growing population inherently leads to higher baseline demand.

4.2.4 Urbanization Trends

Urban population percentage exhibits a consistent upward trend throughout the forecast horizon. The model ensures monotonic growth by training on differential values, thereby avoiding unrealistic fluctuations in the urbanization trajectory.

Urbanization is a critical factor in electricity demand growth, as urban households typically exhibit higher electricity consumption compared to rural households. Increased urbanization is associated with greater appliance ownership, higher standards of living, and increased reliance on electricity for daily activities.

The continued rise in urban population share indicates a structural shift toward more electricity-intensive lifestyles, further reinforcing the upward trend in baseline demand.

4.2.5 Electricity Access and Electrification Saturation

Electricity access is assumed to reach near-complete saturation at 99%, reflecting national electrification goals. This assumption implies that almost all households are connected to the electricity grid in the forecast period.

While the contribution of increasing access to demand growth diminishes as saturation is reached, it remains an important factor in earlier stages of the dataset. In the forecast period, electricity demand growth is driven more by increased usage per consumer rather than expansion of access.

This transition from access-driven growth to consumption-driven growth is characteristic of maturing power systems.

4.2.6 Electricity Consumption per Capita

Electricity consumption per capita shows a strong upward trend over the forecast horizon, increasing significantly between 2026 and 2030. This reflects rising living standards, increased appliance usage, and greater reliance on electricity across residential, commercial, and industrial sectors.

The growth in per capita consumption is particularly important because it captures behavioral and technological changes that are not directly reflected in population or GDP alone. It represents increased intensity of electricity use per individual, which is a key driver of long-term demand growth.

4.2.7 Summary of Forecasted Macro Drivers

The forecasted values of the macro-level drivers for the period 2026–2030 are summarized in Table 2.

Table 2: Forecasted Macro Drivers (2026–2030)

Year	GDP (Billion USD)	Total Population	Urban Population (%)	Electricity per Capita (kWh)	Electricity Access (%)
2026	45.56	29,909,140	66.98	513.46	99
2027	46.89	29,948,050	67.16	561.76	99
2028	48.07	30,028,620	67.33	619.87	99
2029	49.28	30,134,100	67.49	668.10	99

2030	50.34	30,186,290	67.65	712.12	99

These projections indicate a consistent increase across all key drivers, reinforcing the expectation of sustained growth in electricity demand.

4.2.8 Baseline Electricity Demand Forecast

The baseline electricity demand represents the portion of total demand driven solely by macroeconomic and demographic factors, excluding additional contributions from electric vehicles and electric cooking.

The forecast results show that baseline demand increases significantly over the period 2026–2030, reaching approximately **23.79 TWh by 2030**. This represents a substantial increase compared to historical values and reflects the combined effect of GDP growth, population increase, urbanization, and rising per capita consumption.

The growth pattern of baseline demand is nonlinear, exhibiting an accelerating trend over time. This behavior is consistent with compounding effects of macro drivers and is effectively captured by the LSTM model through the use of log-transformed targets during training.

4.2.9 Interpretation of Baseline Demand Growth

The baseline demand forecast highlights that even in the absence of electrification scenarios, electricity demand is expected to grow rapidly due to structural socio-economic changes.
Two key observations can be made:

First, the growth in baseline demand is primarily driven by increasing electricity consumption per capita and urbanization, rather than population growth alone. This indicates a shift toward more electricity-intensive lifestyles.

Second, the baseline demand serves as a critical reference case for evaluating the impact of electrification. By isolating the demand driven by macro-level factors, it becomes possible to quantify the additional burden imposed by electric mobility and electric cooking in subsequent sections.

4.2.10 Implications for Demand Forecasting

The results demonstrate that baseline electricity demand is not static but evolves dynamically with socio-economic development. Accurate modeling of macro-level

drivers is therefore essential for reliable long-term forecasting.

Furthermore, the baseline demand establishes the foundation upon which scenario-based demand increments are added. Any underestimation or overestimation at this stage would propagate through the entire forecasting framework, affecting the final integrated demand results.

Therefore, the robust modeling and validation of macro drivers and baseline demand form a crucial component of the overall methodology.

4.3 EV and Electric Cooking Annual Energy Contribution

While the baseline demand reflects electricity consumption driven by macroeconomic and demographic factors, the transition toward electrification introduces additional demand components that significantly alter the overall energy trajectory. In this study, two major electrification pathways electric mobility and electric cooking are explicitly modeled and incorporated into the total electricity demand forecast.

This section quantifies the annual energy contributions of electric vehicles (EVs) and induction-based electric cooking over the forecast period (2026–2030). By comparing these components with the baseline demand, the analysis provides a clear understanding of their relative magnitude, growth behavior, and combined impact on total electricity requirements.

The results are derived from the aggregated dataset energy_demand_forecast_results.csv, and are visually represented in the stacked energy forecast plot.

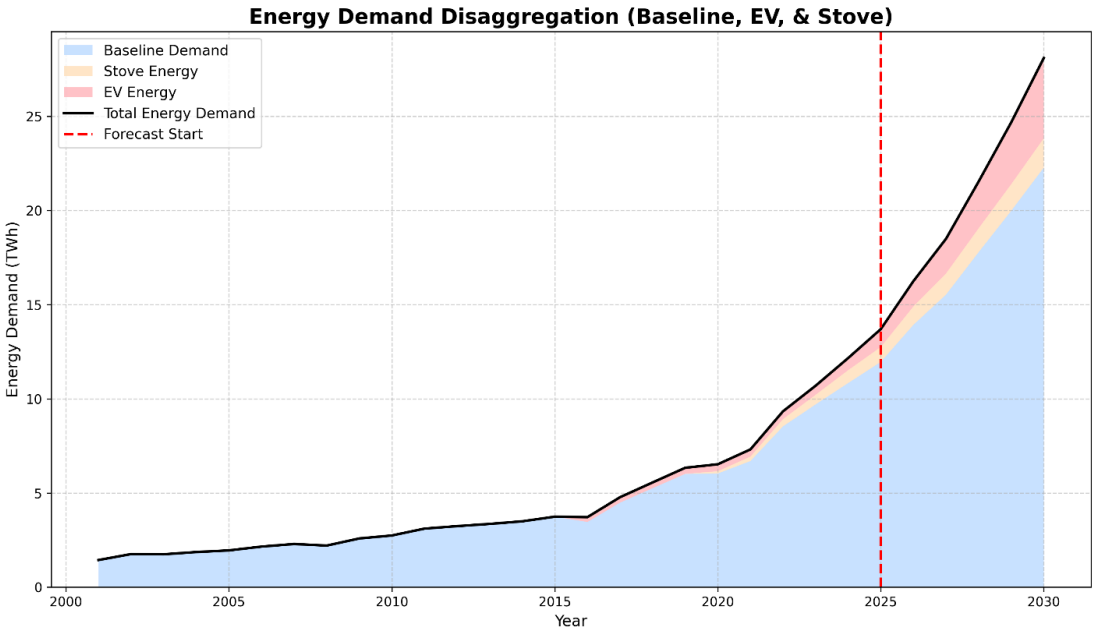

Figure 7: Stacked Annual Electricity Demand Forecast Showing Contributions of Baseline, EV, and Electric Cooking (2026–2030)

4.3.1 Forecasted EV Energy Demand

The projected EV energy demand exhibits a rapid and accelerating increase over the forecast horizon. This trend reflects the early-stage adoption followed by a scaling phase typical of technological diffusion in the transport sector.

Between 2026 and 2030, EV energy demand increases from approximately **0.906 TWh to 3.14 TWh**, representing more than a threefold increase within five years.

This growth pattern indicates that EV adoption is expected to become a major driver of electricity demand in the near future. The steep increase suggests strong policy alignment and technological uptake, consistent with electrification targets in developing energy systems.

Unlike baseline demand, which grows steadily due to structural factors, EV demand introduces an additional dynamic component characterized by rapid expansion.

4.3.2 Forecasted Electric Cooking Energy Demand

Electric cooking demand, derived from cumulative induction stove adoption, shows a steady and gradual increase over the forecast period.

The annual cooking energy demand rises from approximately **1.152 TWh in 2026 to**

1.837 TWh in 2030.

Compared to EV demand, the growth of cooking energy is more linear and less volatile. This reflects the household-level adoption pattern, where the transition to electric cooking occurs progressively rather than abruptly.

The estimation of cooking energy is based on a fixed daily energy consumption per stove, aggregated across the cumulative number of installed units. This provides a physically interpretable and policy-aligned estimate of cooking-related electricity demand.

4.3.3 Comparative Analysis of EV and Cooking Demand

A comparison of EV and cooking energy demand reveals distinct characteristics in both magnitude and growth behavior.

- **Magnitude**: EV demand is consistently higher than cooking demand throughout the forecast period. By 2030, EV demand (3.14 TWh) is nearly three times larger than cooking demand (1.837 TWh).
- **Growth Rate**: EV demand exhibits a faster growth rate, reflecting rapid adoption, whereas cooking demand grows more steadily due to gradual household penetration.
- **Nature of Demand**: EV demand is driven by mobility electrification and is expected to scale quickly. Cooking demand is driven by residential behavior and policy-driven appliance adoption.

This comparison highlights that while EVs dominate in terms of annual energy contribution, electric cooking introduces a more stable and predictable demand component.

4.3.4 Total Annual Electricity Demand

The total electricity demand is calculated as the sum of baseline demand, EV demand, and cooking demand:

$$\text{Total Demand} = \text{Baseline Demand} + \text{EV Demand} + \text{Cooking Demand}$$

The projected values for the forecast period are summarized in Table 3.

Table 3: Annual Energy Demand Disaggregation (2026–2030)

Year	Baseline (TWh)	EV (TWh)	Cooking (TWh)	Total (TWh)
2026	14.365	0.907	1.152	16.424
2027	16.262	1.287	1.324	18.872
2028	18.760	1.776	1.495	22.031
2029	21.330	2.389	1.666	25.385
2030	23.790	3.140	1.837	28.74

The results indicate that total electricity demand increases sharply over the forecast horizon, more than doubling between 2025 and 2030. This growth is driven by both baseline expansion and additional electrification loads.

4.3.5 Interpretation of Stacked Energy Results

The stacked energy forecast (Figure 7) visually illustrates the contribution of each component to total demand. The baseline demand forms the largest portion, while EV and cooking demand progressively increase their share over time.
Several important observations can be made:

First, the contribution of EV demand becomes increasingly significant in later years, indicating its growing importance in the overall energy mix.

Second, cooking demand, although smaller in magnitude, consistently contributes to total demand and cannot be neglected in long-term planning.

Third, the gap between baseline demand and total demand widens over time, highlighting the cumulative effect of electrification.

This visualization reinforces the importance of considering multiple demand components simultaneously rather than relying on a single aggregated forecast.

4.3.6 Implications for Electricity Demand Growth

The results clearly demonstrate that electrification significantly accelerates electricity demand growth beyond baseline projections.

Two key implications emerge:

- **Energy Growth Impact**: EV adoption is the primary contributor to additional energy demand, driving a substantial increase in total annual consumption.

- **Complementary Role of Cooking**: Electric cooking, while contributing less energy annually, represents a consistent and policy-driven addition to demand that becomes increasingly relevant over time.

Importantly, the combined effect of EV and cooking demand leads to a substantial upward shift in total electricity requirements.

4.3.7 Importance of Scenario-Based Forecasting

The comparison between baseline and total demand highlights the necessity of incorporating electrification scenarios into demand forecasting models.

If EV and cooking demand were ignored, the total electricity requirement would be significantly underestimated. For instance, in 2030, the difference between baseline demand (23.79 TWh) and total demand (28.76 TWh) exceeds **4.97TWh**, representing a substantial planning gap.

Such underestimation could lead to inadequate generation capacity planning, grid congestion, and reliability issues.

Therefore, scenario-based forecasting, as implemented in this study, provides a more realistic and policy-relevant assessment of future electricity demand.

This section demonstrates that electric mobility and electric cooking introduce significant additional demand beyond baseline projections. EV demand emerges as the dominant contributor to annual energy growth, while cooking demand provides a steady and consistent increase.

Together, these components substantially reshape the future electricity demand trajectory, emphasizing the need for integrated and scenario-aware forecasting approaches. The next section extends this analysis to the hourly level, where the temporal distribution of demand; particularly the impact of cooking on load profiles becomes critically important.

4.4 Hourly Baseline + EV Load Forecasting Results

While annual energy forecasting provides the magnitude of future electricity demand, it does not capture how this demand is distributed across time. For power system planning and operation, the temporal structure of demand particularly at hourly resolution is equally critical. Therefore, this study employs an informed Long Short-

Term Memory (LSTM) model with physics-inspired constraints to generate hourly demand profiles corresponding to the forecasted annual energy.

At this stage of the framework, the hourly load represents baseline demand combined with EV and cooking demand. This intermediate result is essential, as it forms the structural backbone of the final integrated demand profile.

The hourly forecasting process is implemented through the training and forecasting scripts (pinn_train.py and pinn_forecast.py), with outputs stored in pinn_forecast_combined.csv.

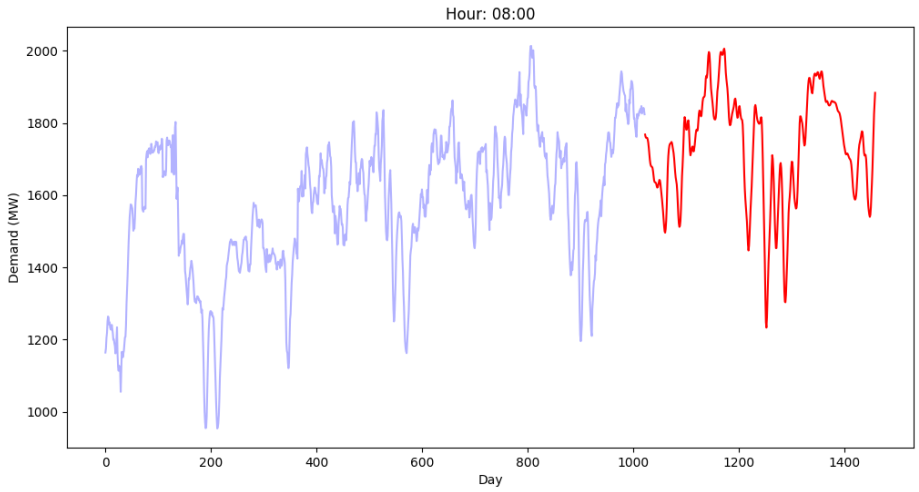

Figure 8: Example Profile of Hourly Load Forecast for Baseline + EV Demand + Cooking Demand for 8:00 AM (2080-2083)

4.4.1 Role of the Informed LSTM (PINN Framework)

The hourly forecasting model is based on an informed LSTM architecture, which incorporates both data-driven learning and physical consistency constraints. Unlike conventional time-series models that rely purely on historical patterns, this approach integrates domain knowledge in the form of annual energy targets.

The model takes as input:

- Historical hourly demand data
- Temporal features (day of week, seasonal encoding)
- A normalized representation of annual energy targets

The inclusion of annual energy information ensures that the hourly forecasts are not independent of the yearly projections, thereby linking different temporal scales within

a unified framework.

This approach can be interpreted as a simplified Physics-Informed Neural Network (PINN), where the "physics" corresponds to energy conservation constraints rather than physical laws.

4.4.2 Loss Function Design: Shape and Energy Constraints

A key strength of the hourly forecasting model lies in its dual-objective loss function, which combines:

- **Shape Loss (MSE Loss)**
  This component minimizes the difference between predicted and actual hourly load values, ensuring that the model accurately captures the temporal structure of demand.
- **Annual Energy Loss**
  This component ensures that the total energy obtained by integrating the predicted hourly load over time matches the corresponding annual energy target.

The combined loss function can be expressed conceptually as:

$$\text{Total Loss} = \lambda_{shape} \cdot \text{Shape Loss} + \lambda_{energy} \cdot \text{Energy Loss} \quad (4.1)$$

where the weighting factors balance the importance of temporal accuracy and energy consistency.

The implementation assigns higher weight to shape accuracy while still enforcing the energy constraint, ensuring that the model produces realistic load curves without deviating from annual projections.

4.4.3 Forecasting Methodology

The forecasting process proceeds sequentially, generating hourly demand for future days based on learned temporal patterns and evolving annual energy targets.

Key steps include:

- Scaling historical demand data for stable training
- Encoding temporal features such as seasonality and day-of-week effects
- Incorporating annual energy targets as an additional input feature

- Iteratively generating future daily load profiles using a rolling prediction window

The final output consists of a continuous hourly demand series spanning the forecast horizon, which is then combined with historical data and exported as pinn_forecast_combined.csv.

4.4.4 Consistency Between Annual and Hourly Demand

One of the most critical aspects of the proposed framework is the consistency between annual and hourly demand.

The hourly forecasts are not arbitrary extrapolations; instead, they are constrained such that their time-integrated energy matches the annual targets derived from the baseline and EV forecasting stage. During training, the model explicitly minimizes the difference between predicted annual energy (obtained by summing hourly outputs) and the actual annual energy target.

The results show that the forecasted annual energy derived from hourly predictions closely matches the predefined targets. For example, the forecasted energy for the year 2026 is aligned with the target value of approximately **16,424.2 GWh**, demonstrating the effectiveness of the energy constraint mechanism.

This consistency ensures that the hourly demand profiles are physically meaningful and directly compatible with system-level energy planning.

4.4.5 Temporal Characteristics of Hourly Load

The predicted hourly demand profiles exhibit clear temporal patterns consistent with real-world electricity consumption behavior. These include:

- **Daily cycles**, characterized by morning ramp-up, midday variation, and evening peaks
- **Seasonal variations**, reflecting changes in demand across different times of the year
- **Day-to-day variability**, capturing short-term fluctuations in demand

The model successfully preserves these patterns in the forecast period, indicating that it has effectively learned the underlying temporal structure of the demand data.

An example of the hourly forecast is illustrated in Figure, which shows the evolution of daily load profiles over the forecast horizon.

4.4.6 Advantages Over Unconstrained Hourly Forecasting

Traditional hourly forecasting approaches often rely on extrapolating historical patterns without enforcing consistency with annual energy projections. This can lead to discrepancies where the sum of hourly demand does not match the expected annual total.

The proposed approach addresses this limitation through the integration of energy constraints. The advantages include:

- **Energy Consistency**: Ensures alignment between annual and hourly forecasts
- **Physical Interpretability**: Produces demand profiles that are consistent with system-level energy requirements
- **Improved Reliability**: Reduces the risk of overestimation or underestimation in long-term forecasts

By combining data-driven learning with constraint-based calibration, the model achieves a balance between accuracy and realism.

4.4.7 Role in the Overall Framework

The hourly baseline-plus-EV demand serves as the foundational layer for the final integrated demand profile. At this stage, the demand reflects:

- Macro-driven baseline consumption
- Additional energy from EV adoption
- Realistic temporal distribution of demand

However, it does not yet include the effects of electric cooking, which are introduced in subsequent stages.

Therefore, this intermediate result represents the structural backbone of the final demand profile, onto which additional components are later superimposed.

This section demonstrates that the informed LSTM-based hourly forecasting model successfully bridges the gap between annual energy projections and high-resolution demand profiles. By incorporating both temporal learning and energy constraints, the

model produces hourly forecasts that are both accurate and physically consistent.

The resulting baseline-plus-EV hourly demand captures realistic load patterns and aligns with annual energy targets, providing a robust foundation for further demand disaggregation and integration.

In the next section, the focus shifts to electric cooking demand, where the temporal concentration of load introduces additional complexity into the overall demand profile.

4.5 Electric Cooking Disaggregation Results

While the previous section established the hourly demand profile for baseline and EV-driven electricity consumption, this section focuses on the disaggregation and characterization of electric cooking demand. Unlike EV demand, which primarily contributes to overall energy growth, electric cooking introduces time specific load concentrations, making it a critical factor in shaping intraday demand patterns.

The results presented in this section are derived from the predicted cooking profiles and associated datasets, including cooking_profiles_latest_365d.csv and the computed cooking share over a 24-hour cycle. The analysis highlights how cooking demand is distributed across time and how it interacts with the baseline load structure.

4.5.1 Temporal Distribution of Cooking Demand

The disaggregated cooking demand exhibits a highly non-uniform distribution across the day, with distinct peaks corresponding to typical meal preparation times. The results indicate two primary periods of elevated cooking activity:

- **Morning peak** (approximately 06:00–02:00)
- **Evening peak** (approximately 17:00–22:00)

Outside these intervals, cooking demand remains minimal, contributing negligibly to the overall load.

This temporal concentration reflects realistic household behavior patterns and confirms that electric cooking demand is inherently event driven rather than continuous.

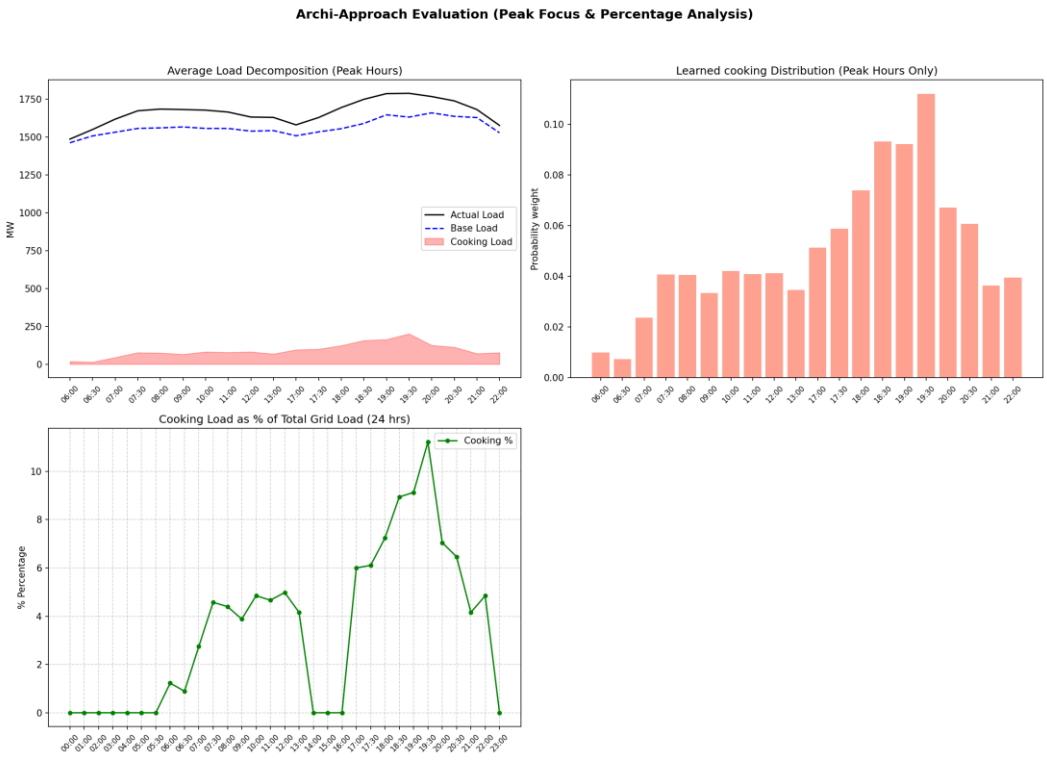

Figure 9: Predicted Intraday Electric Cooking Demand Distribution (24-Hour Profile)

4.5.2 Cooking Load as a Share of Total Demand

To quantify the relative importance of cooking demand, the cooking load was expressed as a percentage of total grid demand across the 24-hour cycle.
The results show that:

- Cooking contributes a significant share of demand during peak hours, particularly in the evening period.
- During off-peak hours, the cooking contribution is negligible.
- The average daily cooking share is moderate, but peak-hour contribution is disproportionately high.

This indicates that the impact of cooking demand is not adequately represented by annual energy values alone. Instead, its significance lies in its ability to amplify demand during already high-load periods.

4.5.3 Variability Across Days

The analysis of the latest 365 days of cooking profiles reveals that while the general shape of the cooking load remains consistent, there is noticeable variability in

magnitude across days.

This variation can be attributed to:

- Differences in daily usage intensity
- Seasonal behavioral patterns
- Variability in active stove population

Despite these fluctuations, the timing of peaks remains stable, reinforcing the conclusion that cooking demand is strongly tied to habitual daily routines.

4.5.4 Interaction with Baseline Load

When compared with the baseline-plus-EV load profile, cooking demand is observed to coincide with existing demand peaks, particularly in the evening period.

This overlap has important implications:

- Cooking demand does not create entirely new peaks but intensifies existing ones
- The combined effect leads to sharper and higher peak loads
- The system experiences increased stress during already critical periods

This interaction highlights the importance of considering not only the magnitude but also the timing of additional demand components.

4.5.5 Implications for Load Shape

The introduction of cooking demand significantly alters the overall load shape in the following ways:

- **Increased peak sharpness**: Load curves become steeper around peak hours
- **Higher peak-to-average ratio**: The difference between average and peak demand increases
- **Greater temporal concentration**: Demand becomes more clustered within specific time windows

These changes make the demand profile more challenging to manage from a grid operation perspective.

4.5.6 Significance Relative to Annual Energy

Although electric cooking contributes less to total annual energy compared to EV demand, its impact on the load profile is more pronounced.

This distinction is critical:

- EV demand primarily affects total energy consumption
- Cooking demand primarily affects load distribution and peak demand

Therefore, both components play complementary roles in shaping future electricity demand, and neither can be neglected in comprehensive forecasting studies.

4.5.7 Interpretation in the Context of Electrification

The results demonstrate that electric cooking represents a behavior-driven load component that reflects daily human activity patterns. As electrification policies promote the adoption of induction stoves, the aggregated effect of these individual behaviors becomes increasingly significant at the system level.

The concentration of cooking demand within specific time intervals suggests that widespread adoption of electric cooking could lead to system-wide synchronization effects, where large numbers of households draw power simultaneously.

Such synchronization has important implications for:

- Load balancing
- Demand-side management
- Infrastructure planning

This section shows that electric cooking demand is characterized by strong temporal concentration and consistent daily patterns. While its contribution to annual energy demand is relatively modest, its impact on the intraday load profile is substantial.

The results highlight that electric cooking plays a crucial role in shaping peak demand and overall load variability. When combined with baseline and EV demand, it introduces additional complexity into the demand profile, necessitating careful consideration in future grid planning.

The next section builds upon these findings by presenting the final calibration and integration process, where all demand components are combined into a unified, energy-

consistent demand profile.

4.6 Final Calibration and Energy-Consistent Data Processing

The preceding sections presented individual components of the forecasting framework, including annual energy projections, hourly baseline + EV demand, and disaggregated electric cooking profiles. While each component provides valuable insights, they originate from different models and operate at different temporal scales. Therefore, a final calibration and integration step is required to ensure that all components are mutually consistent and physically meaningful.

This section describes the final data processing stage, in which the outputs from multiple models are transformed, aligned, and combined into a unified demand dataset. The objective of this stage is to ensure that the final hourly demand profiles are consistent with both historical energy data and projected future energy scenarios.

4.6.1 Need for Calibration

The outputs of machine learning models, particularly when trained independently, may not automatically satisfy system-level constraints such as total annual energy consumption. For example:

- Hourly forecasts may exhibit correct temporal patterns but deviate from expected yearly energy totals
- Cooking profiles may capture realistic usage patterns but may not align with projected annual cooking energy
- Baseline and EV demand may be accurate at the aggregate level but not directly compatible with hourly profiles

Without calibration, these inconsistencies can lead to unrealistic demand projections and reduce the reliability of the results.

Therefore, a structured calibration process is essential to enforce energy consistency across temporal scales.

4.6.2 Scaling and Normalization of Demand Profiles

The first step in the calibration process involves transforming the hourly demand data into normalized energy representations.

Using the scaling procedure, the hourly demand values are converted into:

- **Hourly energy fractions** representing the proportion of daily energy distributed across time intervals
- **Daily scaling factors** representing the proportion of annual energy assigned to each day

This transformation allows the separation of load shape (temporal distribution) from energy magnitude (total consumption).

The resulting scaled dataset preserves the structure of the demand profile while enabling flexible adjustment of total energy levels.

4.6.3 Metadata-Based Energy Alignment

A key component of the calibration process is the use of metadata to store yearly energy totals. This metadata acts as a reference for reconstructing demand in physical units.

In this study, the metadata was carefully updated to reflect both historical observations and future projections:

- For the last three historical years, the yearly energy values were replaced with actual observed energy data
- For the forecast year, the yearly energy was updated using the sum of baseline and EV demand projections
- For cooking demand, the metadata was separately updated using predicted cooking energy values

This selective replacement ensures that the calibration process remains grounded in real-world data while incorporating scenario-based projections.

4.6.4 Upscaling to Physical Demand Values

Following normalization and metadata correction, the scaled demand profiles are converted back into physical units (MW) through an upscaling process.

This step reconstructs hourly demand using:

- The normalized load shape
- The corrected daily scaling factors

- The updated yearly energy values

The resulting demand profiles satisfy two critical conditions:

1. **Temporal accuracy**: The shape of the load profile is preserved
2. **Energy consistency**: The integrated hourly demand matches the target annual energy

This ensures that the final demand data is both realistic and aligned with system-level constraints.

4.6.5 Integration of Demand Components

After calibration, the baseline-plus-EV demand and cooking demand are combined to form the final integrated demand profile.

The integration process involves:

- Aligning the cooking demand profiles with the corresponding time period in the baseline demand
- Adding cooking demand to the baseline-plus-EV demand for the relevant time intervals
- Generating a complete demand dataset spanning multiple years

The final dataset includes both the full multi-year demand series and a focused subset representing the latest year, which is used for detailed analysis in subsequent sections.

4.6.6 Resulting Data Consistency

The calibrated and integrated dataset exhibits a high degree of consistency across all levels of analysis:

- Annual energy values match projected targets
- Daily energy distribution aligns with normalized scaling factors
- Hourly demand profiles retain realistic temporal patterns

This consistency confirms the effectiveness of the calibration process in reconciling outputs from different models.

4.6.7 Importance of the Calibration Framework

The calibration stage represents a critical contribution of this study. Rather than relying on direct outputs from individual models, the framework ensures that all results are harmonized within a unified energy-consistent structure.

This approach offers several advantages:

- **Improved realism**: Demand projections reflect both statistical patterns and physical constraints
- **Cross-scale consistency**: Annual and hourly results are fully aligned
- **Flexibility**: Scenario adjustments can be incorporated through metadata updates
- **Robustness**: Reduces propagation of model-specific errors

By enforcing these properties, the calibration framework enhances the reliability of the final demand projections.

This section presented the final calibration and data processing stage of the forecasting framework. Through scaling, metadata correction, and upscaling, the study ensures that all demand components are consistent across temporal scales and aligned with both historical data and future projections.

The calibrated dataset forms the basis for the final integrated demand analysis, where the combined effects of baseline demand, EV adoption, and electric cooking are examined in detail.

The next section presents the resulting integrated demand profiles and their implications for overall load behavior.

4.7 Final Integrated Demand Results

Following the calibration and energy alignment process, the final step in the forecasting framework involves the integration of all demand components into a unified electricity demand profile. This section presents the resulting integrated demand, combining:

- Baseline demand driven by macroeconomic factors
- Additional demand from electric vehicle (EV) adoption
- Time-specific demand from electric cooking

The integration produces a fully calibrated hourly demand dataset, which represents the most realistic projection of future electricity demand under the considered electrification scenarios. The results discussed in this section are derived from the final combined dataset generated through the integration process and visualized using demand plots.

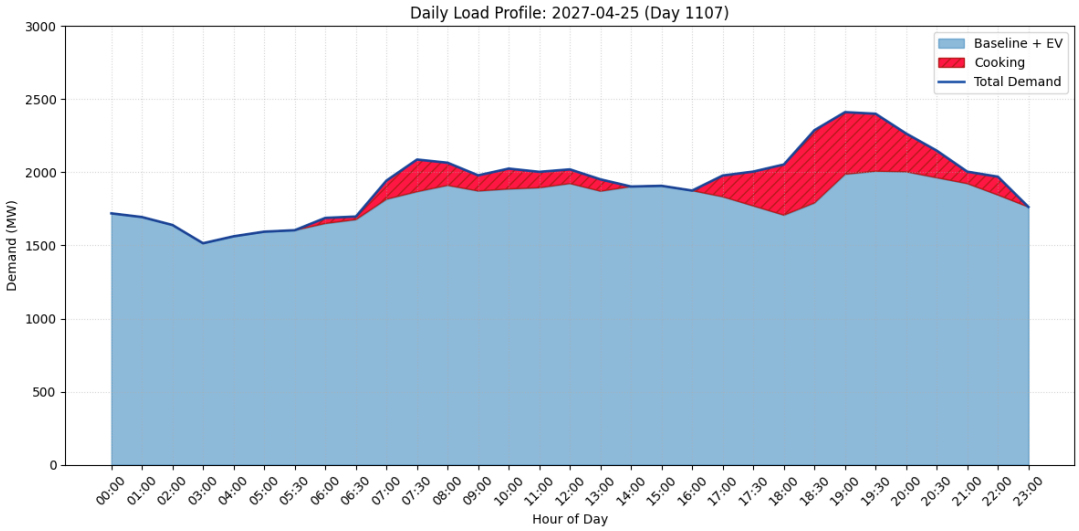

Figure 10: Integrated Electricity Demand Showing Baseline + EV and Cooking Contributions

4.7.1 Structure of the Integrated Demand

The final demand profile consists of two primary components:

- **Baseline + EV Demand**
  This represents the underlying demand structure, including macro-driven growth and electrification of mobility.
- **Electric Cooking Demand**
  This is superimposed on the baseline demand and contributes additional load during specific time intervals.

The integration process ensures that cooking demand is added only to the relevant time periods, resulting in a demand profile that reflects both continuous and event-driven consumption patterns.

4.7.2 Characteristics of the Integrated Load Profile

The integrated demand profile exhibits several important characteristics:

- **Overall increase in demand level**: The inclusion of EV demand raises the baseline load across all time periods.
- **Localized load intensification**: Cooking demand introduces additional peaks during specific hours of the day.
- **Preservation of temporal structure**: The underlying daily and seasonal patterns remain consistent with historical behavior.

These characteristics demonstrate that the final demand profile is not merely an aggregate of components but a structured combination that reflects both magnitude and timing of electricity use.

4.7.3 Daily Demand Profiles

Analysis of daily demand profiles reveals how different components interact over a typical day.

The results show that:

- The baseline + EV demand forms a smooth curve with gradual variations throughout the day
- The cooking demand appears as distinct spikes during meal preparation times
- The total demand reflects the superposition of these effects, resulting in sharper peaks

In particular, the evening period shows the most pronounced increase in demand due to the alignment of cooking activity with already high baseline consumption.

Representative daily plots further illustrate that the addition of cooking demand significantly modifies the load curve, especially during peak hours, while having minimal impact during off-peak periods.

4.7.4 Seasonal Variation in Integrated Demand

The integrated demand profile also exhibits seasonal variations, reflecting differences in electricity usage across the year.

The results indicate that:

- Baseline demand varies across seasons due to climatic and behavioral factors

- Cooking demand remains relatively consistent in timing but varies in magnitude
- Peak demand periods may shift slightly depending on seasonal conditions

Seasonal shading in the demand plots highlights how the combined effect of baseline and cooking demand evolves over time, providing insight into potential seasonal stress on the grid.

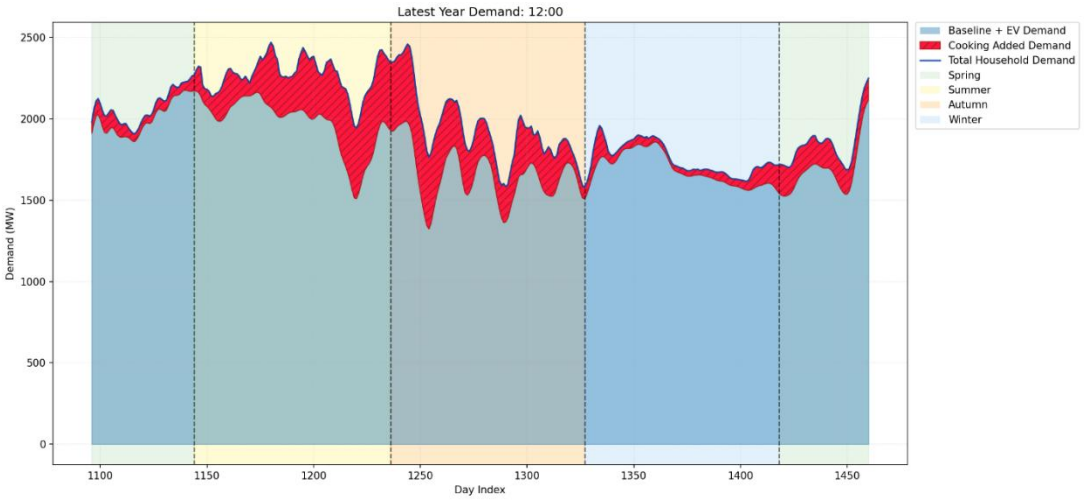

Figure 11: Seasonal Variation of Electricity Demand Across the Latest Forecast Year

4.7.5 Contribution of Cooking Demand to Total Load

The contribution of cooking demand to the total load is most visible when comparing the integrated demand with the baseline + EV demand.

The results show that:

- Cooking demand has a negligible impact during off-peak hours
- During peak hours, it contributes a noticeable increase in total demand
- The magnitude of this increase varies depending on the day and overall load conditions

This reinforces the earlier observation that cooking demand plays a critical role in shaping peak demand rather than significantly increasing total energy consumption.

4.7.6 Comparison with Baseline-Only Scenario

A comparison between the integrated demand profile and the baseline-only scenario highlights the cumulative impact of electrification.

Key observations include:

- The baseline-only profile underestimates both total demand and peak intensity
- The baseline + EV profile captures overall demand growth but lacks peak amplification
- The fully integrated profile reflects both increased energy consumption and intensified peak demand

This comparison demonstrates that each additional component contributes uniquely to the overall demand profile, and all must be considered for accurate forecasting.

4.7.7 Implications for Grid Operation

The integrated demand results have several important implications for power system operation:

- **Increased system load**: Higher overall demand requires additional generation capacity
- **Enhanced peak stress**: Concentrated cooking demand increases peak load requirements
- **Greater variability**: The combination of continuous and event-driven demand introduces complexity in load management

These factors highlight the need for advanced demand management strategies and infrastructure planning to accommodate future electricity demand.

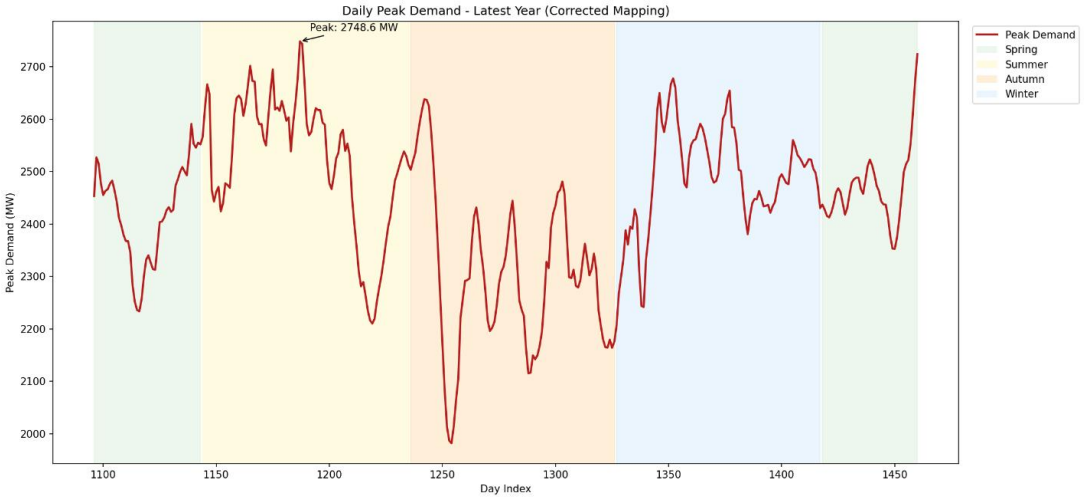

Figure 12: Peak Demand of the forecasted Year

4.7.8 Role in the Overall Framework

The integrated demand profile represents the culmination of the forecasting framework, combining all modeled components into a single, coherent dataset.
This dataset serves as the basis for:

- Peak demand analysis
- Daily and seasonal load assessment
- Grid planning and policy evaluation

By ensuring consistency across all stages, the final integrated demand provides a reliable foundation for assessing the impact of electrification on the power system.

This section presented the final integrated demand results, demonstrating how baseline demand, EV adoption, and electric cooking collectively shape future electricity consumption.

The results show that while EV demand primarily increases overall energy consumption, electric cooking significantly alters the load profile by introducing time-specific demand peaks. The combined effect results in a more complex and demanding load structure.

The next section builds upon these findings by analyzing daily and seasonal demand behavior in greater detail, providing further insight into the temporal dynamics of electricity demand.

4.8 Daily Demand Behavior and Seasonal Variation

While the integrated demand profile provides an overall view of future electricity consumption, a deeper understanding requires analysis at finer temporal scales. In particular, daily and seasonal variations reveal how demand evolves over time and how different components interact under varying conditions.

This section examines the behavior of electricity demand on a daily basis and across different seasons, using the final integrated dataset. The analysis focuses on identifying recurring patterns, variability in load profiles, and the influence of electric cooking on both daily and seasonal demand characteristics.

4.8.1 Daily Load Profile Characteristics

The daily load profiles exhibit a consistent and structured pattern throughout the year. A typical day is characterized by three main phases:

- **Morning rise**: Demand increases as households and commercial activities begin
- **Midday stabilization**: Load levels vary moderately depending on activity patterns
- **Evening peak**: Demand reaches its maximum due to combined residential and commercial usage

The inclusion of EV demand results in a general upward shift in the load curve, while the addition of cooking demand introduces sharp increases during specific time intervals.

The daily demand curves maintain a high degree of consistency in shape, indicating that the model effectively preserves temporal load patterns even under changing demand conditions.

4.8.2 Influence of Electric Cooking on Daily Profiles

Electric cooking has a distinct impact on daily demand behavior. Its influence is concentrated within specific time windows, leading to noticeable modifications in the load curve.

Key observations include:

- **Amplification of existing peaks**: Cooking demand coincides with periods of high baseline demand, particularly in the evening
- **Sharp transitions**: The load curve becomes steeper during cooking periods, reflecting rapid increases in demand
- **Minimal off-peak impact**: Outside cooking hours, the demand profile remains largely unaffected

These effects demonstrate that cooking demand does not alter the overall structure of the load curve but significantly modifies its intensity during critical periods.

4.8.3 Day-to-Day Variability

Although the general shape of the daily load profile remains consistent, there is observable variability in demand magnitude across different days.

This variability arises from several factors:

- Changes in baseline demand due to economic and social activity
- Seasonal influences such as temperature and daylight duration
- Variations in cooking intensity and usage patterns

Despite these fluctuations, the timing of peak demand remains relatively stable, indicating that daily routines strongly influence electricity usage patterns.

4.8.4 Seasonal Demand Variation

The analysis of seasonal trends reveals that electricity demand exhibits noticeable variation across different periods of the year.

The results indicate that:

- **Higher demand periods** occur during certain seasons, reflecting increased usage of electrical appliances and lighting
- **Lower demand periods** correspond to seasons with reduced energy needs

The overall demand level shifts across seasons while maintaining a consistent daily structure. Seasonal shading in the demand plots illustrates these variations, providing a clear visual representation of how demand evolves throughout the year.

4.8.5 Interaction Between Seasonality and Cooking Demand

Electric cooking demand interacts with seasonal variation in a manner that further influences the load profile.

Key findings include:

- Cooking demand remains temporally consistent across seasons, with peaks occurring at similar times each day
- The magnitude of cooking demand varies depending on the overall demand level
- During high-demand seasons, cooking demand contributes to more pronounced

peak loads

This interaction suggests that cooking demand can exacerbate seasonal peak conditions, particularly when it coincides with periods of already elevated baseline demand.

4.8.6 Implications for Load Variability

The combined effect of daily and seasonal variations results in a demand profile that is both structured and dynamic.
Important implications include:

- **Increased variability**: The demand profile becomes more complex due to the interaction of multiple components
- **Predictable peak timing**: Despite variability, peak periods remain relatively consistent
- **Higher operational complexity**: Managing demand requires consideration of both daily cycles and seasonal shifts

These characteristics highlight the importance of high-resolution demand forecasting in modern power systems.

4.8.7 Representative Daily Profiles

Representative daily plots from different seasons further illustrate the variability in demand behavior.
These plots show that:

- The overall shape of the load curve remains consistent across seasons
- Peak demand levels vary depending on seasonal conditions
- Cooking demand consistently appears as localized spikes within the daily profile

Such visual analysis reinforces the quantitative findings and provides intuitive insight into demand dynamics.

4.8.8 Relevance to Power System Planning

Understanding daily and seasonal demand behavior is essential for effective power system planning and operation.

The results indicate that:

- Generation scheduling must account for predictable daily peaks
- Seasonal variations require adaptive planning strategies
- Demand-side management may be necessary to mitigate peak loads

The integration of electric cooking further emphasizes the need for strategies that address time-specific demand increases.

This section demonstrates that electricity demand exhibits structured daily patterns combined with seasonal variability. The addition of electric cooking enhances peak intensity without significantly altering the timing of demand.

The results highlight the importance of analyzing demand at multiple temporal scales, as both daily and seasonal variations play a critical role in determining overall grid behavior.

The next section builds on this analysis by focusing on peak demand, providing a detailed assessment of the maximum load conditions that the power system must accommodate.

4.9 Peak Demand Analysis

Peak demand represents the most critical operating condition of a power system, as it defines the maximum instantaneous load that must be supplied. While annual energy demand reflects the total electricity requirement, peak demand determines infrastructure sizing, system reliability, and operational constraints. Therefore, assessing peak demand is essential to directly evaluate the impact of electrification on grid demand, as highlighted in the title of this study.

In this work, peak demand is extracted from the final integrated hourly dataset using a dedicated analysis procedure. The method computes daily maximum demand, identifies the corresponding peak time, and ranks the highest-demand days in the latest forecast year.

4.9.1 Overall Peak Demand Result

The analysis shows that the maximum system peak demand reaches 2748.61 MW, which represents the highest load condition in the forecast horizon.

- **Peak Demand:** 2748.61 MW
- **Date:** 14 July 2026
- **Time:** 19:00

This value is not an isolated statistical output but a physically meaningful result derived from the fully integrated demand framework. It reflects the combined influence of:

- Baseline demand growth,
- Ev-driven load increase, and
- Electric cooking demand concentrated in peak hours.

Thus, this peak value directly represents the maximum stress point of the future electricity system.

4.9.2 Top 10 Peak Demand Days

To understand the distribution of system stress, the top 10 peak-demand days were identified and ranked, as shown in Table 4.

Table 4:Top 10 Peak Demand Days in the Latest Forecast Year

Rank	Day	Date	Peak Demand (MW)	Peak Time
1	1187	2026-07-14	2748.61	19:00
2	1188	2026-07-15	2744.08	19:00
3	1460	2027-04-12	2724.43	19:30
4	1165	2026-06-22	2702.02	19:00
5	1175	2026-07-02	2695.12	19:30
6	1352	2026-12-26	2678.19	18:30
7	1186	2026-07-13	2677.45	19:00
8	1459	2027-04-11	2673.40	19:30
9	1189	2026-07-16	2673.36	19:00
10	1166	2026-06-23	2673.14	19:00

4.9.3 Distribution and Clustering of Peak Days

The results indicate that peak demand is **not limited to a single extreme day**, but occurs across multiple days with similar magnitude. The relatively small difference between the highest and tenth-highest peak (approximately 75 MW) suggests that the system repeatedly operates close to its maximum capacity.

A clear seasonal clustering of peak days is observed:

- **June–July (summer period):** dominant concentration of highest peaks
- **April (spring period):** secondary cluster
- **December (winter period):** isolated high-demand events

This distribution indicates that peak demand is influenced by both seasonal baseline demand variations and electrification effects, rather than random fluctuations.

4.9.4 Temporal Characteristics of Peak Demand

A key finding is the strong consistency in peak timing:

- Most peak events occur between **19:00 and 19:30**
- A few occur slightly earlier around **18:30**

This consistency reflects the alignment of peak demand with evening activity periods, when multiple electricity uses coincide. The narrow time window of peak occurrence indicates that demand is highly synchronized during evening hours.

4.9.5 Causes of Peak Demand Formation

The observed peak demand results from the interaction of three major demand components:

4.9.5.1 Baseline Demand

Baseline demand provides the fundamental load structure, driven by macroeconomic factors such as GDP growth, population increase, urbanization, and rising electricity consumption per capita.

4.9.5.2 Electric Vehicle Demand

EV demand significantly increases the overall load level. As shown in the annual analysis, EV energy demand grows rapidly over the forecast period, contributing

substantially to total electricity consumption.

4.9.5.3 Electric Cooking Demand

Electric cooking demand is highly concentrated in time and occurs primarily during meal preparation periods. This demand coincides with existing peak hours, thereby amplifying load intensity.

4.9.5.4 Combined Effect

The system peak is therefore not caused by any single component but by their simultaneous occurrence. The peak demand emerges from the coincidence of high baseline load, elevated EV demand, and synchronized electric cooking activity during evening hours.

4.9.6 Role of Electric Cooking in Peak Amplification

One of the most important findings of this study is the role of electric cooking in shaping peak demand.

Although cooking demand contributes less to total annual energy, it has a disproportionately large impact on peak load because:

- It is concentrated within specific time intervals,
- It coincides with existing demand peaks, and
- It amplifies already high load conditions.

This confirms that electric cooking acts as a peak amplifier, significantly influencing the maximum system load.

4.9.7 Peak Demand vs Annual Energy Demand

The results reveal a critical distinction between energy demand and peak demand. The Annual Energy is found to be the prime driver of EV Demand whereas Peak Demand Formation is found to be the prime driver of Cooking Demand.

This distinction is essential for system planning:

- Annual energy determines long-term generation requirements
- Peak demand determines real-time capacity and infrastructure limits

Ignoring this difference would lead to underestimation of system stress conditions.

4.9.8 Implications for Grid Planning

The peak demand analysis has several important implications:

- **Generation Capacity**: The system must be capable of supplying approximately **2750 MW** to meet future peak demand.
- **Transmission and Distribution**: Infrastructure must handle highly concentrated demand during peak periods, requiring reinforcement of network capacity.
- **Demand-Side Management**: Strategies such as time-of-use pricing and load shifting may be necessary to reduce peak demand intensity.
- **Operational Flexibility**: Hydropower-dominated systems must provide rapid response to steep evening demand increases.

The final integrated demand reveals that electrification increases not only total electricity consumption but also intensifies peak demand, making peak load the primary constraint for future grid planning.

This section directly addressed the grid-impact dimension of the study by analyzing peak demand under electrification scenarios. The results show that the maximum system demand reaches **2748.61 MW**, occurring during evening hours when baseline, EV, and cooking demand coincide.

The analysis demonstrates that peak demand is more critical than total energy demand for system planning, as it defines the most demanding operating condition. Furthermore, electric cooking plays a key role in amplifying peak load despite its smaller contribution to annual energy.

Overall, the peak-demand results provide a realistic and actionable understanding of future grid stress, reinforcing the importance of scenario-based, high-resolution demand forecasting in modern power systems.

4.10 Overall Discussion and Grid Planning Implications

This section synthesizes the findings from the preceding analyses and interprets them in the context of power system planning. The study integrates annual energy forecasting, hourly load modeling, electric mobility demand, and electric cooking demand into a unified framework. As a result, the discussion moves beyond isolated

results and focuses on the combined implications of electrification on both energy demand and load behavior.

The central objective of this thesis is to assess how electric cooking and electric mobility influence future grid demand. The results demonstrate that their impact is multi-dimensional, affecting not only the magnitude of electricity consumption but also its temporal distribution and peak characteristics.

4.10.1 Implications of Annual Demand Growth

The annual forecasting results indicate a substantial increase in total electricity demand over the forecast horizon. This growth is driven by two primary factors:

- Structural socio-economic changes reflected in baseline demand
- Additional electrification loads from EV adoption and electric cooking

Among these, EV demand emerges as the dominant contributor to incremental annual energy growth. Its rapid expansion significantly increases the total electricity requirement, effectively shifting the demand trajectory upward.

Electric cooking, while contributing less to total annual energy, still represents a consistent and policy-driven increase in demand. When combined with baseline growth, these components lead to a substantial increase in total electricity consumption.

From a planning perspective, this implies that future generation capacity must be expanded to meet not only baseline growth but also the additional energy demand associated with electrification.

4.10.2 Implications of Hourly Load Structure

While annual energy demand determines the overall scale of electricity requirements, the hourly distribution of demand determines how the system must operate in real time.

The hourly forecasting results demonstrate that:

- Baseline demand establishes the fundamental load structure
- EV demand increases the overall load level across all hours
- Cooking demand introduces concentrated load additions during specific time intervals

The inclusion of cooking demand significantly modifies the load curve, particularly

during peak periods. This results in sharper demand transitions and increased load concentration within specific time windows.

These findings highlight that the future electricity system will not only face higher demand but also more complex and dynamic load behavior.

4.10.3 Implications of Peak Demand

Peak demand represents the most critical condition that the power system must be designed to handle. The analysis of the final integrated demand profile shows that peak demand is influenced by the combined effect of all demand components.

The results indicate that:

- EV demand increases the overall load level, raising the baseline upon which peaks occur
- Electric cooking intensifies demand during peak hours due to its temporal concentration
- The system peak emerges from the overlap of these effects

This demonstrates that peak demand is not simply a function of total energy growth but is strongly influenced by the timing of demand components.

From a planning perspective, this means that ensuring adequate generation capacity alone is insufficient. The system must also be capable of handling short duration high load events, which may place additional stress on transmission and distribution infrastructure.

4.10.4 Relevance to Hydropower-Dominated Systems

The findings of this study are particularly relevant in the context of a hydropower-dominated electricity system, such as that of Nepal.

Hydropower systems are generally well-suited for meeting base-load and flexible generation requirements. However, they may face challenges under the following conditions:

- **High peak demand periods**, especially when water availability is limited
- **Seasonal variability**, which affects generation capacity
- **Rapid demand fluctuations**, requiring responsive load balancing

The increase in peak demand and load variability observed in this study suggests that future electricity systems may require:

- Enhanced operational flexibility
- Improved storage solutions
- Better coordination between generation and demand

The integration of electric cooking and EV demand therefore introduces new operational considerations that extend beyond traditional hydropower planning.

4.10.5 Need for Coordinated Energy Planning

The results emphasize the importance of coordinated planning across multiple dimensions of the power system.

Key considerations include:

- **Generation planning**: Ensuring sufficient capacity to meet both annual energy demand and peak load requirements
- **Transmission and distribution planning**: Upgrading infrastructure to handle increased and more concentrated demand
- **Demand-side management**: Implementing strategies to shift or reduce peak demand

The interaction between baseline demand, EV adoption, and cooking demand highlights that these components cannot be treated independently. Instead, a holistic approach is required to ensure system reliability and efficiency.

4.10.6 Importance of Scenario-Based Forecasting

One of the key contributions of this study is the use of scenario-based forecasting to explicitly incorporate electrification effects into demand projections.
The results show that:

- Ignoring EV and cooking demand leads to significant underestimation of future electricity requirements
- Annual-only forecasting fails to capture the temporal concentration of demand
- Scenario-based hourly forecasting provides a more realistic representation of

future grid conditions

By integrating multiple demand components and temporal scales, the proposed framework enables a more comprehensive assessment of future electricity demand.

4.10.7 Energy vs Peak: A Critical Distinction

A central insight from this study is the distinction between energy demand and peak demand.

- EV demand primarily affects total energy consumption
- Cooking demand primarily affects peak load and load shape

This distinction is crucial for system planning. While energy demand determines long-term generation requirements, peak demand dictates short-term operational capacity and infrastructure limits.

Effective planning must therefore address both aspects simultaneously.

4.10.8 Implications for Policy and Electrification Strategies

The results have important implications for policy design and electrification strategies. Policies promoting electric mobility and cooking should consider:

- The potential increase in total electricity demand
- The impact on peak load and load distribution
- The need for supporting infrastructure and demand management measures

For example, encouraging staggered usage patterns or time-of-use pricing could help mitigate peak demand effects.

4.10.9 Key Findings

The overall findings of this study can be summarized as follows:

- Electricity demand is expected to grow significantly due to both baseline factors and electrification
- EV demand is the primary driver of additional annual energy consumption
- Electric cooking has a strong impact on intraday load distribution and peak demand

- The combined effect results in a more complex and demanding load profile
- Scenario-based hourly forecasting provides a more accurate representation of future grid conditions than traditional methods

This section synthesized the results of the study and discussed their implications for power system planning. The findings highlight that electrification affects electricity demand in multiple dimensions, including total energy, load shape, and peak demand.

The study demonstrates the importance of integrating annual and hourly forecasting approaches and incorporating scenario-based demand components to obtain realistic and actionable insights.

The final section concludes the chapter by summarizing the key outcomes and linking them to the broader objectives of the research.

This chapter presented a comprehensive analysis of future electricity demand by integrating annual forecasting, hourly load modeling, electric mobility demand, and electric cooking demand within a unified framework. The results were discussed progressively, beginning with the validation of the annual forecasting model and extending through to the final integrated demand and peak analysis.

The evaluation of the forecasting model demonstrated that the LSTM-based approach provides reliable and accurate predictions of baseline electricity demand, thereby establishing a strong foundation for scenario-based analysis. The subsequent examination of macro-level drivers confirmed that structural socio-economic changes, including GDP growth, urbanization, and increasing electricity consumption per capita, will continue to drive baseline demand upward in the coming years.

The incorporation of electrification scenarios revealed that electric mobility significantly increases total annual energy demand, while electric cooking introduces additional demand that is more modest in magnitude but highly concentrated in time. This distinction was further emphasized in the hourly analysis, where EV demand contributed to an overall upward shift in load, whereas cooking demand altered the intraday load structure by intensifying peak periods.

The calibrated integration of all demand components ensured consistency across temporal scales, resulting in a realistic representation of future electricity demand. The analysis of daily and seasonal variations highlighted the persistence of structured load

patterns, alongside increased variability and peak intensity due to electrification.

Most importantly, the peak demand analysis demonstrated that the combined effect of baseline growth, EV adoption, and electric cooking leads to a significant increase in maximum system load. This finding directly addresses the core objective of the study, showing that electrification affects not only total energy requirements but also the most critical operating conditions of the power system.

Overall, the results highlight the necessity of adopting scenario-based and high-resolution forecasting approaches for effective energy planning. The integrated framework developed in this study provides a more comprehensive understanding of future demand dynamics compared to conventional methods that rely solely on aggregated projections.

CHAPTER FIVE: CONCLUSION AND FUTURE WORK

5.1 Conclusion

This study presented a comprehensive framework for assessing the impact of electric cooking and electric mobility on future electricity demand through a scenario-based hourly load forecasting approach. By integrating macro-level annual forecasting, high-resolution hourly modeling, demand disaggregation, and final energy-consistent calibration, the research provides a detailed and realistic representation of future grid demand.

The results demonstrate that electricity demand is expected to increase significantly due to both structural socio-economic growth and electrification. The baseline demand, driven by GDP growth, population increase, urbanization, and rising electricity consumption per capita, establishes a strong upward trajectory in energy consumption. The forecasting model, validated through comparison with persistence and ARIMA benchmarks, achieved high accuracy and reliability, confirming its suitability for long-term demand prediction.

The incorporation of electrification scenarios reveals that electric mobility is the dominant contributor to additional annual energy demand. EV energy demand increases rapidly over the forecast period, significantly raising total electricity consumption and shifting the overall demand curve upward. In contrast, electric cooking contributes a comparatively smaller share of annual energy but introduces highly concentrated demand within specific time intervals.

A key contribution of this study is the integration of annual and hourly forecasting scales. The informed LSTM-based hourly model ensures that the predicted load profiles are consistent with annual energy targets while preserving realistic temporal patterns. This cross-scale consistency enhances the reliability and physical interpretability of the results.

The disaggregation of electric cooking demand further highlights the importance of temporal analysis. Cooking demand is shown to be strongly concentrated during morning and evening periods, aligning with household activity patterns. When integrated with baseline and EV demand, this results in sharper and higher peaks in the overall load profile.

The peak demand analysis provides the most critical insight of the study. The results indicate that the system peak reaches approximately **2748.61 MW**, occurring during evening hours when baseline demand, EV load, and cooking demand coincide. This demonstrates that electrification affects not only total energy requirements but also the most critical operating conditions of the grid.

A fundamental distinction emerges between the roles of EV and electric cooking:

- EV demand primarily drives annual energy growth
- Electric cooking primarily influences intraday load structure and peak demand

This distinction is crucial for power system planning. While energy demand determines long-term generation requirements, peak demand dictates real-time operational constraints and infrastructure capacity.

Overall, the study shows that conventional annual-only forecasting approaches are insufficient for capturing the full impact of electrification. Scenario-based hourly forecasting provides a more accurate and actionable representation of future demand by accounting for both magnitude and temporal distribution.

The findings are particularly relevant for hydropower-dominated systems, where the ability to meet peak demand and manage temporal variability is as important as total energy availability. The results highlight the need for integrated planning strategies that consider both energy growth and peak load dynamics.

5.1.1 Contributions of the Study

This research makes several important contributions to the field of electricity demand forecasting and energy planning:

- **Integrated Multi-Scale Framework**
  The study combines annual forecasting, hourly load modeling, and demand disaggregation into a unified framework, ensuring consistency across temporal scales.
- **Scenario-Based Demand Modeling**
  Explicit incorporation of electric mobility and electric cooking enables a realistic assessment of future electrification impacts.
- **Energy-Consistent Calibration Approach**

The scale–metadata–upscale framework ensures alignment between model outputs and physical energy constraints, improving reliability.

- **High-Resolution Demand Insights**
  The use of hourly forecasting reveals detailed load patterns and peak behavior that are not captured by aggregate models.
- **Peak Demand Characterization**
  The study provides a clear understanding of how electrification influences peak demand, identifying cooking demand as a key peak driver.

5.1.2 Implications for Power System Planning

The results of this study have direct implications for future electricity planning and policy development:

- **Generation Planning**
  Future capacity expansion must account for both increased annual energy demand and higher peak load requirements.
- **Grid Infrastructure**
  Transmission and distribution systems must be upgraded to handle concentrated demand during peak periods.
- **Demand-Side Management**
  Strategies such as time-of-use pricing and load shifting may be necessary to mitigate peak demand.
- **Operational Flexibility**
  Hydropower and other flexible resources must be managed to respond to rapid changes in demand, particularly during evening peaks.
- **Policy Design**
  Electrification policies should consider not only energy benefits but also their impact on load patterns and system stress.

5.2 Future Work

Several directions for future research can build upon the findings of this study:

- Integration with Supply-Side Modeling: Future work can incorporate

hydropower generation modeling, including seasonal water availability and reservoir operation, to assess supply-demand balance.

- EV Charging Behavior Modeling: More detailed modeling of EV charging patterns, including fast charging, home charging, and smart charging strategies, can improve accuracy.
- Demand Response and Load Management: Incorporating demand-side management strategies, such as time-of-use tariffs and smart appliances, can help evaluate peak reduction potential.
- Climate and Weather Integration: Including temperature, rainfall, and climate variability can improve both annual and hourly demand forecasts.
- Long-Term Forecast Extension: Extending the analysis to 2040 or 2045 would align with long-term policy targets and net-zero commitments.
- Spatial Demand Modeling: Future studies can analyze demand distribution across regions to support localized grid planning.
- Real-Time Grid Simulation: Integration with power system simulation tools can provide insights into voltage stability, frequency response, and network constraints.

5.3 Final Remarks

This study demonstrates that electrification is not merely an increase in electricity consumption but a transformation of demand behavior. The combined effects of electric mobility and electric cooking reshape both the magnitude and timing of electricity demand, creating new challenges and opportunities for power system planning.

By adopting a scenario-based, high-resolution forecasting approach, this research provides a more comprehensive understanding of future grid demand and offers a robust foundation for informed decision-making in the transition toward electrified energy systems.

REFERENCES

Adhikari, M., Ghimire, L. P., Kim, Y., Aryal, P., & Khadka, S. B. (2020). Identification and Analysis of Barriers against Electric Vehicle Use. *Sustainability 2020, Vol. 12, Page 4850*, *12*(12), 4850. https://doi.org/10.3390/SU12124850

Alizadegan, H., Rashidi Malki, B., Radmehr, A., Karimi, H., & Ilani, M. A. (2025). Comparative study of long short-term memory (LSTM), bidirectional LSTM, and traditional machine learning approaches for energy consumption prediction. *Energy Exploration and Exploitation*, *43*(1), 281–301. https://doi.org/10.1177/01445987241269496;PAGEGROUP:STRING:PUBLICATION

Amir, M., Zaheeruddin, Haque, A., Bakhsh, F. I., Kurukuru, V. S. B., & Sedighizadeh, M. (2024). Intelligent energy management scheme-based coordinated control for reducing peak load in grid-connected photovoltaic-powered electric vehicle charging stations. *IET Generation, Transmission & Distribution*, *18*(6), 1205–1222. https://doi.org/10.1049/gtd2.12772

Baral, A., Parajuli, R., & Aryal, B. (2000). Institutional responses to electric vehicle promotion in Nepal. *Studies in Nepali History and Society*, *5*(1), 89–125.

Bhandari, R., & Pandit, S. (2018). Electricity as a Cooking Means in Nepal—A Modelling Tool Approach. *Sustainability 2018, Vol. 10, Page 2841*, *10*(8), 2841. https://doi.org/10.3390/SU10082841

Birk Jones, C., Vining, W., Lave, M., Haines, T., Neuman, C., Bennett, J., & Scoffield, D. R. (2022). Impact of Electric Vehicle customer response to Time-of-Use rates on distribution power grids. *Energy Reports*, *8*, 8225–8235. https://doi.org/10.1016/j.egyr.2022.06.048

Clements, W., Silwal, K., Pandit, S., Leary, J., Gautam, B., Williamson, S., Tran, A., & Harper, P. (2020a). Unlocking electric cooking on Nepali micro-hydropower mini-grids. *Energy for Sustainable Development*, *57*, 119–131. https://doi.org/10.1016/j.esd.2020.05.005

Clements, W., Silwal, K., Pandit, S., Leary, J., Gautam, B., Williamson, S., Tran, A., & Harper, P. (2020b). Unlocking electric cooking on Nepali micro-hydropower mini-grids. *Energy for Sustainable Development*, *57*, 119–131. https://doi.org/10.1016/J.ESD.2020.05.005

Deb, S., Kalita, K., & Mahanta, P. (2017). Review of impact of electric vehicle charging station on the power grid. *2017 International Conference on Technological Advancements in Power and Energy (TAP Energy)*, 1–6. https://doi.org/10.1109/TAPENERGY.2017.8397215

Demirci, A., Tercan, S. M., Cali, U., & Nakir, I. (2023). A Comprehensive Data Analysis of Electric Vehicle User Behaviors Toward Unlocking Vehicle-to-Grid Potential. *IEEE Access*, *11*, 9149–9165. https://doi.org/10.1109/ACCESS.2023.3240102

Ghanbari, R., & Borna, K. (2021). Multivariate Time-Series Prediction Using LSTM Neural Networks. *26th International Computer Conference, Computer Society of Iran, CSICC 2021*. https://doi.org/10.1109/CSICC52343.2021.9420543

Giri, T., Paneru, B., Bhattarai, N., Chaudhary, J., Paneru, B., & Poudyal, R. (2026). Enhancing EV charging in Nepal: Strategic sizing and placement of solar – Powered battery system in Byasi Feeder. *Renewable Energy*, *256*, 124145. https://doi.org/10.1016/J.RENENE.2025.124145

Gould, C. F., Bejarano, M. L., De La Cuesta, B., Jack, D. W., Schlesinger, S. B., Valarezo, A., & Burke, M. (2023). Climate and health benefits of a transition from gas to electric cooking. *Proceedings of the National Academy of Sciences*, *120*(34). https://doi.org/10.1073/pnas.2301061120

Guayanlema, V., Martínez-Gómez, J., Fontalvo, J., & Espinoza, V. S. (2024). Modeling the Benefits of Electric Cooking in Ecuador: A Long-Term Perspective. *Processes*, *12*(11), 2400. https://doi.org/10.3390/pr12112400

Jenn, A., & Highleyman, J. (2022). Distribution grid impacts of electric vehicles: A California case study. *IScience*, *25*(1), 103686. https://doi.org/10.1016/j.isci.2021.103686

Jha, A. K., Darlami, H. B., Bhattarai, N., Karn, S., & Neupane, G. (2025). Current State and Energy Policy Roadmap for Sustainable Adoption of Electric Vehicles in Nepal. *International Journal of Energy Economics and Policy*, *15*(4), 272–281. https://doi.org/10.32479/IJEEP.18634

Kadurek, P., Ioakimidis, C., & Ferrao, P. (2009). Electric Vehicles and their impact to the electric grid in isolated systems. *2009 International Conference on Power Engineering, Energy and Electrical Drives*, 49–54. https://doi.org/10.1109/POWERENG.2009.4915218

Kafle, U. R. (2025a). *Environmental, Energy Security, and Equity (3E) Implications of Decarbonization Pathways in Nepal: An Open-Source OSeMOSYS Analysis*. https://doi.org/10.2139/SSRN.5693322

Kafle, U. R. (2025b). *Policy-Aligned Energy Transition Pathways for Nepal: Demand Projections and Decarbonization Strategies Through 2035*. https://doi.org/10.2139/SSRN.5679684

Kafle, U. R., Bhattarai, S., Shakya, S. R., Bajracharya, T. R., & Prajapati, A. (2026). *High access, low use: Distribution-grid readiness and suppressed demand in rural electrification*. https://doi.org/10.2139/SSRN.6168257

Kene, R. O., & Olwal, T. O. (2023). Energy Management and Optimization of Large-Scale Electric Vehicle Charging on the Grid. *World Electric Vehicle Journal*, *14*(4), 95. https://doi.org/10.3390/wevj14040095

Leach, M., Mullen, C., Lee, J., Soltowski, B., Wade, N., Galloway, S., Coley, W., Keddar, S., Scott, N., & Batchelor, S. (n.d.). *Modelling the costs and benefits of moving to Modern Energy Cooking Services-methods & application to three case studies Working Paper 29 th April 2021*. Retrieved www.mecs.org.uk

Leary, J., Leach, M., & Batchelor, S. (2022). *Nepal eCooking Market Assessment*.

Li, Y., & Jenn, A. (2024). Impact of electric vehicle charging demand on power distribution grid congestion. *Proceedings of the National Academy of Sciences*, *121*(18). https://doi.org/10.1073/pnas.2317599121

Lombardi, F., Riva, F., Sacchi, M., & Colombo, E. (2019). Enabling combined access to electricity and clean cooking with PV-microgrids: new evidences from a high-

resolution model of cooking loads. *Energy for Sustainable Development*, *49*, 78–88. https://doi.org/10.1016/j.esd.2019.01.005

Mali, B., Shrestha, A., Chapagain, A., Bishwokarma, R., Kumar, P., & Gonzalez-Longatt, F. (2022). Challenges in the penetration of electric vehicles in developing countries with a focus on Nepal. *Renewable Energy Focus*, *40*, 1–12. https://doi.org/10.1016/J.REF.2021.11.003

Malla, S., Timilsina, G. R., & Heger, M. P. (2025). Economics of Household Cooking Using Electricity in Nepal. *Development Research*.

Miri, I., Fotouhi, A., & Ewin, N. (2021). Electric vehicle energy consumption modelling and estimation—A case study. *International Journal of Energy Research*, *45*(1), 501–520. https://doi.org/10.1002/er.5700

Morais, H., Sousa, T., Vale, Z., & Faria, P. (2014). Evaluation of the electric vehicle impact in the power demand curve in a smart grid environment. *Energy Conversion and Management*, *82*, 268–282. https://doi.org/10.1016/j.enconman.2014.03.032

Nationally Determined Contribution (NDC) 3.0 Government of Nepal Kathmandu. (2025).

NEPAL ELECTRICITY AUTHORITY. (n.d.). Retrieved February 13, 2025, from https://www.nea.org.np/yearlyOperationalReports

Neupane, S., Shakya, B., & Author, C. (2024). Factors Influencing Adoption of Two-Wheeler Electric Vehicles in Nepal. *Journal of Productive Discourse*, *2*(1), 63–82. https://doi.org/10.3126/PROD.V2I1.65734

Odoi-Yorke, F. (2024). A systematic review and bibliometric analysis of electric cooking: evolution, emerging trends, and future research directions for sustainable development. *Sustainable Energy Research*, *11*(1), 24. https://doi.org/10.1186/s40807-024-00119-x

Powell, S., Cezar, G. V., Min, L., Azevedo, I. M. L., & Rajagopal, R. (2022). Charging infrastructure access and operation to reduce the grid impacts of deep electric vehicle adoption. *Nature Energy*, *7*(10), 932–945. https://doi.org/10.1038/s41560-022-01105-7

Qiu, Y. L., Wang, Y. D., Iseki, H., Shen, X., Xing, B., & Zhang, H. (2022). Empirical grid impact of in-home electric vehicle charging differs from predictions. *Resource and Energy Economics*, *67*, 101275. https://doi.org/10.1016/j.reseneeco.2021.101275

Roy, P., Ilka, R., He, J., Liao, Y., Cramer, A. M., Mccann, J., Delay, S., Coley, S., Geraghty, M., & Dahal, S. (2023). Impact of Electric Vehicle Charging on Power Distribution Systems: A Case Study of the Grid in Western Kentucky. *IEEE Access*, *11*, 49002–49023. https://doi.org/10.1109/ACCESS.2023.3276928

Saha, A., Razzak, Md. A., & Khan, M. R. (2021). Electric Cooking Diary in Bangladesh: Energy Requirement, Cost of Cooking Fuel, Prospects, and Challenges. *Energies*, *14*(21), 6910. https://doi.org/10.3390/en14216910

Scott, N., Leach, M., & Clements, W. (2024). Energy-Efficient Electric Cooking and Sustainable Energy Transitions. *Energies*, *17*(13), 3318. https://doi.org/10.3390/en17133318

Search | World Bank Data360. (n.d.). Retrieved April 9, 2026, from https://data360.worldbank.org/en/search

Shrestha, A., Dixit, A., Rimal, N. N., Bhandari, D., Basnet, S., Acharya, D., & Sharma, R. (2024). Electric Cooking in Nepal. *Institue for Social Amd Envrionment Transition Nepal (ISETN). Accessed on October*, *11*.

Sinha, P., Paul, K., Deb, S., & Sachan, S. (2023). Comprehensive Review Based on the Impact of Integrating Electric Vehicle and Renewable Energy Sources to the Grid. *Energies*, *16*(6), 2924. https://doi.org/10.3390/en16062924

Sustainable Development Goals | United Nations Development Programme. (n.d.). Retrieved April 8, 2026, from https://www.undp.org/sustainable-development-goals

Veldman, E., & Verzijlbergh, R. A. (2015). Distribution Grid Impacts of Smart Electric Vehicle Charging From Different Perspectives. *IEEE Transactions on Smart Grid*, *6*(1), 333–342. https://doi.org/10.1109/TSG.2014.2355494

Waqas, M., & Humphries, U. W. (2024). A critical review of RNN and LSTM variants in hydrological time series predictions. *MethodsX*, *13*, 102946. https://doi.org/10.1016/j.mex.2024.102946

Yangka, D., & Diesendorf, M. (2016). Modeling the benefits of electric cooking in Bhutan: A long term perspective. *Renewable and Sustainable Energy Reviews*, *59*, 494–503. https://doi.org/10.1016/j.rser.2015.12.265

Zheng, J., Xu, C., Zhang, Z., & Li, X. (2017). Electric load forecasting in smart grids using Long-Short-Term-Memory based Recurrent Neural Network. *2017 51st Annual Conference on Information Sciences and Systems, CISS 2017*. https://doi.org/10.1109/CISS.2017.7926112

FY (BS)	FY (AD)	Two-wheelers (units)	Three-wheelers (units)	Four-wheelers (units)	Buses (units)	Commercial (units)	Total EV units	Energy (TWh)
2072/73	2015/16	248	102690	0	0	0	102938	0.112826883
2073/74	2016/17	1212	10114	1297	29	0	12652	0.015169168
2074/75	2017/18	347	332	5239	0	0	5918	0.008399572
2075/76	2018/19	2047	0	4745	0	0	6792	0.007789263
2076/77	2019/20	1349	208	15516	5	0	17078	0.024420508
2077/78	2020/21	2333	4250	249	9	559	7400	0.008017405
2078/79	2021/22	5455	7322	1807	92	797	15473	0.020400381
2079/80	2022/23	11184	7463	4050	451	289	23437	0.045625232
2080/81	2023/24	9894	12171	11701	1330	961	36057	0.116899121
2081/82	2024/25	13984	16505	13578	3132	2295	49494	0.238122116
	energy	295.416	1098	1514.13	60073.28	3119.895		
	km	8952	18000	12310	58112	25365		
	effi	3.3	6.1	12.3	103.375	12.3		

Figure 13: Import data of Electric Vehicles and energy calculations

year	cumulative_stoves	energy
2019	10435	0.008989
2020	165423	0.142495
2021	323687	0.278824
2022	528080	0.454888
2023	699012	0.602129
2024	936448	0.806656
2025	1083383	0.933226
2026	1337739	1.152328
2027	1536461	1.323508
2028	1735183	1.494687
2029	1933905	1.665866
2030	2132627	1.837045

Figure 14: Energy Consumption due to Electric Stove (TWh)

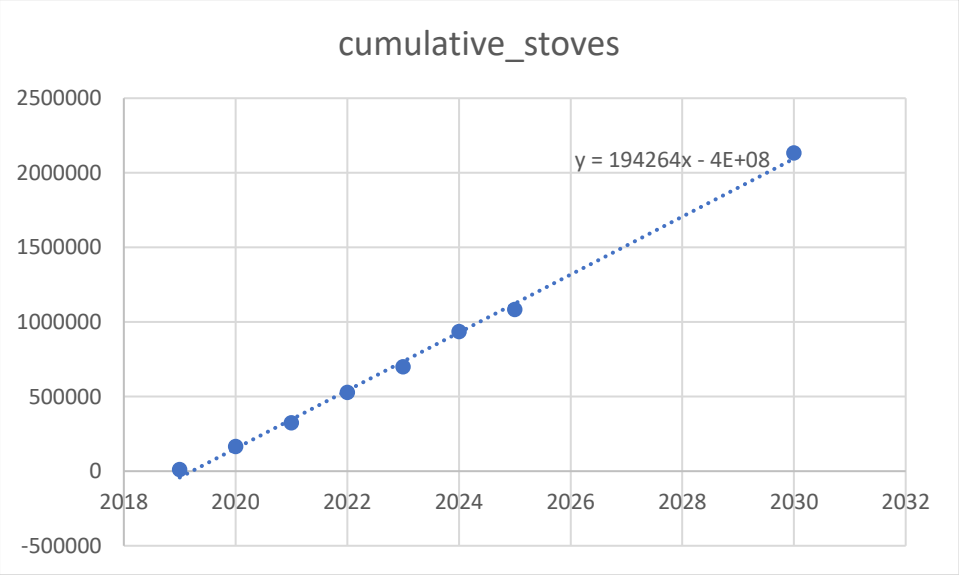

Figure 15: Historic and NDC target data of Electric Stove

EV Energy	
year	energy
2016	0.112827
2017	0.127996
2018	0.136396
2019	0.144185
2020	0.168605
2021	0.176623
2022	0.197023
2023	0.242648
2024	0.359548
2025	0.59767
2026	0.8926
2027	1.2701
2028	1.757
2029	2.3671
2030	3.1142

Figure 16: Energy Consumption due to EV (TWh)

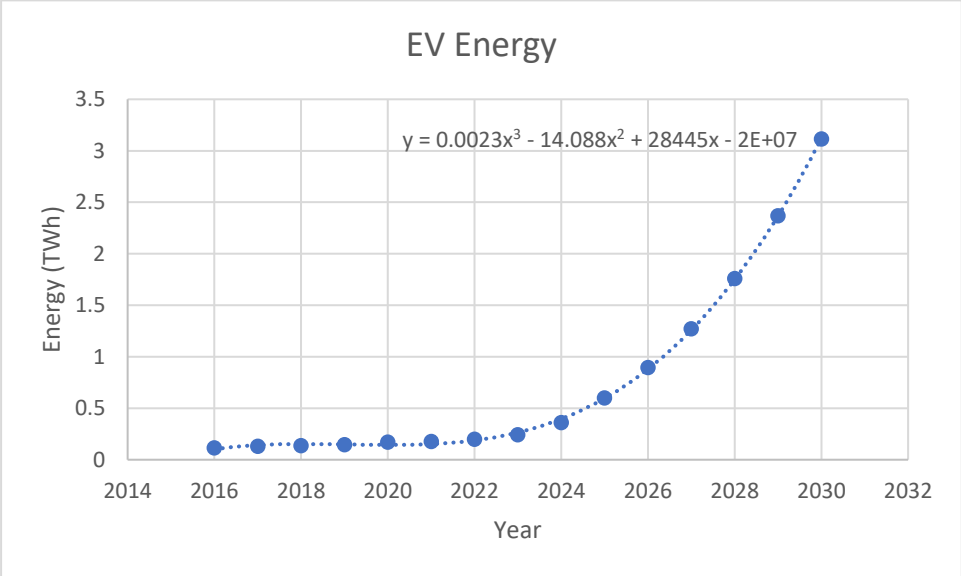

Figure 17: EV Energy Historic and Extrpolated trend

Year	GDP	total_Population	urban_population_by_percentage	net_national_income_per_capita	electricity_per_capita	Electricity_access	energy_Demand
2001	6.01E+09	24946748	31.1	556	63	24.6	1.441
2002	6.05E+09	25328981	32.8	552	66	36.4	1.757
2003	6.33E+09	25688758	35.0	560	69	39.6	1.746
2004	7.27E+09	26016656	38.0	569	73	37.2	1.865
2005	8.13E+09	26309458	41.6	581	75	46.1	1.952
2006	9.04E+09	26565425	45.5	590	82	51.2	2.154
2007	1.03E+10	26788492	49.5	602	86	52.6	2.292
2008	1.25E+10	26990037	53.4	624	82	56	2.208
2009	1.29E+10	27173035	56.9	653	96	59.3	2.586
2010	1.6E+10	27341952	59.9	667	101	68.6	2.744
2011	2.16E+10	27464494	62.0	789	114	67.3	3.108
2012	2.17E+10	27534915	63.1	788	119	75.2	3.24
2013	2.22E+10	27589996	63.7	803	133	77.4	3.358
2014	2.27E+10	27672370	64.1	821	142	84.9	3.496
2015	2.44E+10	27823629	64.6	875	141	82	3.743
2016	2.45E+10	27955462	65.0	877	176	90.7	3.718
2017	2.9E+10	28011258	65.3	1034	204	86.6	4.776
2018	3.31E+10	28079689	65.6	1179	230	93.9	5.56
2019	3.42E+10	28414064	65.8	1200	231	89.9	6.338
2020	3.34E+10	28966574	66.0	1154	257	89.9	6.525
2021	3.69E+10	29475010	66.1	1252	304	89.9	7.313
2022	4.12E+10	29715436	66.1	1385	321	91.3	9.336
2023	4.1E+10	29694614	66.3	1382	380	94	10.693
2024	4.29E+10	29651054	66.5	1447	400	95	12.165
2025	4.38E+10	29618118	66.8	1535	465	98	13.699

Figure 18: Macroeconomics and Demographic Parameters

APPENDICES II: HOURLY DEMAND DATA

Hrs / Day	00:00	01:00	02:00	03:00	04:00	05:00	05:30	06:00	06:30	07:00	07:30	08:00	09:00	10:00	11:00	12:00	13:00	14:00	15:00	16:00	17:00	17:30	18:00	18:30	19:00	19:30	20:00	20:30	21:00	22:00	23:00
1	1318	1282	1275	1242	1236	1284	1343	1404	1414	1437	1463	1509	1494	1424	1410	1368	1333	1408	1400	1348	1356	1287	1264	1312	1431	1369	1573	1571	1532	1450	1317
2	1226	1209	1182	1228	1224	1267	1281	1354	1336	1440	1452	1514	1577	1612	1592	1633	1631	1606	1657	1659	1603	1589	1461	1702	1870	1857	1776	1704	1648	1553	1450
3	1396	1356	1343	1291	1316	1317	1367	1403	1527	1517	1607	1663	1490	1528	1631	1549	1523	1649	1700	1621	1684	1569	1466	1752	1837	1815	1756	1720	1666	1572	1498
4	1455	1422	1384	1354	1356	1387	1399	1437	1509	1575	1635	1628	1581	1602	1654	1620	1596	1592	1572	1441	1469	1365	1240	1261	1685	1668	1696	1669	1572	1521	1432
5	1354	1363	1373	1330	1283	1328	1367	1459	1526	1467	1518	1539	1593	1613	1585	1613	1638	1641	1672	1626	1559	1508	1482	1547	1808	1808	1789	1741	1708	1657	1527
6	1510	1457	1425	1385	1375	1408	1458	1463	1528	1568	1608	1601	154	1579	1617	1638	1319	1673	1712	1685	1615	1580	1457	1537	1832	1815	1744	1720	1645	1612	1566
7	1470	1403	1369	1364	1342	1385	1428	1479	1532	1566	1603	1626	1641	1720	1726	1721	1696	1621	1549	1595	1545	1470	1539	1615	1797	1765	1731	1713	1675	1595	1542
8	1496	1460	1429	1408	1426	1420	1430	1500	1546	1580	1547	1646	1615	1629	1591	1543	1516	1393	1416	1410	1391	1348	1507	1607	1734	1722	1708	1692	1663	1540	1566
9	1538	1477	1439	1420	1419	1438	1468	1536	1609	1683	1732	1665	1685	1756	1768	1703	1735	1692	1727	1727	1667	1628	1511	1776	1917	1873	1840	1796	1771	1661	1532
10	1551	1528	1502	1492	1464	1483	1517	1526	1603	1609	1502	1676	1718	1720	1725	1760	1690	1670	1711	1756	1723	1741	1578	1855	1984	1998	1922	1862	1838	1715	1669
11	1583	1587	1542	1529	1511	1533	1545	1623	1707	1614	1684	1640	1618	1706	1728	1730	1682	1595	154	1526	1584	1579	1520	1735	1963	1959	1912	1885	1835	1718	1612
12	1608	1581	1560	1520	1524	1546	1569	1641	1743	1762	1809	1815	1635	1647	1698	1694	1658	1646	1597	1664	1556	1543	1688	1769	1977	1966	1884	1879	1851	1754	1667
13	1624	1605	1533	1519	1507	1523	1547	1691	1792	1779	1754	1104	1814	1795	1729	1718	1718	1794	1769	1788	1777	1736	1688	1835	1837	1834	1899	1873	1972	1781	1685
14	1561	1488	1488	1432	1430	1458	1494	1580	1500	1630	1697	1727	1700	1662	1789	1771	1689	1771	1790	1716	1727	1641	1538	1573	2011	1956	1856	1832	1813	1721	1620
15	1593	1552	1532	1564	1536	1507	1507	1495	1505	1452	1485	1549	1582	1554	1567	1526	1466	1543	1534	1512	1513	1513	1446	1403	1885	1889	1821	1851	1817	1570	1651
16	1532	1543	1492	1467	1456	1475	1471	1505	1525	1666	1757	1802	1808	1831	1833	1817	1750	1698	1751	1696	1676	1632	1604	1751	1927	1919	1874	1877	1777	1698	1649
17	1595	1544	1492	1469	1455	1465	1482	1513	1586	1673	1727	1811	1752	1823	1834	1818	1827	1783	1809	1765	1706	1703	1605	1746	1846	1905	1968	1910	1873	1822	1735
18	1670	1626	1583	1547	1539	1551	1560	1561	1542	1651	1788	1780	1777	1827	1836	1815	1766	1700	1713	1737	1716	1678	1753	1856	1902	1939	1880	1840	1830	1710	1639
19	1570	1524	1493	1476	1455	1451	1464	1528	1459	1549	1609	1554	1528	1528	1633	1559	1572	1579	1613	1528	1534	1524	1497	1467	1915	1947	1863	1848	1870	1723	1651
20	1577	1564	1532	1457	1400	1450	1540	1531	1540	1685	1756	1771	1763	1806	1811	1826	1795	1789	1758	1760	1728	1639	1530	1594	1908	1909	1919	1844	1791	1643	1548
21	1539	1471	1415	1118	1125	1156	1156	1200	1498	1665	1772	1786	1732	1781	1786	1795	1774	1842	1864	1806	1710	1718	1530	1741	1816	1799	1741	1721	1838	1783	1610
22	1550	1495	1477	1463	1471	1489	1476	1559	1464	1599	1597	1622	1639	1596	1565	1613	1614	1656	1634	1606	1543	1540	1493	1708	1888	1860	1827	1808	1730	1650	1555
23	1555	1471	1445	1411	1417	1429	1452	1515	1537	1667	1721	1666	1794	1826	1819	1832	1813	1857	1870	1843	1812	1776	1606	1818	1872	1900	1901	1816	1756	1694	1583
24	1544	1496	1453	1441	1419	1459	1491	1421	1536	1646	1727	1728	1654	1706	1696	1778	1762	1811	1816	1800	1745	1603	1410	1400	1794	1672	1622	1615	1608	1576	1545
25	1515	1468	1442	1432	1445	1454	1458	1493	1532	1671	1698	1656	1539	1483	1561	1531	1586	1503	1601	1493	1434	1431	1352	1401	1465	1517	1494	1475	1471	1342	1307
26	1296	1192	1200	1145	1156	1231	1323	1297	1549	1467	1474	1500	1524	1578	1574	1525	1536	1556	1564	1547	1422	1399	1389	1539	1598	1535	1515	1529	1457	1389	1334
27	1262	1245	1249	1235	1239	1262	1329	1446	1425	1560	1626	1632	1591	1636	1615	1597	1579	1596	1592	1590	1586	1585	1465	1631	1751	1748	1646	1563	1529	1464	1407
28	1407	1295	1272	1273	1237	1267	1279	1367	1468	1545	1608	1593	1545	1594	1690	1638	1648	1708	1706	1679	1576	1592	1521	1584	1780	1758	1706	1694	1651	1592	1624
29	1450	1394	1365	1384	1390	1411	1412	1421	1426	1428	1503	1520	1563	1483	1500	1516	1496	1522	1528	1547	1493	1425	1346	1529	1690	1746	1789	1789	1673	1649	1477
30	1423	1199	1177	1076	1077	1102	1156	1206	1208	1334	1419	1416	1432	1449	1386	1415	1432	1463	1443	1475	1354	1490	1499	1371	1590	1568	1569	1519	1516	1429	1006
31	1362	1348	1317	1353	1361	1395	1431	1518	1402	1500	1577	1568	1616	1631	1618	1568	1612	1687	1714	1747	1659	1619	1546	1628	1772	1870	1838	1785	1740	1624	1484

Figure 19: Hourly Electricity Demand of Baisakh 2081 (Mega Watt)

Hrs / Day	00:00	01:00	02:00	03:00	04:00	05:00	05:30	06:00	06:30	07:00	07:30	08:00	09:00	10:00	11:00	12:00	13:00	14:00	15:00	16:00	17:00	17:30	18:00	18:30	19:00	19:30	20:00	20:30	21:00	22:00	23:00
1	1221	1207	1176	1187	1192	1260	1348	1436	1563	1651	1760	1775	1725	1547	1476	1438	1298	1325	1260	1269	1304	1471	1679	1722	1723	1691	1636	1478	1375	1386	1257
2	1187	1145	1091	1041	1095	1147	1237	1252	1313	1465	1465	1476	1497	1641	1617	1612	1500	1498	1408	1500	1570	1595	1876	1901	1876	1876	1780	1704	1386	1532	1532
3	1532	1532	1181	1153	1166	1182	1264	1356	1442	1576	1694	1651	1682	1671	1701	1659	1612	1592	1628	1530	1488	1427	1490	1933	1884	1867	1832	1809	1502	1510	1430
4	1243	1208	1202	1175	1179	1236	1281	1391	1553	1702	1779	1819	1839	1943	1735	1656	1561	1508	1544	1528	1412	1377	1490	1931	1908	1888	1847	1837	1615	1368	1308
5	1211	1211	1206	1170	1169	1211	1305	1333	1457	1500	1673	1710	1692	1829	1476	1444	1318	1319	1331	1308	1291	1468	1703	1804	1777	1734	1399	1340	1280	1048	1270
6	1162	1139	1129	1119	1159	1191	1286	1356	1476	1704	1764	1670	1640	1701	1674	1596	1528	1551	1529	1541	1485	1617	1865	1900	1867	1525	1422	1353	1280	1426	1237
7	1239	1149	1144	1195	1194	1230	1323	1367	1414	1483	1571	1829	1476	1535	1679	1686	1587	1520	1468	1467	1519	1648	1824	1921	1845	1762	1751	1714	1595	1471	1314
8	1253	1176	1202	1190	1192	1242	1312	1363	1462	1416	1421	1878	1728	1658	1666	1597	1546	1499	1508	1386	1218	1272	1868	1933	1840	1794	1696	1613	1544	1477	1305
9	1222	1202	1173	1194	1177	1212	1299	1418	1559	1511	1566	1471	1411	1569	1637	1542	1583	1574	1452	1388	1366	1240	1818	1938	1556	1535	1788	1703	1527	1493	1388
10	1247	1204	1184	1194	1179	1232	1337	1437	1567	1557	1969	1854	1896	1803	1635	1638	1569	1586	1599	1667	1669	1737	1888	1917	1857	1851	1499	1504	1463	1470	1252
11	1219	1151	1173	1174	1180	1255	1317	1360	1472	1549	1835	1775	1391	1719	1733	1641	1544	1549	1505	1509	1692	1708	1858	1935	1901	1836	1810	1744	1558	1408	1337
12	1227	1177	1186	1191	1167	1290	1231	1319	1387	1398	1418	1550	1720	1528	1568	1413	1377	1306	1308	1373	1310	1077	1761	1817	1477	1484	1699	1662	1662	1371	1258
13	1147	1119	1105	1076	1110	1124	1223	1293	1387	1611	1731	1713	1719	1656	1575	1499	1438	1516	1510	1433	1395	1130	1881	1948	1860	1833	1808	1715	1473	1414	1346
14	1222	1252	1285	1225	1250	1279	1325	1394	1548	1619	1922	1912	1966	1961	1605	1570	1532	1542	1548	1602	1460	1766	1737	1972	1921	1894	1564	1535	1537	1416	1311
15	1291	1254	1237	1134	1178	1257	1307	1435	1553	1617	1875	1938	2054	1782	1688	1602	1553	1536	1493	1524	1400	1518	1793	1899	1587	1556	1541	1541	1363	1430	1306
16	1241	1180	1173	1186	1179	1181	1266	1350	1496	1620	1767	1785	1722	1592	1512	1531	1419	1379	1316	1363	1379	1542	1737	1842	1790	1742	1647	1633	1589	1407	1274
17	1232	1190	1187	1167	1163	1216	1275	1341	1505	1726	1741	1859	1769	1624	1618	1572	1545	1503	1480	1507	1426	1576	1677	1875	1842	1767	1741	1696	1660	1396	1303
18	1217	1221	1217	1194	1182	1268	1285	1392	1504	1515	1826	1891	1732	1588	1610	1532	1530	1503	1507	1508	1291	1221	1923	1926	1849	1860	1802	1700	1642	1436	1299
19	1273	1245	1216	1202	1216	1266	1332	1391	1499	1448	1674	1713	1364	1536	1775	1340	1333	1291	1306	1306	1208	1262	1442	1867	1830	1733	1682	1683	1661	1378	1206
20	1206	1170	1184	1174	1164	1227	1268	1347	1462	1612	1803	1778	1692	1592	1572	1560	1514	1498	1479	1525	1404	1697	1806	1997	1659	1583	1365	1384	1338	1399	1274
21	1263	1202	1201	1225	1212	1282	1400	1464	1626	1817	1945	1932	1863	1652	1706	1628	1520	1513	1568	1558	1370	1621	1787	1921	1877	1836	1773	1728	1726	1413	1304
22	1209	1209	1188	1166	1172	1270	1292	1168	1399	1922	1833	2079	1657	1597	1635	1539	1477	1493	1514	1463	1404	1663	1817	1934	1855	1787	1728	1670	1635	1375	1281
23	1243	1216	1214	1173	1174	1233	1274	1427	1567	1623	1600	1503	1319	1589	1591	1457	1457	1497	1491	1485	1660	1334	1433	1978	1952	1862	1637	1508	1420	1385	1279
24	1237	1244	1210	1202	1186	1252	1352	1420	1504	1880	1846	1820	1410	1646	1640	1532	1508	1501	1517	1543	1414	1775	1830	1999	2008	1893	1828	1667	1562	1379	1323
25	1341	1239	1194	1205	1205	1268	1333	1425	1569	1557	1562	1449	1494	1663	1639	1595	1527	1543	1517	1550	1687	1608	1866	1989	1923	1884	1682	1656	1572	1383	1306
26	1306	1306	1257	1251	1225	1243	1284	1337	1431	1450	1469	1370	1553	1547	1470	1373	1333	1338	1334	1090	1232	1552	1748	1840	1848	1754	1695	1650	1597	1280	1205
27	1187	1154	1123	1077	1087	1188	1272	1340	1461	1510	1615	1680	1638	1566	1569	1505	1561	1494	1496	1483	1431	1506	1671	1940	1842	1808	1709	1669	1687	1332	1252
28	1274	1228	1226	1206	1237	1270	1358	1469	1575	1634	1484	1835	1789	1941	1675	1694	1612	1582	1567	1555	1125	1779	1826	1885	1778	1818	1746	1635	1565	1324	1218
29	1226	1152	1152	1130	1140	1247	1305	1356	1495	1538	1733	1772	1294	1505	1575	1527	1481	1516	1522	1509	1388	1650	1805	1959	1822	1725	1653	1580	1375	1315	1261
30	1187	1160	1175	1137	1162	1200	1253	1401	1514	1797	1761	1766	1586	1611	1579	1489	1433	1469	1479	1498	1317	1515	1791	1855	1782	1751	1666	1705	1519	1302	1219

Figure 20: Hourly Electricity Demand of Magh 2081 (Mega Watt)

Gmail **Prashant Paudyal Sharma <paudyalprashant98@gmail.com>**

[JIEE] Editor Decision

1 message

postmaster@nepjol.info <postmaster@nepjol.info> 5 May 2026 at 20:55
Reply-To: Raj Kumar Chaulagain <rajkrc12@tcioe.edu.np>
To: Prashant Paudyal <paudyalprashant98@gmail.com>, Sanjaya Neupane <sanjaya@pcampus.edu.np>

Prashant Paudyal, Sanjaya Neupane:

We have reached a decision regarding your submission to Journal of Innovations in Engineering Education, "Forecasting Nepal's Electricity Demand under Transport and Cooking Electrification Using Deep Learning".

Our decision is to: Accept the Submission with minor corrections on the attached concerns

---

Journal of Innovations in Engineering Education

Prashant Paudyal

Impact assessment of Electric Cooking and Electric Mobility on Grid Demand A Scenario Based Hourly Load Forecasting Stud...

University Grants Commission, Nepal

Document Details

Submission ID
trn:oid:::3117:589990733

Submission Date
May 13, 2026, 9:19 AM GMT+5:45

Download Date
May 13, 2026, 9:23 AM GMT+5:45

File Name
Impact assessment of Electric Cooking and Electric Mobility on Grid Demand A Scenario Based H....pdf

File Size
2.1 MB

127 Pages

30,368 Words

182,605 Characters

4% Overall Similarity

The combined total of all matches, including overlapping sources, for each database.

Filtered from the Report

- Bibliography
- Quoted Text
- Cited Text
- Small Matches (less than 8 words)

Match Groups

85 Not Cited or Quoted 4%
Matches with neither in-text citation nor quotation marks

0 Missing Quotations 0%
Matches that are still very similar to source material

0 Missing Citation 0%
Matches that have quotation marks, but no in-text citation

0 Cited and Quoted 0%
Matches with in-text citation present, but no quotation marks

Top Sources

4% Internet sources
2% Publications
0% Submitted works (Student Papers)

Integrity Flags

1 Integrity Flag for Review

Replaced Characters
73 suspect characters on 16 pages
Letters are swapped with similar characters from another alphabet.

Our system's algorithms look deeply at a document for any inconsistencies that would set it apart from a normal submission. If we notice something strange, we flag it for you to review.

A Flag is not necessarily an indicator of a problem. However, we'd recommend you focus your attention there for further review.

Match Groups

- **85** Not Cited or Quoted 4%
  Matches with neither in-text citation nor quotation marks
- **0** Missing Quotations 0%
  Matches that are still very similar to source material
- **0** Missing Citation 0%
  Matches that have quotation marks, but no in-text citation
- **0** Cited and Quoted 0%
  Matches with in-text citation present, but no quotation marks

Top Sources

4% Internet sources
2% Publications
0% Submitted works (Student Papers)

Top Sources

The sources with the highest number of matches within the submission. Overlapping sources will not be displayed.

1	Internet	elibrary.tucl.edu.np 1%
2	Internet	www.mdpi.com <1%
3	Internet	fastercapital.com <1%
4	Internet	worldwidescience.org <1%
5	Internet	hdl.handle.net <1%
6	Internet	ebin.pub <1%
7	Publication	Navin Kumar Jha, Sunil Prasad Lohani. "Understanding household biogas failures ... <1%
8	Internet	www.econjournals.com <1%
9	Internet	www.ijisrt.com <1%
10	Publication	Mohammed Fathy El-Amin. "Advances and Applications of Machine Learning in Fl... <1%

11 Internet
iieta.org <1%

12 Internet
sciencepg.org <1%

13 Internet
www.biorxiv.org <1%

14 Internet
iconline.ipleiria.pt <1%

15 Internet
repository.tudelft.nl <1%

16 Publication
Bhargava K. Reddy, Dursun Delen. "Predicting hospital readmission for lupus pati... <1%

17 Internet
dspace.cbe.ac.tz:8080 <1%

18 Internet
pmc.ncbi.nlm.nih.gov <1%

19 Internet
pollution.sustainability-directory.com <1%

20 Internet
gggi.org <1%

21 Publication
Mohammad-Reza Andervazh, Shahram Javadi, Mahmood Hosseini Aliabadi. "Activ... <1%

22 Internet
repository.nusystem.org <1%

23 Publication
"Cooperative Information Systems", Springer Science and Business Media LLC, 20... <1%

24 Publication
Dipesh K.C., Sunil Prasad Lohani, Ramchandra Bhandari, Sushil Aryal. "Feasibility ... <1%

25 Publication

Lecture Notes in Computer Science, 2015. <1%

26 Publication

Sabzi, Shahab. "AI-Based Electric Vehicles Charging Strategy Considering User Be... <1%

27 Internet

d197for5662m48.cloudfront.net <1%

28 Internet

edepot.wur.nl <1%

29 Internet

taksarnews.com <1%

30 Publication

Agyemang, Edmund Fosu. "Sequential Data Modeling of Influenza A via Tradition... <1%

31 Publication

Ali Razzaghi, Sayyed Majid Miri Larimi, Hamid Reza Baghaee. "Reliability-, security... <1%

32 Publication

Dal-Ri dos Santos, Iago. "Transport of Firebrand Particles in the Turbulent Atmos... <1%

33 Publication

Melanie Maliti, Aaron Zimba. "A White-box Approach to Forecasting Petrol Prices i... <1%

34 Publication

Smart Innovation Systems and Technologies, 2014. <1%

35 Internet

arxiv.org <1%

36 Internet

isjem.com <1%

37 Internet

pypi.org <1%

38 Internet

wci.t.u-tokyo.ac.jp <1%

39 Publication

An Jiang, Jiehong Qiu, Aiyuan Li, Guangnan Zhang. "An Empirical Analysis Framew... <1%

40 Publication

B. Gunapriya, B. Santosh Kumar, B. Rajalakshmi, Kannan Palanisamy. "Cost-Efficie... <1%

41 Publication

C. Guedes Soares, F.C. Salvado. "Innovations in Maritime Technology and Enginee... <1%

42 Publication

D. Sivabalaselvamani, G. Revathy, Ranjit Singh Sarban Singh. "Advanced AI and D... <1%

43 Publication

Kirk R. Smith, Howard Frumkin, Kalpana Balakrishnan, Colin D. Butler et al. "Ener... <1%

44 Publication

Luis Rodrigo Asturias Schaub, Luis Alberiko Gil-Alana, Benjamín Leiva. "Fractional... <1%

45 Publication

Maynard, Logan. "Advanced Machine Learning and Low-Dimensionality Projectio... <1%

46 Publication

Meng, Qingjia. "The effects of eicosapentaenoic acid (EPA) treatments on the oxid... <1%

47 Publication

Sunil Malla. "An outlook of end-use energy demand based on a clean energy and ... <1%

48 Publication

Xydas, Erotokritos, Charalampos Marmaras, Liana M. Cipcigan, Nick Jenkins, Stev... <1%

49 Internet

d-nb.info <1%

50 Internet

dirros.openscience.si <1%

51 Internet

img.saurenergy.com <1%

52 Internet

orca.cardiff.ac.uk <1%

53 Internet

pure.solent.ac.uk <1%

54 Internet

research.usq.edu.au <1%

55 Internet

sun-connect.org <1%

56 Internet

wecs.gov.np <1%

57 Internet

www.jewe.ir <1%

58 Internet

www.pnas.org <1%